# [NOT A FINAL NAME, NEEDS WORK] LEU+ TO HALEU TRANSITIONS IN ADVANCED REACTOR FUEL CYCLES

BY

NATHAN SEAN RYAN

THESIS

Submitted in partial fulfillment of the requirements
for the degree of Master of Science in Nuclear, Plasma, Radiological Engineering
in the Graduate College of the
University of Illinois at Urbana-Champaign, 2025

Urbana, Illinois

Master's Committee:

Assistant Professor Madicken Munk
Associate Professor Kathryn D. Huff
Professor Rizwan Uddin

# Abstract

This is the abstract.

**Keywords:** Cyclus, TRISO, HALEU, LEU+, Serpent, Nuclear Fuel Cycle, Memory Efficiency

# Acknowledgments

I would like to thank Prof. Madicken Munk, who mentored me as a student and who constantly inspires me to think big and find the impact in my work. Relatedly, I would like to thank Prof. Kathryn Huff, who has been a mentor to me at every step of my collegiate education and who shows me how to be a happy warrior.

I want to thank my fellow graduate students and the members of Advanced Reactors and Fuel Cycles (ARFC); particularly Dr. Amanda Bachmann, Sam Dotson, Nataly Panczyk, Olek Yardas, Zoë Richter, Dr. Gwendolyn Chee, Dr. Sun Myung Park, Rhys MacMillian, and Ceser Zambrano. I would like to especially thank Luke Seifert for his assistance in running the Serpent simulations in this work.

Throughout the years, I have learned much from my group mates, advisors, and mentors, but I would be remiss not to acknowledge that I went to the school of open source and learned much from countless developers who work openly to better science. Particularly the CYCLUS community, especially Prof. Paul P.H. Wilson, Dr. Katie Mummah, Jin Whan Bae, and Dr. Eva Davidson.

I owe many thanks to my parents, brother, grandparents, family, partner, and friends who have reminded me—sometimes to my chagrin—that life keeps going outside the walls of my office. To my cousin Matthew, I can not wait to explain this part of my life to you someday when we are reunited because I know you will have questions.

This research was performed, in part, using funding received from the DOE Office of Nuclear Energy's Nuclear Energy University Program (Project 23-29656 DE-NE0009390) 'Illuminating Emerging Supply Chain and Waste Management Challenges'.

This research was supported in part by an appointment to the Oak Ridge National Laboratory Research Student Internships Program, sponsored by the U.S. Department of Energy and administered by the Oak Ridge Institute for Science and Education.

# Table of Contents

**List of Tables** . . . vi

**List of Figures** . . . vii

**Chapter 1 Introduction** . . . 1

**Chapter 2 Background** . . . 5
- 2.1 Energy System Modeling . . . 7
- 2.2 The Nuclear Fuel Cycle . . . 8
  - 2.2.1 Front End of the Fuel Cycle . . . 9
  - 2.2.2 Reactor Operation . . . 11
  - 2.2.3 Back-End of the Fuel Cycle . . . 11
- 2.3 LEU Plus (LEU+) . . . 12
- 2.4 TRISO Fuel . . . 14
- 2.5 Reactor Models . . . 15
  - 2.5.1 MMR-like Reactor . . . 16
  - 2.5.2 Xe-100-like Reactor . . . 18
  - 2.5.3 AP1000 Reactor . . . 21
- 2.6 CYCLUS . . . 22
  - 2.6.1 Fuel Depletion . . . 23

**Chapter 3 Deployment Scenarios** . . . 25
- 3.1 Transition Scenarios . . . 25
- 3.2 Metrics . . . 30
  - 3.2.1 Separative Work Units . . . 31
  - 3.2.2 Energy Output . . . 32
  - 3.2.3 Mass of Fuel . . . 32
- 3.3 Greedy Deployment . . . 32
  - 3.3.1 Number of Reactors . . . 33
  - 3.3.2 SWU Results . . . 35
  - 3.3.3 Fresh Fuel Results . . . 37
  - 3.3.4 Used Fuel Results . . . 38
- 3.4 Random Deployment . . . 40
  - 3.4.1 Number of Reactors . . . 41
  - 3.4.2 SWU Results . . . 43
  - 3.4.3 Fresh Fuel Results . . . 45
  - 3.4.4 Used Fuel Results . . . 46
- 3.5 Initially Random, Greedy Deployment . . . 48
  - 3.5.1 Number of Reactors . . . 49
  - 3.5.2 SWU Results . . . 50
  - 3.5.3 Fresh Fuel Results . . . 52
  - 3.5.4 Used Fuel Results . . . 54

**Chapter 4 Reactor Power and Market Interactions** . . . . . 56
4.1 Archetypes and Time Management . . . . . 56
4.2 Trading On-Demand Reactor . . . . . 58
4.3 Dynamic Power Reactor . . . . . 60

**Chapter 5 Conclusions** . . . . . 63
5.1 Transition Scenarios Conclusions . . . . . 63
5.1.1 Future Work . . . . . 64
5.2 Reactor Power and Market Interaction Conclusions . . . . . 65
5.2.1 Future Work . . . . . 65

**References** . . . . . 67

**Appendix A LWRs Simulated** . . . . . 70

**Appendix B Considered Deployment Schemes** . . . . . 74
B.1 Capped Deployment . . . . . 74
B.2 Pre-Determined Distribution Deployment . . . . . 76

**Appendix C Availability of Work** . . . . . 78

# List of Tables

2.1 Enrichment levels and their ranges. . . . . . . . . . 13
2.2 Advanced reactor design specifications. . . . . . . . . . 15

3.1 Deployment schemes. . . . . . . . . . 26
3.2 Demand growth scenarios. . . . . . . . . . 26
3.3 Transition scenario simulations run. . . . . . . . . . 27
3.4 Capacity difference between results and projection. . . . . . . . . . 30
3.5 SWU calculation values for each fuel type. . . . . . . . . . 32
3.6 Average greedy total operating reactors by design. . . . . . . . . . 35
3.7 Average greedy yearly SWU by design in kseparative work units (SWU). . . . . . . . . . 37
3.8 Average greedy yearly fresh fuel by design in tonnes. . . . . . . . . . 38
3.9 Average greedy yearly used fuel by design in tonnes. . . . . . . . . . 40
3.10 Average random total operating reactors by design. . . . . . . . . . 43
3.11 Average random yearly SWU by design in tonnes of SWU. . . . . . . . . . 45
3.12 Average random yearly fresh fuel by design in tonnes. . . . . . . . . . 46
3.13 Average random yearly used fuel by design in tonnes. . . . . . . . . . 48
3.14 Average initially random, then greedy total operating reactors by design. . . . . . . . . . 50
3.15 Average initially random, then greedy yearly SWU by design in kSWU. . . . . . . . . . 52
3.16 Average initially random, then greedy yearly fresh fuel by design in tonnes. . . . . . . . . . 54
3.17 Average initially random, then greedy yearly used fuel by design in tonnes. . . . . . . . . . 55

4.1 Trading On-Demand (TOD) reactor and CYCAMORE reactor profiles. . . . . . . . . . 58

5.1 Average yearly percentage SWU increases from the no-growth scenario to the double scenario. . . . . 64

A.1 LWR fleet simulated, A-K. . . . . . . . . . 71
A.2 LWR fleet simulated, L-St. . . . . . . . . . 72
A.3 LWR fleet simulated, Su-Z. . . . . . . . . . 73

# List of Figures


1.1 US LWR capacity through 2024. Reproduced from [25]. . . . . 2
1.2 US once-through fuel cycle. . . . . 3

2.1 Global energy consumption (exajoules) by source from 1800–2017. Reproduced from [66]. . . . . 6
2.2 Hypothetical closed fuel cycle. . . . . 9
2.3 Foreign and domestic uranium purchases over time. Reproduced from [60]. . . . . 10
2.4 TRISO fuel particle layers [8]. . . . . 14
2.5 USNC MMR design [54]. . . . . 16
2.6 USNC Micro Modular Reactor (MMR) fuel renderings [55]. . . . . 17
2.7 Serpent model of the USNC MMR core. . . . . 18
2.8 X-Energy Xe-100 rendition [63]. . . . . 19
2.9 X-Energy Xe-100 fuel pebble [62]. . . . . 20
2.10 Top-down view of the X-Energy Xe-100 core model. . . . . 21

3.1 Total and new nuclear capacity deployed in each scenario. . . . . 29
3.2 Energy capacity difference between projection and scheme predictions. . . . . 30
3.3 Greedy deployment diagram. . . . . 33
3.4 Greedy multi-fuel reactor deployment. . . . . 34
3.5 Greedy single-fuel reactor deployment. . . . . 34
3.6 Greedy yearly SWU capacity multi-fuel, no growth scenario. . . . . 35
3.7 Greedy multi-fuel SWU. . . . . 36
3.8 Greedy single-fuel SWU. . . . . 36
3.9 Greedy multi fresh fuel demanded. . . . . 37
3.10 Greedy single fresh fuel demanded. . . . . 38
3.11 Greedy multi used fuel accumulation. . . . . 39
3.12 Greedy single used fuel accumulation. . . . . 39
3.13 Random deployment diagram. . . . . 41
3.14 Multiple fuels random reactor deployment. . . . . 42
3.15 Single-fuel random reactor deployment. . . . . 42
3.16 Random reactor yearly SWU capacity. . . . . 43
3.17 Random reactor multi-fuel SWU. . . . . 44
3.18 Random reactor single-fuel SWU. . . . . 44
3.19 Random multi fresh fuel demanded. . . . . 45
3.20 Random single fresh fuel demanded. . . . . 46
3.21 Random multi used fuel accumulation. . . . . 47
3.22 Random single used fuel accumulation. . . . . 47
3.23 Initially random, greedy deployment diagram. . . . . 48
3.24 Multiple fuels initially random, then greedy reactor deployment. . . . . 49
3.25 Single-fuel initially random, then greedy reactor deployment. . . . . 50
3.26 Initially random, then greedy yearly SWU capacity. . . . . 51
3.27 Initially random, then greedy multi-fuel SWU. . . . . 51

3.28 Initially random, then greedy single-fuel SWU. . . . . . 52
3.29 Initially random, then greedy multi fresh fuel demanded. . . . . . 53
3.30 Initially random, then greedy single fresh fuel demanded. . . . . . 53
3.31 Initially random, then greedy multi used fuel accumulation. . . . . . 54
3.32 Initially random, then greedy single used fuel accumulation. . . . . . 55

4.1 Simple A-B-C scenario. . . . . . 56
4.2 Acceptance of $^{239}$Pu into the sink with a frequency of 50 months. . . . . . 57
4.3 Time clock values for the TOD and CYCAMORE reactors. . . . . . 59
4.4 Number of instructions and instructions per cycle from the TOD and CYCAMORE reactors. . . . . . 59
4.5 Clinton Clean Energy Center (Clinton) reactor daily power percent 2021-2024. . . . . . 60
4.6 Difference in daily power capacity between Dynamic Power Reactor (DPR) and Clinton. . . . . . 61
4.7 2024 power capacity of the CYCAMORE reactor and DPR. . . . . . 62

B.1 Capped deployment diagram. . . . . . 75
B.2 Pre-determined distribution deployment diagram. . . . . . 76

# Chapter 1

# Introduction

While the world grapples with the effects of climate change, the demand for clean and firm energy continues to increase. Utilities and decision-makers face rising energy demands of machine learning and data center companies, which require a constant and reliable energy source. The escalation of data center demand and electrification in the economy has led the U.S. Energy Information Administration (EIA) to forego publishing its annual energy outlook report in 2023 as it evaluates its models under emergent market pressures [59]. New nuclear reactors—designed to be more efficient, flexible, and resilient than the reactors that have come before them—can provide clean, firm energy to meet these demands.

Since 1959, the United States (U.S.) has commercially operated large Light Water Reactor (LWR) designs at nuclear power plants. These reactors use light water as a coolant and moderator and can be categorized as either Pressurized Water Reactors (PWRs) or Boiling Water Reactors (BWRs). As shown in Figure 1.1, the LWR fleet in the U.S. expanded power capacity over roughly 20 years before achieving just over 99 GWe in 1990 and remained roughly constant in the years since then. With the recent connection of Vogtle Units 3 and 4 to the grid, the U.S. has seen the first new LWR units come online in 8 years–following the completion of Watts Bar-2 in 2016.

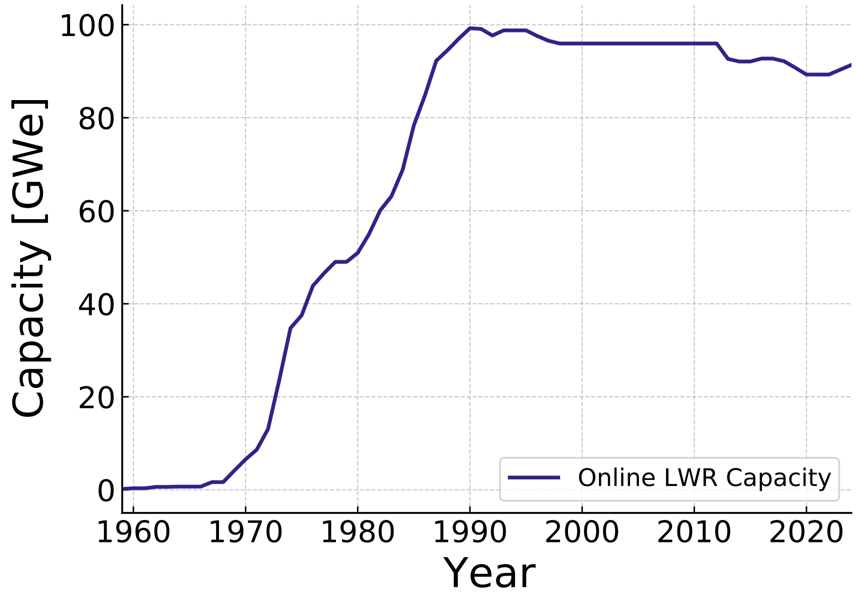


Figure 1.1: US LWR capacity through 2024. Reproduced from [25].

According to the EIA, nuclear power plants produced 18% of utility-scale electricity generation in 2023 [61], meaning nuclear energy was 46.5% of total clean energy generation and the largest clean energy source in the country. The last license in the fleet will now expire in 2063 following the completion of Vogtle Unit 4; however, to meet growing energy demands, the U.S. will need to replace and expand the current fleet as it retires over that time; deploying new reactors at a rate that has not been seen since the 1970s. The U.S. Department of Energy (DOE) has published a liftoff report on how nuclear energy can expand to meet future demands and has outlined myriad scenarios that could lead to a 100% net zero carbon by 2050 [26]. One of the striking takeaways from the liftoff report is the necessity of tripling nuclear energy demand by 2050 due to new capacity demand, the retirement of fossil fuels, electrification of the economy, and other behind-the-meter applications of nuclear technologies. The future DOE outlines is not without its challenges; the EIA 2023 Domestic Uranium Production Report highlights the decrease in uranium concentrate production in the U.S. and the number of fuel cycle facilities that are dormant or have been decommissioned [10].

Despite these deployment challenges, the DOE liftoff report asserts that high-value propositions in low land use, firm energy generation, direct heat applications, local economic benefits, and the low transmission build-out associated with nuclear energy make it a compelling choice. Some of these benefits can be reflected in the 73% increase in uranium production workers from 2022 to 2023, the 4x increase in exploration of uranium resources, and a $20 million increase in resource investment [10] —the private sector is starting to move on the value proposition of nuclear energy.

The current fleet of LWRs has been the backbone of the commercial nuclear industry, but the industry is on the precipice of a different generation of reactor technologies. The fleet of LWRs uses a ceramic uranium-oxide fuel that is enriched to 3-5% $^{235}$U, but there is a panoply of advanced reactor designs at various stages of deployment using decades of experience with creating nuclear energy. These reactors vary in size from large gigawatt-scale reactors to smaller reactors designed to fit on the back of a truck. The design space is vast, but one innovation that has been a focus of the nuclear industry is the TRi-structural ISOtropic (TRISO) fuel particle. This fuel particle is a small sphere of uranium fuel coated in carbon and silicon carbide layers. TRISO is designed to be more robust than traditional fuel and to be used in various reactor designs that require high-assay low-enriched uranium (HALEU) (5-20%).

The nuclear fuel cycle (NFC) describes the steps nuclear fuel goes through in its life cycle. In Figure 1.2, we have outlined a simple *once-through* fuel cycle (so-called because the fuel goes through the cycle once in its lifetime). The fuel cycle begins with mining uranium ore, typically from uraninite or pitchblende deposits. Then, the ore must be milled and refined into yellowcake, which can then be converted into uranium hexafluoride. To power the reactors in the U.S., the uranium hexafluoride is then enriched to the desired percentage of $^{235}$U and converted into uranium dioxide. Reactor operators receive the fuel in rods after it has been fabricated into fuel pellets from uranium dioxide. Upon receiving the fuel, workers load the rods into the reactor to generate heat. The heat generates steam, which drives a turbine and generates electricity. After years of operation, workers remove the used fuel from the reactor and store it in a spent fuel pool. After cooling, transporters move the used fuel to dry cask storage, where it will remain until policymakers act to enable a long-term solution.

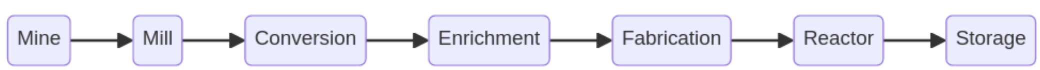


Figure 1.2: US once-through fuel cycle.

Although we have linearly presented them, these steps are interwoven with multilateral relationships and long-term purchasing agreements that complicate the establishment of new supply chains. Consequently, the availability of services at each step in the fuel cycle is difficult to model; this is where we use the CYCLUS [22] tool. CYCLUS is a nuclear fuel cycle simulator that allows users to model the material movement between facilities in discrete-event simulations. These facilities are run by agents that make decisions and interact with other agents. Because CYCLUS is designed to be technology agnostic, we can use it to model a variety of fuel cycles and reactor types–although it is not primarily a physics engine, so coupling it with physics software can be necessary for some problems.

Partners in industry, academia, and government are building the body of literature surrounding TRISO fuel cycles. This thesis is a timely evaluation of various energy-demand scenarios and an optimization of the deployment of advanced reactors building off of the method established by Bachmann et al. [4] for HALEU fuel, incorporating a phased enrichment demand that advanced reactor companies could explore as the HALEU supply chain develops. This thesis seeks to understand the potential for advanced reactor deployment in the U.S. and the implications of the fuel cycle on the deployment of these reactors, as some designs adopt a staggered enrichment demand for various TRISO fuels. We have chosen to focus on separative work units (SWU), energy output, mass of fuel, and reactor deployment to understand the performance of each deployment scenario. In service of this goal, this thesis will also examine the computational efficiency of the Dynamic Resource Exchange (DRE) in CYCLUS to contribute to a robust tool for future analysis.

The structure of this thesis is as follows:

- Chapter 2 outlines energy system modeling, the reactors investigated in this work, the types of fuel, and the CYCLUS tool as it pertains to this work.
- Chapter 3 discusses the deployment schemes analyzed in this work, the metrics used to evaluate the scenarios, and presents the results of each.
- Chapter 4 outlines two reactor archetypes developed in this work, and compares them to the CYCAMORE reactor.
- Chapter 5 concludes the work in Chapters 3 and 4, discusses the assumptions and limitations, and presents directions for future work.
- Appendix A shows the details for each reactor in what we call the "existing fleet" in this work.
- Appendix B discusses the implemented reactor deployment schemes that were not used in this work.
- Appendix C discusses the availability and reproducibility of this work.

# Chapter 2

# Background

The United States contributed over 12.5% of total global carbon emissions in 2020 [12]. Local, state, and national governmental bodies have announced myriad programs to support clean energy projects in response to growing climate concerns; however, when you add lenses of environmental justice and life cycle analysis, these transitions might result in displacement instead. In 2012, Richard York from the Oregon State Department of Sociology and Environmental Studies published a study of the 50-year history of alternative-energy installations to the modern grid asserting that "to displace 1 kWh of fossil-fuel electricity requires generating more than 11 kWh of non-fossil-fuel electricity," [65]. This conversion was based on six models of fossil fuel use from 1960-2009, accounting for levels of urbanization, manufacturing, age, and a variety of energy technologies.

This result challenges the assumption that energy facilities with comparable power have a one-to-one relationship. In 2019, York and co-author Shannon Bell further developed this idea by saying that such proportional representation studies "do not focus their discussions on or graphically present the absolute quantity of energy in their assessments of purported energy transitions" [66]. They demonstrate in Figure 2.1 that the proportional representation misses how the total demand for energy has dramatically increased since the Industrial Revolution. What may have looked like a transition in the mid-1800s from biofuels to coal is merely a displacement, and they show that the energy consumption of biofuel has increased since the early 1900s.

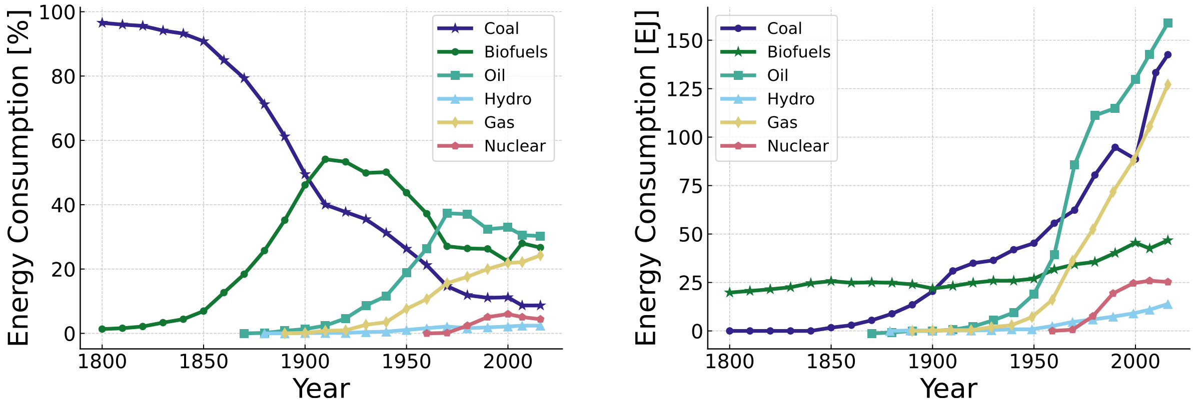


(a) Proportional Energy Use.

(b) Total Energy Use.

Figure 2.1: Global energy consumption (exajoules) by source from 1800–2017. Reproduced from [66].

Similarly, what looks in Figure 2.1a like a transition away from coal in the early 1900s, with the introduction of alternatives like oil and hydroelectricity, belies the continued increase in coal consumption into the early 2000s. If what we have axiomatically understood as a transition is not happening, we arrive at the kernel of several grand challenges to society and elected officials. The semantic difference between a transition and a displacement is not the core concern; instead, we must focus on realistically presenting the increasing energy needs of society.

The policy inertia behind the monetary valuation of energy system is something that future generations could overcome, upending the incentives policymakers might implement to drive an actual transition instead of a displacement, as we have discussed. If decision-makers focus on what a policy will do only for the term of their service, they drastically undervalue the impact that daily climate actions will have hundreds of years down the line. We see this dichotomy in the 2020 grid failings in Texas during the unseasonably cold front they experienced. From the outside, we can see how an extreme weather event would create a great demand. This case is a microcosm of a drastic change in a society's values for an energy grid. In a couple of weeks, a state that had praised its sustained grid [52] experienced massive failures only for its service to resume.

Since 2020, the Electric Reliability Council of Texas (ERCOT) has been working to update its grid to be more resilient to such events. The Grid Deployment Office of the U.S. Department of Energy (DOE) published a report in 2024 outlining $270 billion in savings that resulted from increasing connections to the Texas Interconnection [57]. Concurrent with this announcement, the DOE announced a $1.5 billion transmission investment that would go to four projects in Texas, New Mexico, Louisiana, Mississippi, Maine, Oklahoma, and Arizona [56]. These projects are expected to be completed by 2026 and will increase the grid capacity by 1.5 GW. This is a step in the right direction, but it is not enough to ensure that the grid will be resilient to future extreme weather events.

We can legislate for such changes by developing policy frameworks that bring in the community and address changing values for energy systems. Elisa Papadis and George Tsatsaronis set out to update the vision for a well-designed policy package in their 2020 paper, surmising that "carefully introduced targeted investment subsidies, performance standards and mandates, communication and education campaigns and a $CO_2$ tax for global aviation and shipping" constitutes achieving this legislative framework [38]. This approach will require geographically bespoke solutions that draw in stakeholders to focus on serving the needs of the future. They advocate for expansion and maintenance investments in the complex United States (U.S.) power grid to accommodate flexibly generated capacity.

Flexibility is a ubiquitous goal of decarbonizing industries, like chemical producers, which highlight big emitters that are large volume/ low-profit goods (disincentivizing development) [31], or farm researchers who highlight the growing importance of human intervention as climate change impacts their crop in a negative feedback cycle [14]. Focusing efforts where investment can have the largest impact in the shortest time and consulting the changing valuation of stakeholders in how modifications to the grid are carried out would further this goal of flexibility.

## 2.1 Energy System Modeling

Nations such as the U.S. and the United Kingdom (UK) centralized their electrical infrastructure as it developed, stemming from an attitude that Dieter Helm from the University of Oxford describes as prevailing until the end of the 1970s [19]. Due to the heavy state involvement, energy planning is a concept that has existed for many decades. Evidence of contemporary planning can be found as far back as 1967 in nationalized industry reports from the UK [53] and was a top-of-mind consideration in the U.S. and other countries.

In 1973, Michael Posner from the University of Cambridge published his book *Fuel Policy A Study In Applied Economics* [41], which describes methods large institutions could use to make energy decisions. In connection with the 1973 oil crisis, this book was a wake-up call for many countries to enhance their predictive capabilities for energy markets. The crisis led to the development of energy planning models that could be used to evaluate the impact of different policies on energy systems as disruptions tend to do [40]. The International Institute for Applied Systems Analysis (IIASA), founded in 1972, and the International Energy Agency (IEA), founded in 1974, have served international communities with Energy System Model (ESM) tools since the oil crisis. The resulting models were used to develop long-term energy plans to help countries increase their energy security, facilitate economic development, and better legislate with increasingly complex energy systems.

Today, utilities, countries, and other organizations use ESMs to model the behavior of energy systems in different economic contexts, such as the cost of energy, the price of carbon, and the availability of financing. These contexts can focus on developing favorable conditions for new technologies, understanding the relationship between actors, predicting future trends, and the impact of different policies on energy systems. Decision-makers compare the behavior of energy systems in various scenarios to a baseline, such as business-as-usual scenarios compared with low-carbon or high-renewable scenarios. These are effective across regulated, competitive, and hybrid markets. As ESMs have evolved, they have become more sophisticated. Now, they can model the behavior of energy systems in different social contexts, such as the adoption of energy efficiency measures, the acceptance of energy technologies, and the resistance to new energy projects. The Osier tool [9] is a framework for multi-objective optimization over traditional cost constraints that incorporates public preferences and user-defined parameters.

Pfenninger et al. [39] describe four paradigms of energy system modeling: optimization, simulation, econometric, and hybrid models. In the optimization paradigm, the modeler seeks a normative solution to a problem by minimizing or maximizing an objective function subject to constraints. In the simulation paradigm, the modeler aims to predict the behavior of the energy system by simulating the interactions between different system components. In the econometric, or market, paradigm, the modeler seeks to understand the relationship between different operational variables in the energy system by estimating the parameters of a statistical model. The hybrid paradigm is a catch-all for narrative scenarios that combine the paradigms to develop a more comprehensive understanding of the energy system.

Although there are myriad paradigms of ESM, two philosophies (top-down and bottom-up) to their construction dictate the restrictions a model will place on the type of questions it can answer. In the top-down approach, the modeler starts with a high-level view of the energy system and then drills into the details. This approach aids in understanding the overall behavior of the energy system and the impact of different policies on the system [27]. In the bottom-up approach, the modeler starts with the details of the energy system and then builds up to a high-level view. This approach is useful for understanding the behavior of individual components of the energy system and the impact of different technologies on the system [20, 27].

## 2.2 The Nuclear Fuel Cycle

Starting with President Eisenhower's Atoms for Peace speech in 1953 [11], the international community has been working toward the peaceful use of nuclear energy while reducing proliferation routes. Nuclear safeguards were formally introduced with the creation of the International Atomic Energy Agency (IAEA) in 1957, which conducts inspections and verifies compliance with safeguards agreements and supports states building facilities to meet its standards [24]. Compliance is verified through regular inspections, data analysis, and cooperation between the IAEA and member states. Countries must declare their nuclear activities, and inspectors perform unannounced visits to nuclear facilities to ensure compliance. As of November 2024, the IAEA has 180 member states, with the addition of the Cook Islands and Somalia.

The nuclear fuel cycle (NFC) spans various IAEA members and is a series of industrial processes that produce and consume fuel. Here, we present a high-level overview to establish the context for this thesis with modeling the fuel cycle in later chapters. Commonly, these processes are grouped into two categories (the front end and back end). In the U.S., we keep these facilities separate, in the front end of the fuel cycle, in a "collect and wait" pathway [21]. Without a long-term or interim solution for the Used Nuclear Fuel (UNF), the back end of the nuclear fuel cycle (NFC) is collocated with the reactors that burn the fuel (with the minor exception of the consolidated storage facility in Morris, Illinois). This thesis will restrict discussion of the fuel cycle to fuel alone, although some work has been done to consider byproducts and non-fuel wastes in related work in this field.

Companies can reprocess and recycle nuclear fuel into a different fuel type that can produce usable power for several cycles, called a "closed" fuel cycle. As outlined in Figure 1.2, the "open" fuel cycle is a one-time use of fuel that is then stored in a repository. The closed fuel cycle is a more sustainable option, as it reduces the amount of waste stored in a repository by adding an extra step for reprocessing and recycling the used fuel into new fuel–as shown in Figure 2.2. However, a closed fuel cycle is currently more expensive and may pose proliferation risks associated with reprocessing fuel. The open fuel cycle is less costly and has fewer proliferation risks, but it produces more waste that must be stored in a repository. The choice between an open and closed fuel cycle is a policy decision for the country using nuclear technology.

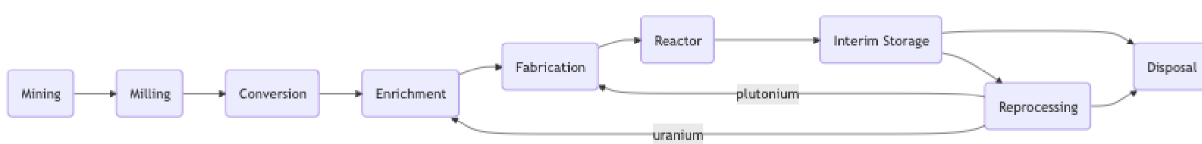


Figure 2.2: Hypothetical closed fuel cycle.

### 2.2.1 Front End of the Fuel Cycle

At the time of writing, the Nuclear Energy Agency (NEA) and IAEA have not released their 2024 *Red Book*. We will extrapolate trends from the 2022 *Red Book* report on global Uranium availability, which covers January 2019 to January 2021 and updates the projections from 54 countries of their uranium supply and resources through 2040 [32].

Globally, Australia holds the most significant reasonably assured resources of uranium at roughly 28% of the world's total. However, total identified recoverable resources declined 2% from 2019 to 2021–in contrast with slight increases reported in previous versions of the report–as countries increased mining efforts, reclassified economic viability of inferred resources, and currency values fluctuated with inflation. Among the most well-established uranium exporters like Australia, Canada, and Kazakhstan re-evaluations of inferred resources accounted for decreases in nearly every quality category, while relatively new exporters, Mongolia and Niger, reported increases in inferred resources [32]. This thesis focuses on the U.S. explicitly and does not incorporate geospatial information.

The U.S. imports more uranium than it produces domestically, as shown in Figure 2.3, from countries with large uranium deposits like Canada, Australia, and Kazakhstan. This trend is expected to continue as the U.S. has only recently begun to invest in new uranium mines since the 1980s.

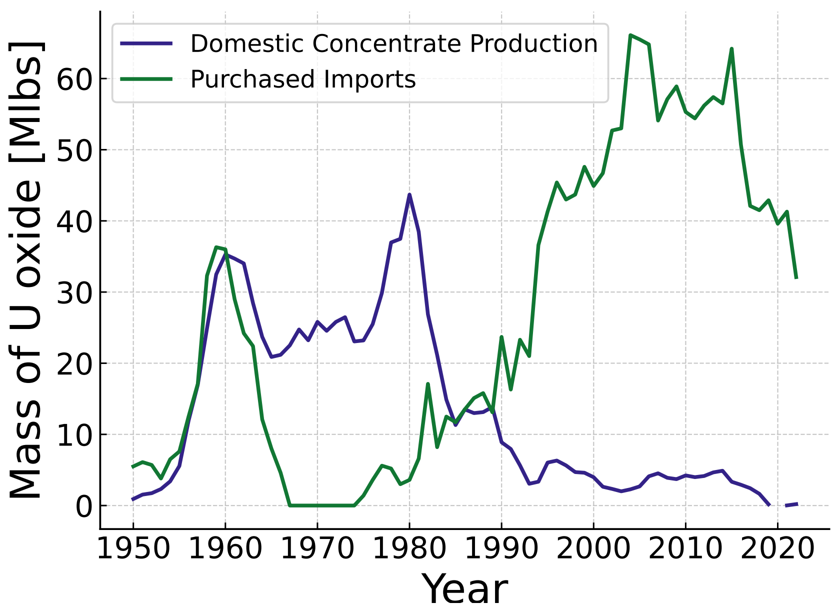


Figure 2.3: Foreign and domestic uranium purchases over time. Reproduced from [60].

As the 2022 *Red Book* notes, the literature surrounding the understanding of best practices for environmental stewardship and remediation of mines is growing. Once-common practices of strip, pit, and underground mining are beginning to be replaced with more sustainable practices that minimize the environmental impact of mining. One method that has garnered interest in the uranium mining community is in-situ leaching, wherein automatic pumps inject a leaching solution into the ground to dissolve the uranium and then pump the solution to the surface for processing [28]. The paradigm shift in uranium mining is from a focus on burial depth to a focus on geological properties. In-situ leaching is limited to areas with favorable permeabilities, but the reduced labor intensity, simplified infrastructure requirements, and lower environmental impact make it an attractive option for uranium mining where applicable.

In-situ leaching also reduces the extent of the milling process as the ratio of desirable material to non-desirable material is higher in the leaching solution than in the resultant material from traditional mining. The milling process generally involves crushing the ore into a fine powder and then leaching the uranium from the ore with a sulfuric acid solution. Workers then extract the uranium from the solution and convert it into yellowcake ($U_3O_8$), a concentrated form of uranium oxide [7]. The yellowcake is then shipped to a conversion facility, where it is converted into uranium hexafluoride ($UF_6$), a gas that cools to a liquid and then a solid before it is transported to be enriched. Uranium hexafluoride is attractive in the enrichment process because fluorine has only one naturally occurring isotope and is easy to ensure isolation from the uranium.

Up to the enrichment stage of the fuel cycle, we have described a process almost entirely agnostic to the end use of the uranium fuel. Leaving the conversion stage of the fuel cycle is a colorless, volatile, and radioactive solid material. Next, the enrichment process aims to achieve a specific concentration or weight percent of $^{235}$U relative to the other uranium isotopes. Today, enrichment relies on centrifuges, which separate the isotopes based on their mass; however, historical gaseous diffusion technology could potentially use laser enrichment if it becomes economically viable. This thesis does not distinguish between enrichment services; instead, using separative work units (SWU), which we will expand on in Section 3.2.1, to quantify the enrichment delivered.

The enriched $UF_6$ is then converted into uranium dioxide ($UO_2$) and fabricated into fuel. For the U.S. fleet of large Light Water Reactors (LWRs), the fuel is made into pellets, stacked into rods, and collected into assemblies. This is not the case for every reactor design, as some reactors use prismatic, pebble, or liquid fuel elements. As with enrichment, the fabrication stage of the fuel cycle is simplified in this work, and we do not incorporate explicit details of the fabrication process.

### 2.2.2 Reactor Operation

Up to now, everything we have laid out is part of the front end of the fuel cycle. The part of the NFC where the fuel is used in the reactor is neither at the front nor back of the fuel cycle. As such, we have created a separate section for it despite the comparatively small amount of processes we outline here. Inside the reactor core, the fuel generates heat through fission, which produces steam, thereby driving a turbine to generate electricity. The fuel remains in the reactor for several years, depending on the reactor design and fuel enrichment.

### 2.2.3 Back-End of the Fuel Cycle

After the fuel has been in the reactor for several years, it is removed and stored in a spent fuel pool. After cooling, the fuel is moved to dry cask storage, where it will remain until a long-term solution is implemented. As this thesis does not focus on closed-fuel cycles, we do not consider fuel reprocessing in this description of the NFC.

When considering a long-term repository for the used fuel, we must consider the macroscopic and microscopic effects of the environment on the repository. On a macroscopic level, climate change will drive shorelines to move, permafrost to recede, and congenital ice sheets to melt. Translating these well-known effects into chemical consequences that dictate the design of a repository will require site-specific adaptations on several fronts. Special attention must be given to the impact in the first few thousand years, as this period will exhibit the highest activity. In the case of meltwater exposure, water saturated with dissolved $O_2$ could infiltrate a repository, potentially altering the oxidizing conditions [18]. Consequently, regulators considering the 100,000-year perspective of a potential repository must account for proximity to such meltwater sources to meet the demands imposed by a changing climate.

Sites experiencing reducing conditions may continue to do so; however, the changing climate will also influence the salinity of groundwater. Changes in salinity affect density, which could either exacerbate or mitigate the spread of contaminants in the event of exposure outside the repository [18]. This change in salinity also has the potential to interact differently with canisters, necessitating that proactive regulators ensure containment is designed to withstand a changing environment over the repository's lifetime.

An additional layer of microscopic consideration for these regulatory concerns is the imminent deployment of new nuclear fuels with different compositions and forms. Some fuels are designed with pyrolytic carbon matrices that can immobilize decay products for much longer than current fuel forms. As new fuel technologies are deployed, NFC facilities will adapt accordingly. These changes, although seemingly slight (the fuel will likely still be uranium-based), can have significant consequences over 100,000 years of storage [23].

## 2.3 LEU Plus (LEU+)

In 2020, a high-assay low-enriched uranium (HALEU) workshop report led by Monica Regalbuto [43] highlighted the unique regulatory challenges of establishing a HALEU fuel cycle in the U.S.. It noted that part of enriching HALEU is first to produce low-enriched uranium plus (LEU+), defined as between 5% and 10% $^{235}U$ enrichment. The report notes that LEU+ facilities would fall under a similar category of regulations as the existing low-enriched uranium (LEU) fuel cycle, allowing existing enrichment servicers to leverage their experience and infrastructure before taking on the increased regulatory burden of producing HALEU. If a reactor could be redesigned to accommodate it, using LEU+ could delay the demand for HALEU. Table 2.1 shows the various levels of enrichment for uranium that we will use in this thesis.

Table 2.1: Enrichment levels and their ranges.

| **Enrichment Level** | **Range [% $^{235}$U]** |
|---|---|
| Natural | < 0.711 |
| LEU | 0.711-5 |
| LEU+ | 5-10 |
| HALEU | 10-20 |
| high-enriched uranium (HEU) | ≥ 20 |

One of the primary advantages of a fuel cycle containing LEU+ is that the facility to produce it would fall under the same licensing category as LEU fuel. The U.S. Nuclear Regulatory Commission (NRC) defines a *special nuclear material of low strategic significance* as meeting one of three criteria, the most notable of which for our purposes is "(3) 10,000 grams or more of uranium-235 (contained in uranium enriched above natural but less than 10 percent in the U–235 isotope)," [35]. This facility definition is where the upper limit of the LEU+ range arises.

To enrich to HALEU, facilities such as TRISO-X LLC and Kairos Power Atlas Fuel Fabrication Facility must increase to *special nuclear material of moderate strategic significance* (Category II). Thus, LEU+ is an attractive intermediary step for servicers wishing to minimize the size of a Category II facility (thereby reducing costs) as it is the same category we have historically licensed for LEU fuel enrichment.

Traditional LWRs could receive benefits from using LEU+ fuel; as outlined by López-Luna et al. [30], incorporating such fuel rods would allow for a 24-month cycle in the Boiling Water Reactor (BWR) design they studied and would reduce the levelized cost of the nuclear fuel cycle they simulated. In October 2024, Framatome announced that their 6 wt% $^{235}$U GAIA fuel assemblies completed their third 18-month fuel cycle at the Vogtle plant in Georgia [16], with the eventual goal of this process being commercialization of new accident-tolerant fuels that can potentially support LEU+. The growing body of work indicates that LEU+ fuels could suit various nuclear technologies; however, the fuel does not exist in a vacuum.

Increased prevalence of higher enrichment fuels will require modifications to the existing supply chain, particularly to ensure the continued safety of workers and the public. A 2022 report from Shaw and Clarity out of Oak Ridge National Laboratory (ORNL) highlighted that existing nuclear fuel vault configurations at BWRs and Pressurized Water Reactors (PWRs) did not have sufficient margins to satisfy regulatory requirements when fully flooded [50]. Their report only studied the impacts of 6.5 wt% and 8 wt% fuel, but they concluded that HALEU fuel would similarly require significant changes to existing fuel storage infrastructure.

## 2.4 TRISO Fuel

This thesis adapts the approach of Bachmann et al. [4] to focus on TRi-structural ISOtropic (TRISO) fueled reactor designs alongside traditional fuel forms at various enrichments. TRISO is not a classification of enrichment; several reactor designs use different fuel enrichments that are all TRISO. Here, we will distinguish the production of TRISO from the traditional metallic fuels used in LWRs outlined in Section 2.2.

Coating the fuel particles is a critical step in the fabrication of TRISO fuel, and the idea has existed in nuclear fuel design spaces since the 1950s [42] with the Dragon project. In 1957, the Harwell facility began coating spherical fuel particles, and in 1961, researchers modified the particle coating to include a silicon carbide layer to trap cesium, strontium, and barium–which diffused through the single pyrolytic carbon layer. Concurrently, in 1958, a report to the Atomic Energy Commission (AEC) introduced the concept of a pebble bed pile (first proposed by Daniels [13]) to the broader nuclear community. Researchers in Germany, China, and the UK have proposed, built, and operated similar designs since then, with companies in the U.S. looking to deploy modern versions of the technology.

In a 2019 paper, authors Demkowicz, Liu, and Hunn [8] authors describe the fuel as a particle encapsulated in layers of pyrolytic carbon and silicon carbide; a fluidized-bed chemical vapor deposition system (FB-CVD) applies each of these layers. As shown in Figure 2.4, the layers are frequently ordered with a fuel kernel at the center, followed by layers of porous carbon buffer, inner pyrolytic carbon, silicon carbide, and outer pyrolytic carbon. The fuel kernel is typically composed of uranium dioxide, and it is surrounded by a porous carbon buffer using acetylene in the FB-CVD as it has a relatively low density. The silicon carbide layer encapsulates the pyrolytic carbon layers and provides a barrier to fission products. A mix of methyltrichlorosilane and hydrogen is sufficient for SiC deposition without argon. The inner and outer pyrolytic carbon layers isolate the silicon carbide layer and provide a barrier to the coolant; the FB-CVD applies these layers using a mix of propylene, acetylene, and argon.

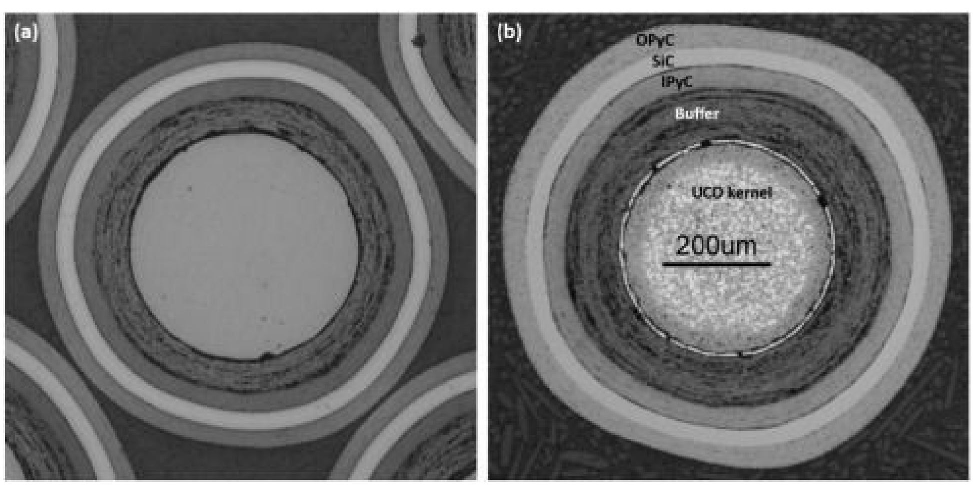


Figure 2.4: TRISO fuel particle layers [8].

Through a heat and pressure setting process, fabricators create a graphite matrix that accepts the coated particles. The resulting fuel type is incredibly robust and can reduce proliferation concerns due to the difficulty of separating the particles from the matrix and the fuel from the particles. The fuel can withstand high temperatures and burnups, which can be advantageous in reactor designs that require high temperatures for efficient operation.

## 2.5 Reactor Models

This thesis explores various transition scenarios for the deployment in the U.S. of the: 1) X-Energy Xe-100 (Xe-100) High-Temperature Gas-cooled Reactor (HTGR); 2) Ultra Safe Nuclear Corporation (USNC) Micro Modular Reactor (MMR) HTGR; and 3) and Westinghouse AP1000 PWR using proxy reactors. To accommodate the assumption that the HALEU-fueled TRISO reactors will first accept LEU+ fuel, we have adapted Bachmann's MMR-like Serpent model [2] and Richter's Xe-100-like Serpent model [46] to accept LEU+ fuel. These reactor models are constructed from publicly available data to approximate their aggregate behavior.

Table 2.2 shows the design specifications for the advanced reactors in this thesis. The MMR and Xe-100 reactors are HTGRs that use TRISO fuel, while the AP1000 is a PWR that uses $UO_2$ fuel. We have listed the enrichment for both the LEU+ and HALEU versions of the fuel accepted by the MMR and Xe-100, respectively, as the only distinguishing variable between the two versions of the reactors. The cycle length, discharge burnup, and reactor lifetime are the same for both versions of the reactors. The AP1000 is assumed to use LEU fuel throughout the simulation.

Table 2.2: Advanced reactor design specifications.

| **Design Criterion** | **MMR-Like** [54] | **Xe-100-Like** [37] | **AP1000** |
|---|---|---|---|
| Reactor type | HTGR | HTGR | PWR |
| Power Output [MWe] | 15 | 100 | 1000 |
| Fuel Type | TRISO | TRISO | $UO_2$ |
| Enrichment [% $^{235}$U] | 9.95, 19.75 | 9.95, 15.5 | 5 |
| Cycle Length | 20 [yrs] | Online Refuel | 18 [months] |
| Discharge Burnup [GWd/MTU] | 82 | 168 | 65 |
| Reactor Lifetime [yrs] | 20 | 60 | 60 |

In the following subsections, we will discuss the reactors in greater detail. One limitation of these models is the approximation that the LEU+-fueled reactors achieve the same burnup and power level as the HALEU-fueled version. This assumption is not necessarily valid, and we will explore the implications of this assumption in future work. However, we expect that the limited deployment of LEU+ fuel allows discrepancies to be well understood.

### 2.5.1 MMR-like Reactor

The future of the once-active partnership between the University of Illinois Urbana-Champaign (UIUC) and USNC to deploy their MMR is uncertain to those not on the project; however, they reached the pre-licensing phase with the NRC and were planning on commencing operation of an on-campus reactor in the 2030s. The USNC MMR is an HTGR that uses TRISO fuel, has an electrical output of 15 $MW_e$, and a cycle length of 20 years. The fuel is enriched to 9.95% $^{235}U$ for LEU+ and 19.75% for HALEU. As modeled, both have a discharge burnup of 82 GWd/MTU, which coincides with the 20-year lifetime of the reactor. In this thesis, the MMR is based on the model developed by Bachmann et al. [2] and is implemented here as-is for the HALEU version of the reactor, while the LEU+ version is adapted from the HALEU version.

Figure 2.5 shows a rendering of the MMR core and reactor vessel. As indicated by the figure, the design is intended to be underground, with an estimated total reactor footprint less than 5 acres. The primary coolant is helium gas, which heats up in the core and deposits its heat in a heat exchanger to generate electricity to the side of the reactor [17]. Helium is transparent to many nuclear interactions and is inert, making it an attractive choice for a coolant.

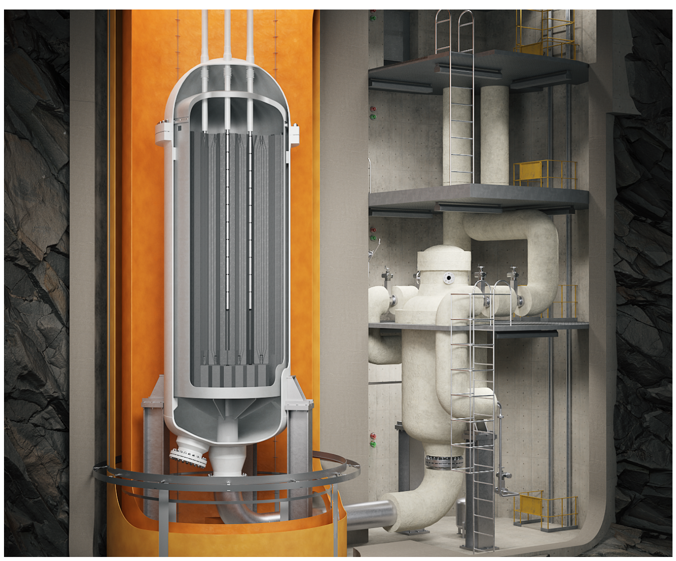

Figure 2.5: USNC MMR design [54].

The proposed deployment of this reactor concept includes an operational *MMR Energy System* consisting of two plants: the *Nuclear Plant* and the *Adjacent Plant*. The *Nuclear Plant* contains multiple MMR units, including all the equipment required to transport the heat to the *Adjacent Plant*. The *Adjacent Plant* consists of the equipment that converts heat to electricity or process heat as needed. The *MMR Energy System* will theoretically store up to

10 hours of power plant thermal output and can be supplemented with hydrogen burners. Auxiliary molten salt thermal storage allows for a flexible electricity and process heat supply.

Electricity and heat would be delivered on demand from the power plant while the MMR unit operates at constant power. The MMR's high-temperature heat has many uses beyond the generation of electricity. District heating, desalination, and chemical or industrial heat highlight the broader point of how fourth generation (GENIV) nuclear reactors are not solely intended for electricity generation as with the current domestic fleet. An MMR could deliver steam temperatures of 660 °C, and they estimate that temperatures up to 950 °C could be possible in future MMR variants [54].

The fuel for this reactor is inspired by the TRISO fuel developed in the 1960s and 1970s. A small sphere of uranium fuel is coated in carbon and silicon carbide layers. As shown in Figure 2.6, the fuel is composed of kernels arranged into a larger fuel pellet. They call their fuel form Fully Ceramic Microencapsulated (FCM) fuel. They additively manufacture each element, allowing for a high packing fraction of fuel, which means their fuel could be adapted to other reactor designs.

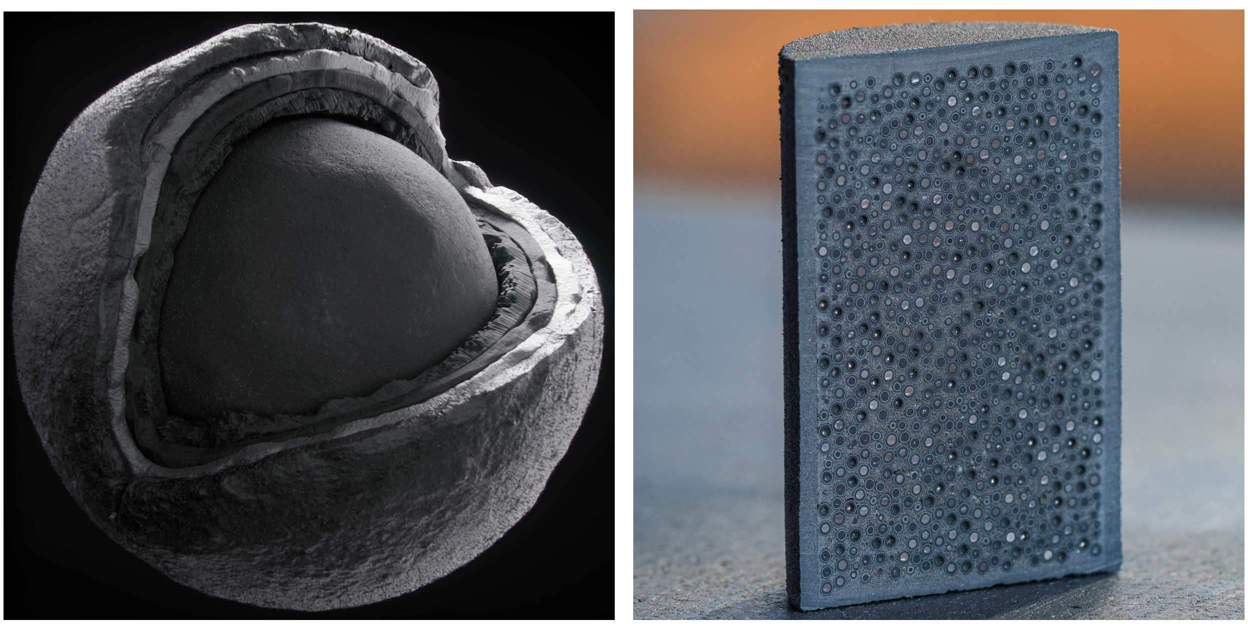

(a) Fuel element layers. (b) Fuel pellet profile.

Figure 2.6: USNC MMR fuel renderings [55].

Figure 2.7 shows a top-down and side view of the MMR Serpent model [2] that we have modified in fuel composition alone. As Bachmann describes [3], the radius of the fuel channel is based on the publicly available size of the FCM pellets (1.15 cm), and the coolant channel has an arbitrarily chosen radius of 3 cm. The entire core is assumed to be in an isothermal state at 800 K. There is a 20 cm thick graphite reflector above and below the stacks of graphite and a 10 cm thick beryllium-oxide reflector on the outside of the graphite blocks of the core, illustrated by the green material in Figure 2.7. The model does not contain control rods or burnable poisons, so the control rod tubes are filled with helium. Five layers of graphite fuel blocks are stacked to form the entire core to approximate the number of fuel blocks described in the publicly available data [54]. The fuel does not move through the core, as the model is designed to use the same fuel for the entire reactor lifetime.

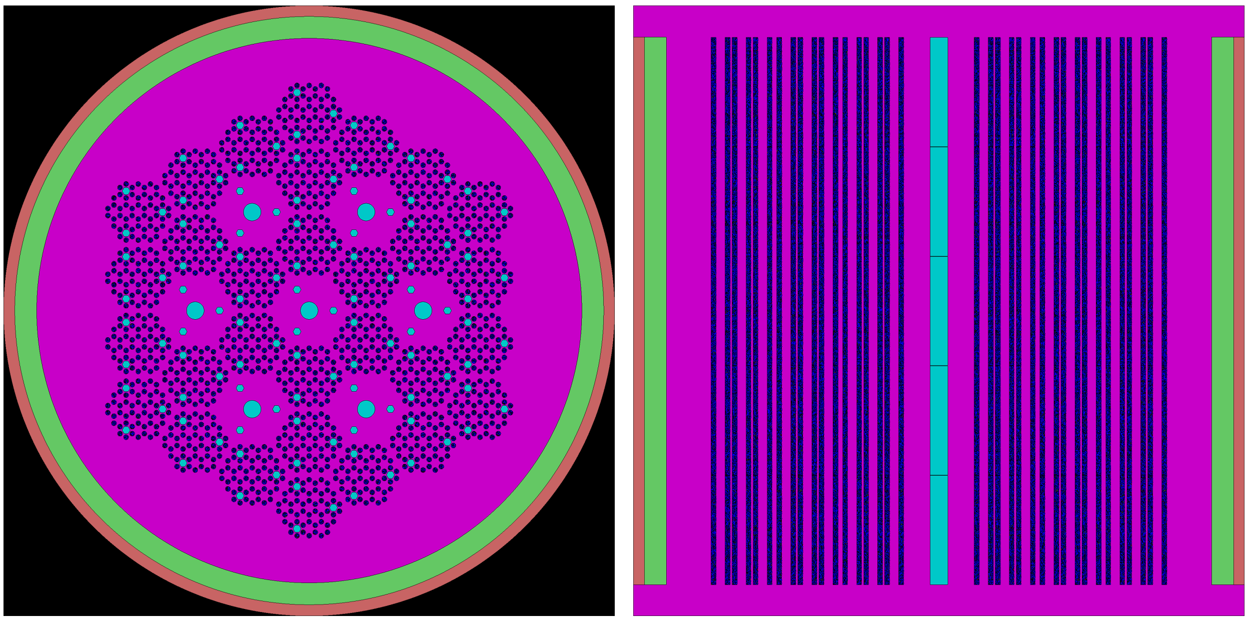

(a) Top-down core view.

(b) Full core side profile.

Figure 2.7: Serpent model of the USNC MMR core.

### 2.5.2 Xe-100-like Reactor

X-Energy has entered into a cooperative agreement with DOE to deploy their Xe-100, is in the pre-licensing phase with the NRC for projects in Texas and Washington, and is expected to be operational in the 2030s. There are similar projects in the early stages in Canada and the UK. The X-Energy Xe-100 is an HTGR that uses TRISO fuel and is expected to operate for 60 years. The reactor has an electical output of 100 MW and uses online refueling. The fuel is enriched to 9.95% $^{235}$U for LEU+ and 15.5% $^{235}$U for HALEU and a discharge burnup of 168 GWd/MTU. The reactor in this thesis is an approximation based on publicly available data and is not based on confidential or proprietary information. The model was developed by Richter et al. [46] and is implemented herein as-is for the HALEU-fueled reactor, while the LEU+ version has a modified fuel composition.

Figure 2.8 shows a rendering of the Xe-100 core and reactor vessel. The Xe-100 reactor is designed to be a small modular reactor that can be deployed in various locations and will be gas-cooled. This design differs from the MMR as the reactor features online refueling due to its pebble-bed nature.

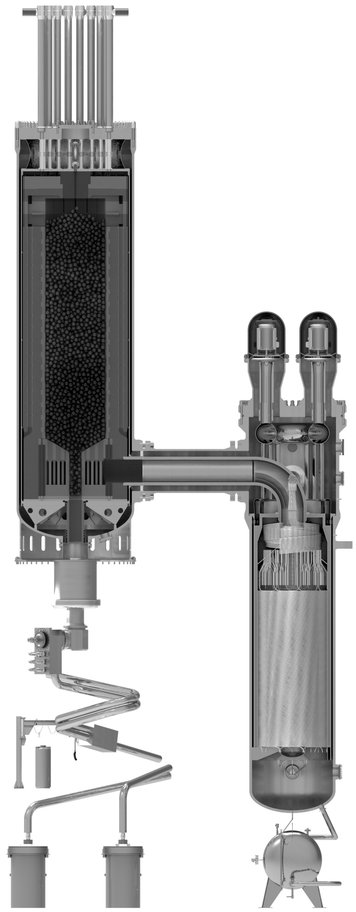

Figure 2.8: X-Energy Xe-100 rendition [63].

Unlike the MMR's annular fuel elements, the Xe-100 pebbles are composed of a graphite matrix that contains the TRISO fuel particles. These TRISO particles are similar to those in the MMR, as shown in Figure 2.9.

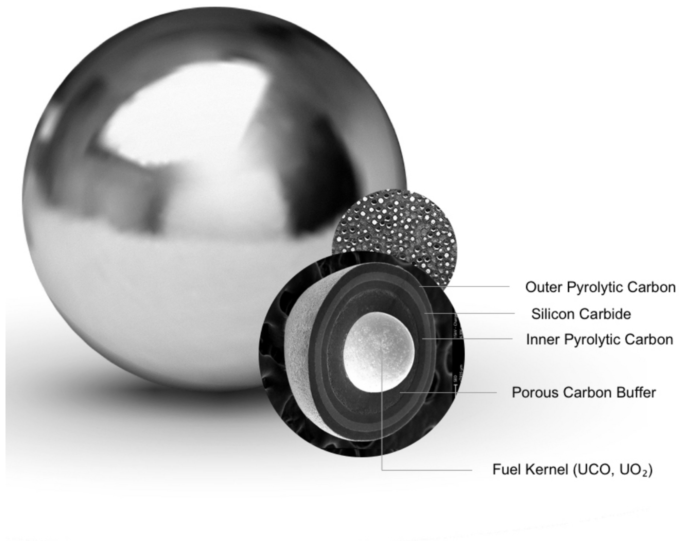


Figure 2.9: X-Energy Xe-100 fuel pebble [62].

We have modified the fuel composition of Richter's Xe-100-like reactor model to accept LEU+ fuel. The LEU+ fuel is assumed to have the same burnup and power level as the HALEU fuel. This assumption is not necessarily valid, and we will explore the implications of this assumption in future work. Due to the limited deployment of LEU+ fuel, the discrepancies are minimal. Figure 2.10 shows the top-down view of the LEU+ Xe-100 core as the HALEU version has been established by Richter [45], and they are visually similar.

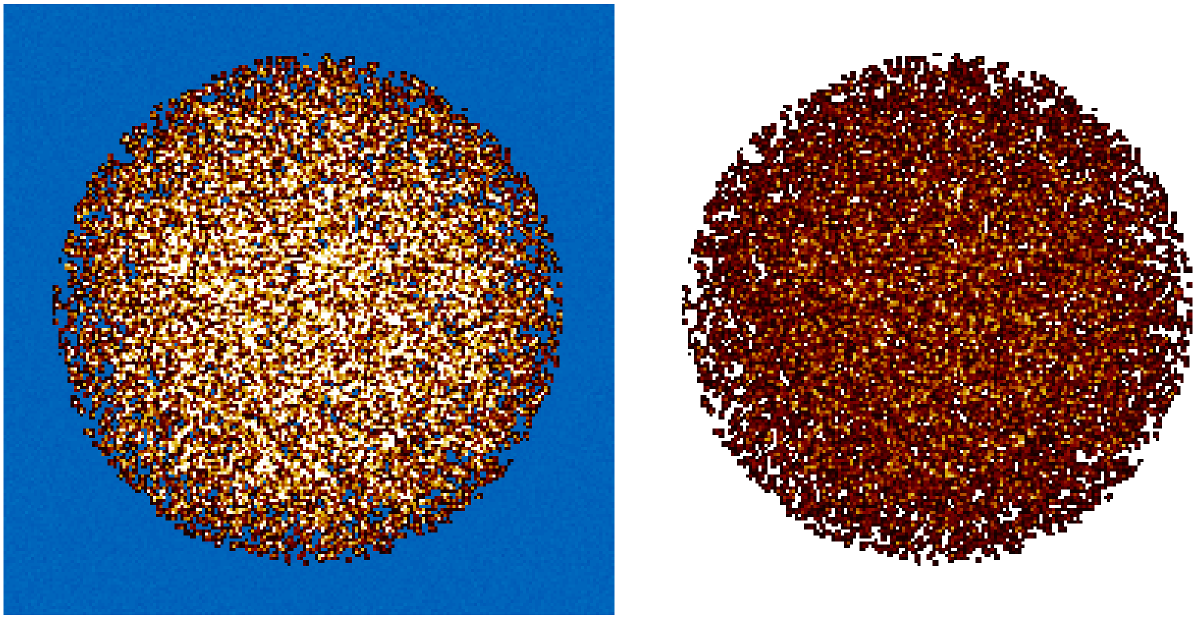

(a) Initial core.

(b) Final core.

Figure 2.10: Top-down view of the X-Energy Xe-100 core model.

Comparing Figures 2.10a and 2.10b, we can see visual differences in the shading of the pebbles. The pebbles are shaded based on the burnup of the fuel, with darker pebbles indicating higher burnup. The pebbles are inserted into the core at the top, and gravity pulls them down through the core. After a brief holding time outside the core, the pebbles are reinserted at the top of the core. This process is repeated until the pebbles reach their targeted number of passes, at which point they are removed from the core and stored.

### 2.5.3 AP1000 Reactor

AP1000s are operational in the U.S. and China, and the UK and India plan to deploy more. The Westinghouse AP1000 is a PWR that uses $UO_2$ fuel. The reactor has an electrical output of 1000 MW, a cycle length of 18 months, and an expected lifetime of 60 years. The fuel is enriched to 5% $^{235}U$ and has a discharge burnup of 65 GWd/MTU. The reactor in this work is an approximation based on publicly available data and is not based on confidential or proprietary information. As this work does not anticipate LEU+ being used in the AP1000, there is no such neutronics model of the reactor, and we have adapted the generic CYCAMORE reactor archetype to represent the AP1000 in the same way we represent the existing LWR fleet.

## 2.6 CYCLUS

CYCLUS [22] is an agent-based NFC simulator that is versatile, open-source, and modular. The software achieves this versatility through a series of generic archetypes that are primarily transaction-based. Over the years, the user community and developers have created a litany of nuclear-facility archetypes for everything from proliferation assessment to fuel burnup. Many standard fuel cycle facility archetypes have been implemented in the CYCAMORE repository [6], which holds technology-agnostic archetypes for material sources, material sinks, enrichment services, separations capabilities, storage services, and a generic reactor.

CYCLUS treats each facility as an agent that can interact with other agents in the simulation. These agents are defined by their capabilities and the resources they can provide or consume. The agents are connected through a unique market mechanism called the Dynamic Resource Exchange (DRE) that allows agents to request resources and respond to requests from other agents. The DRE is responsible for matching resource requests with offers from suppliers and ensuring that the resources are exchanged.

Commodities, in the parlance of the CYCLUS ecosystem, are passed by agents through the DRE in recorded transactions. A commodity can be anything, from raw materials (like uranium ore) to contextual concepts (e.g., money or permits). The transactions are recorded in a database that can be queried to determine the flow of materials through the simulation. As Huff et al. outline in their 2016 paper [22], treating facilities and materials independently allows for flexibility in the level of fidelity for both.

As CYCLUS is a transactions code and not necessarily a physics code, the reactors incorporate physics through pre-defined *recipes*, where the user specifies the concentration of isotopes in a fuel form. Pre-defining recipes can reduce the precision with which fuel compositions are calculated, but it dramatically increases computational efficiency for simulations of complex fuel cycles. For example, depending on how fuel is discharged from a core at the end of a reactor's lifetime, there are instances when the model will over or under-predict the concentration of isotopes, thereby injecting a level of error into calculations. Users approximate the burnup of each fuel element with the same input recipe to be the same; however, in this work, we incorporate a cascading enrichment from LEU+ to HALEU; LEU+ in the short term, while reactor vendors and fuel suppliers work with the government to establish the supply chain for HALEU.

In CYCLUS, the user defines the simulation by specifying the regions, institutions, and facilities that will be present. Regions are collections of institutions, where institutions are collections of facilities, while facilities are the primary agents interacting in the simulation. The user can define the relationships between regions, institutions, and facilities to model the flow of materials and resources through the simulation. Through initial conditions, the user can tailor their simulation for any historical or imagined starting point based on the expected facilities and resources available from the outset.

### 2.6.1 Fuel Depletion

Fuel depletion is a critical aspect of fuel cycle simulations, as it directly influences the characteristics and behavior of UNF. The composition of this fuel, shaped by factors like decay heat, the quantity of fissile material, and the volume of UNF, has profound implications for various stages of the nuclear fuel cycle. The effects of depletion on these properties are the thermal and physical characteristics of the fuel, as well as the practical considerations such as the transportation of UNF, the limits of repository storage, and the potential for reprocessing and recycling of materials. Thus, any comprehensive fuel cycle simulation must account for fuel depletion, ensuring that the resulting data reflect realistic conditions and constraints.

In many fuel cycle simulators, fuel depletion is managed using pre-defined compositions, which allow for rapid calculations and straightforward modeling of fuel cycles. Tools such as VISION [64], the CYCAMORE Reactor archetype in CYCLUS–which uses the aforementioned *recipes*–and ORION utilize this methodology. In these frameworks, the compositions of UNF are established in advance and derived from separate depletion modeling efforts. This approach is particularly effective for once-through fuel cycles, where fresh fuel compositions remain constant across refueling periods, leading to minimal variation in the characteristics of discharged fuel. While this method offers simplicity and speed, it may not capture the nuanced behaviors seen in more complex fuel cycles, where dynamic changes in fuel composition are more pronounced.

Users have developed several archetypes to further expand the capabilities of CYCLUS in modeling fuel depletion. Bright-lite [48], for instance, introduces a comprehensive framework for evaluating fuel compositions based on burnup and criticality. This archetype offers two operational modes—forward and blending mode—allowing users to tailor depletion modeling to specific scenarios. The initial recipe is depleted based on a given fluence in forward mode. In blending mode, the reactor is connected to a fabrication facility that mixes material streams to meet a burnup criticality or conversion ratio. The burnups and material definitions need to be given, which is the first step in implementing this archetype. CyBORG [51], another CYCLUS archetype, integrates CYCLUS with ORIGEN by generating a problem-specific cross section library (which it then feeds to ORIGEN to perform a single depletion calculation for the core), enabling a more nuanced approach to modeling fuel cycles. Although CyBORG requires access to the export-controlled ORIGEN, it enhances the accuracy of UNF compositions. The ann_pwr [5] archetype employs neural networks trained on historical data to predict fuel compositions based on burnup and initial enrichment. While achieving results with less than 1% error 0.23% of the time as ORIGEN, ann_pwr's applicability is limited to PWR designs, highlighting a need for broader models that can encompass diverse reactor types.

Dynamic modeling of fuel depletion represents an evolution in fuel cycle simulations, allowing for real-time updates to fuel compositions as material properties evolve. This approach is crucial for accurately reflecting the influences of fuel depletion on material properties. Various simulators outside the CYCLUS ecosystem, including ORION [15], DYMOND [44], and NFCSim [49], are capable of dynamic modeling. For instance, ORION allows users to define material compositions using recipes and autonomously model decay and depletion. DYMOND enhances accuracy by coupling with ORIGEN2, enabling criticality searches that refine fresh fuel compositions based on updated UNF data. NFCSim's coupling with the Los Alamos Criticality Engine (LACE) further exemplifies this trend by employing fluence-dependent calculations to ascertain the evolving nature of nuclear materials. These advancements in dynamic modeling are essential for improving the fidelity and reliability of fuel cycle simulations, particularly as the nuclear industry moves toward more intricate and sustainable fuel management strategies.

The OpenMCyclus archetype [1] enhances the CYCLUS ecosystem by introducing an open-source real-time fuel depletion tool for CYCLUS simulations, building off of the concept of CyBORG. Unlike traditional approaches that rely on pre-defined recipes for fuel compositions, OpenMCyclus integrates with OpenMC [47] to dynamically update spent fuel compositions throughout the simulation, allowing for greater accuracy and flexibility in modeling various reactor designs. This real-time depletion capability is valuable for assessing the impacts of different fuel cycle strategies, as it accommodates changes in fuel composition and operational conditions without the need for restrictive licensing agreements associated with other depletion tools.

# Chapter 3

# Deployment Scenarios

This chapter discusses proposed transition scenarios for new nuclear reactor deployment in the United States (U.S.) and the reactor models used to simulate them. It also discusses the theoretical framework and key concepts that underpin the research and the results for each deployment scheme.

## 3.1 Transition Scenarios

This chapter explores the deployment schemes implemented in this work—outlined in Table 3.1—and the demand growth scenarios we have considered—outlined in Table 3.2. Appendix B will discuss two additional deployment schemes that I implemented but did not leverage, as they are more useful for problems not considered herein.

As the energy landscape evolves, compounding factors will drive the actual deployment of these reactors in ways this work does not capture. The value of energy system modeling and transition scenarios is to understand the deployment implications compared with and measured relative to business-as-usual cases with similar approximations.

Table 3.1: Deployment schemes.

| Status | Scheme | Description |
|---|---|---|
| Incorporated | Greedy Deployment | Deploy the largest reactor first at each time step, fill in the remaining capacity with the next smallest, and so on. |
| | Random Deployment | Uses a date and hour as seed to sample the reactors list randomly. |
| | Initially Random, Greedy Deployment | Randomly deploy reactors until a reactor bigger than the remaining capacity is proposed for each time step, then fills the remaining capacity with the greedy algorithm. |
| Not Incorporated | Capped Deployment | There is a single-number capacity for one or more of the reactor models. |
| | Pre-Determined Distribution Deployment | One or more reactors have a preset distribution, and a smaller capacity model fills in the gaps. |

These deployment schemes choose reactors to fill demand growth based on two predictions of future. The U.S. Energy Information Administration (EIA) publishes demand expansion projections for the totality of the U.S. [58]. The administration has refrained from publishing AEO 2024 in light of recent accelerations in demand growth. Our assumptions for the low-growth scenarios are that the relative percentage of nuclear power remains constant and that the relative performance of the various fuel cycle metrics we simulate will remain constant. Our high-growth scenarios come from the U.S. Department of Energy (DOE) Liftoff Report [26], which does not reflect this constant percentage assumption for nuclear power in their demand scenarios. Their growth projections are specific to nuclear energy deployment increases, and the number is agnostic to the total increase.

Table 3.2: Demand growth scenarios.

| **Demand Growth** | **Year-to-Year Increase** | **Source** |
|---|---|---|
| No Growth | 0.0% | N/A |
| Low Growth | 0.17% | [58] |
| Low Growth | 0.5% | [58] |
| Low Growth | 1.0% | [58] |
| High Growth | 3.5% | [26] |
| High Growth | 5.6% | [26] |

As shown in Table 3.3, each growth scenario has two regimes: 1) the reactors are never fueled with low-enriched uranium plus (LEU+); 2) the Micro Modular Reactor (MMR) and X-Energy Xe-100 (Xe-100) reactors are fueled with LEU+ until 2040, when they move to high-assay low-enriched uranium (HALEU). MMRs deployed before this fuel transition will continue to use LEU+ fuel until the end of their lifetime as they do not refuel; however, the Xe-100 reactors will refuel with LEU+ until 2040, when they will refuel with HALEU. The AP1000 reactors will continue to use low-enriched uranium (LEU) fuel throughout the simulation.

Table 3.3: Transition scenario simulations run.

| **Run** | **Deployment Scheme** | **Demand Growth** | **Fuel Choice** |
|---|---|---|---|
| I | Greedy | 0.0% | Single |
| II | Greedy | 0.0% | Multi |
| III | Greedy | 0.17% | Single |
| IV | Greedy | 0.17% | Multi |
| V | Greedy | 0.5% | Single |
| VI | Greedy | 0.5% | Multi |
| VII | Greedy | 1.0% | Single |
| VIII | Greedy | 1.0% | Multi |
| IX | Greedy | 3.5% | Single |
| X | Greedy | 3.5% | Multi |
| XI | Greedy | 5.6% | Single |
| XII | Greedy | 5.6% | Multi |
| XIII | Random | 0.0% | Single |
| XIV | Random | 0.0% | Multi |
| XV | Random | 0.17% | Single |
| XVI | Random | 0.17% | Multi |
| XVII | Random | 0.5% | Single |
| XVIII | Random | 0.5% | Multi |
| XIX | Random | 1.0% | Single |
| XX | Random | 1.0% | Multi |
| XXI | Random | 3.5% | Single |
| XXII | Random | 3.5% | Multi |
| XXIII | Random | 5.6% | Single |

| Run | Deployment Scheme | Demand Growth | Fuel Choice |
|---|---|---|---|
| XXIV | Random | 5.6% | Multi |
| XXV | Random + Greedy | 0.0% | Single |
| XXVI | Random + Greedy | 0.0% | Multi |
| XXVII | Random + Greedy | 0.17% | Single |
| XXVIII | Random + Greedy | 0.17% | Multi |
| XXIX | Random + Greedy | 0.5% | Single |
| XXX | Random + Greedy | 0.5% | Multi |
| XXXI | Random + Greedy | 1.0% | Single |
| XXXII | Random + Greedy | 1.0% | Multi |
| XXXIII | Random + Greedy | 3.5% | Single |
| XXXIV | Random + Greedy | 3.5% | Multi |
| XXXV | Random + Greedy | 5.6% | Single |
| XXXVI | Random + Greedy | 5.6% | Multi |

Under each regime, each demand projection is met by deploying reactors using the schemes outlined in Table 3.1. The following sections will discuss the results of these deployment schemes, their limitations, and propose future work. Regardless of the regime, each run will attempt to deploy reactors to meet the capacity outlined in Figure 3.1. The results will focus on the *no growth* and 3.5% growth (corresponding to doubling nuclear by 2050) scenarios.

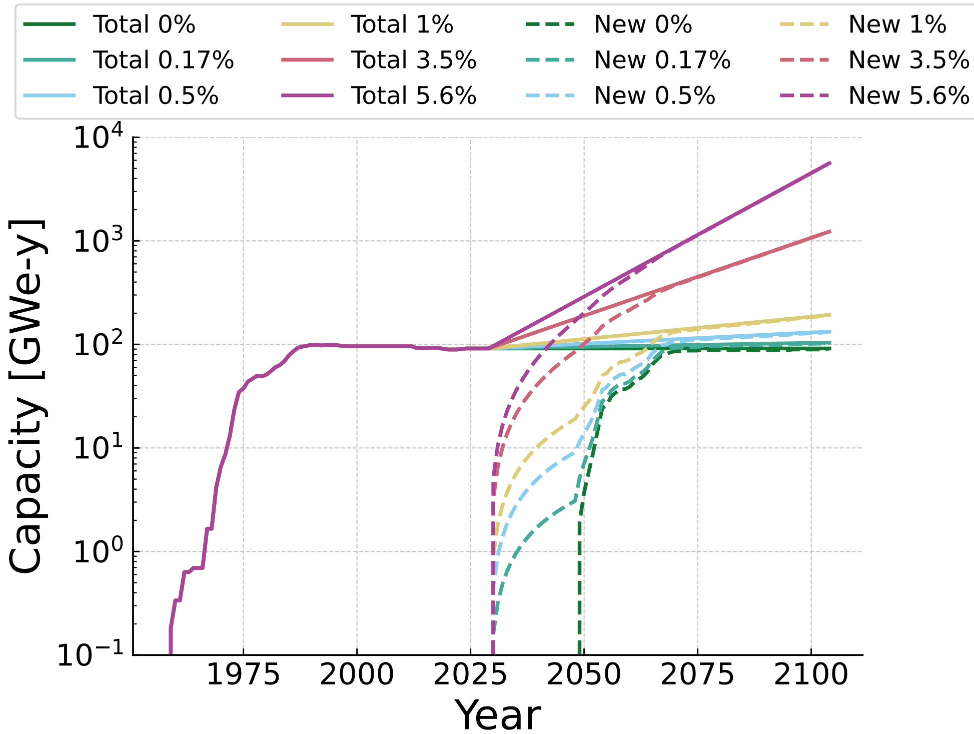


Figure 3.1: Total and new nuclear capacity deployed in each scenario.

As shown, advanced reactors (for this work, the designs are the MMR, Xe-100, and AP1000) begin deployment in 2030. While this is an aggressive deployment schedule, [3] established that the precise deployment start did not significantly impact the total results for this type of analysis and could reasonably serve as an upper bound of deployment. The business-as-usual or, as we will refer to it, *no growth* scenario does not require the deployment of a new nuclear reactor until just before 2050, whereas the other scenarios understandably commence deployment in 2030. As we have presented the capacity on a logarithmic plot, the linear appearance of the data belies the compounding effect that the year-to-year percentage growth requires.

Comparing these projected deployments with the results from the *no growth* and double scenarios, we can consolidate the over- and under- deployments of capacity into Table 3.4 and see that the random deployment scheme showed the least total difference between the results and the projection. The initially random, then greedy deployment scheme showed the largest total difference between the results and the projection, while the greedy deployment scheme was between the two.

Table 3.4: Capacity difference between results and projection.

| Scenario | Deployment Scheme | Total Difference [GWe] |
|---|---|---|
| | Greedy | 19.46 |
| No Growth | Random | -15.21 |
| | Initially Random Then Greedy | 47.26 |
| | Greedy | 103.54 |
| Double | Random | 6.65 |
| | Initially Random Then Greedy | 151.86 |

We show the difference in energy capacity between the results and the projection for the *no growth* and double scenarios over time in Figure 3.2. The difference curves in Figure 3.2b show a tightly perturbed oscillation as more reactors are deployed to meet the increasing demand in the random and the initially random, then greedy schemes. Closer to the start of advanced reactor deployment, the greedy scheme shows a consistently smaller difference than the other schemes, but the difference continues to grow as time progresses.

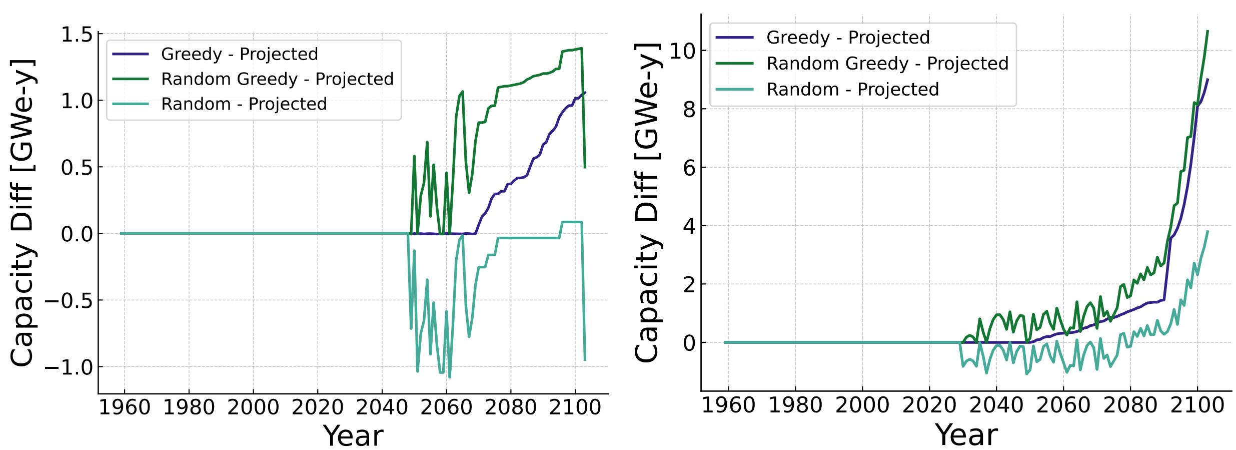


(a) No Growth.

(b) Double.

Figure 3.2: Energy capacity difference between projection and scheme predictions.

## 3.2 Metrics

This thesis develops a nuclear energy model of the U.S. using concepts from Energy System Models (ESMs) on scenarios that compare the transition from our current fleet to incorporate advanced reactor technologies not currently deployed. To compare these scenarios, I have focused on a few key metrics: separative work units (SWU), energy output, mass of fuel, and reactor deployment.

### 3.2.1 Separative Work Units

The process of enriching uranium is a critical step in the nuclear fuel cycle, and is expected to be a bottleneck in the deployment of advanced reactors. The Separative Work Unit (SWU), is a ubiquitous measure of effort that goes into separating isotopes. It is simplified as:

$$SWU = (PV(x_p) + TV(x_t) - FV(x_f))\,t$$

where:

$$V(x_i) = (2x_i - 1)\ln\left(\frac{x_i}{1-x_i}\right)$$

where:

$$\begin{aligned}
SWU &= \text{Separative Work Units [kgSWU]}\\
P &= \text{Product mass flow rate [kg/d]}\\
F &= \text{Feed mass flow rate [kg/d]}\\
T &= \text{Tails mass flow rate [kg/d]}\\
V(x_i) &= \text{Separation Potential [-]}\\
x_i &= \text{Weight fraction of } {}^{235}U \text{ in the i stream [-]}\\
x_p &= \text{Weight fraction of } {}^{235}U \text{ in the product stream [-]}\\
x_f &= \text{Weight fraction of } {}^{235}U \text{ in the feed stream [-]}\\
x_t &= \text{Weight fraction of } {}^{235}U \text{ in the tails stream [-]}\\
t &= \text{Time [d]}
\end{aligned}$$

This thesis compares the SWU required for each scenario to understand the relative effort required to deploy the reactors and provide a stable precursor to economic calculations. As mentioned in Section 2.3, the definition used in the literature for LEU+ can be tied to the upper limit on enrichment for a Category III facility. The LEU+ fuel, as shown in Table 2.2, is enriched to 9.95 w% $^{235}$U, which would fall under the Category III limit. The HALEU fuel would require Category II facilities to achieve the 19.75 w% $^{235}$U and 15.5 w% $^{235}$U enrichment for the MMR and Xe-100 HALEU. Table 3.5 shows the SWU calculation values for each fuel type.

Table 3.5: SWU calculation values for each fuel type.

| **Variable** | **Value** |
|---|---|
| MMR LEU+ $x_p$ | 0.0995 |
| MMR HALEU $x_p$ | 0.1975 |
| Xe-100 LEU+ $x_p$ | 0.0995 |
| Xe-100 HALEU $x_p$ | 0.155 |
| LEU $x_p$ | 0.045 |
| $x_f$ | 0.00711 |
| $x_t$ | 0.002 |

### 3.2.2 Energy Output

The deployment of reactors in this thesis is based on energy demand, which approximates the complicated relationship that generators and utilities have with power expansions. The reactors simulated herein have a static peak energy output, so the nuance in the fleet's ability to meet the demand comes from the deployment scheme and limitations in the fuel supply chain. This thesis discusses the realistic features of each scheme and compares the energy output with the demand scenarios to understand the relative performance of each deployment scheme.

### 3.2.3 Mass of Fuel

CYCLUS tracks the mass of material in each transaction, this thesis characterized the fresh and used fuel accumulation to show the relative mass of fuel required to deploy the reactors in each scenario. From the mass of fuel and fuel design, these results can be converted into cost metrics, transportation indicators, and hypothetical repository space considerations.

## 3.3 Greedy Deployment

The greedy deployment scheme selects the largest reactor first until another reactor exceeds the demand—as outlined in 3.3. Then, it moves to the next largest reactor until the next deployment of the smallest capacity reactor exceeds the demand. This scheme is not a proxy for strategic decisions by individual actors, but it reveals the implications of deploying a minimal number of reactors to meet the demand.

Previous work from Bachmann et al. [4] employed a similar scheme to explore the deployment of advanced reactors in the U.S.. This scheme is computationally efficient and allows for the exploration of the deployment of advanced reactors in a way that is not overly complex. This scheme is most useful for scenarios where the user is interested in comparing metrics relative to the number of specific reactors deployed outside of the context of the problem.

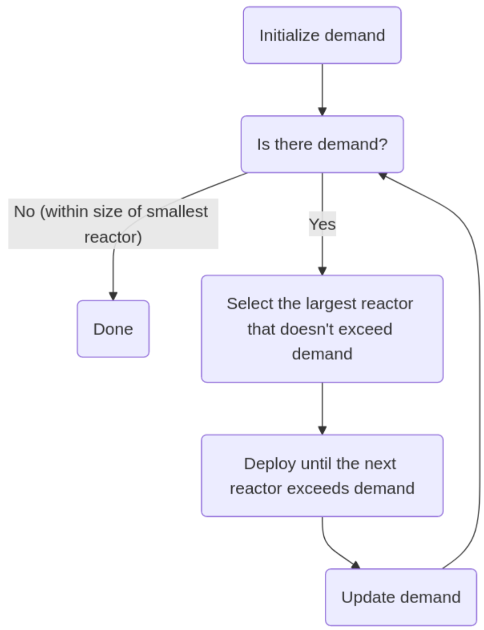


Figure 3.3: Greedy deployment diagram.

The greedy deployment does not attempt to capture the complexity of the deployment problem but rather to explore the implications of deploying a certain number of reactors. The scheme could mirror large actors in a market, but is likely not realistic. The scheme will deploy reactors until the demand is met within the amount of the smallest capacity reactor. Sections 3.3.1, 3.3.2, 3.3.3, and 3.3.4 show the greedy deployment results for the no growth scenario and the double nuclear by 2050 scenario.

### 3.3.1 Number of Reactors

As Section 3.1 mentions, one difference between the no growth scenario and the doubling scenario is that the transition for the no growth scenario will begin closer to 2050 instead of 2030. This trend is reflected in Figures 3.4 and 3.5, where the MMRs, Xe-100s, and AP1000s start as the existing Light Water Reactor (LWR) fleet is retired. Comparing fuel regimes, Figures 3.4a and 3.5a are identical, which typifies the impact of the delayed transition in the no growth scenario.

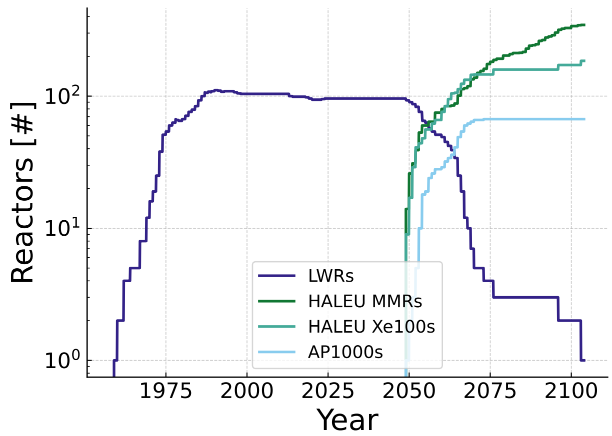


(a) No Growth.

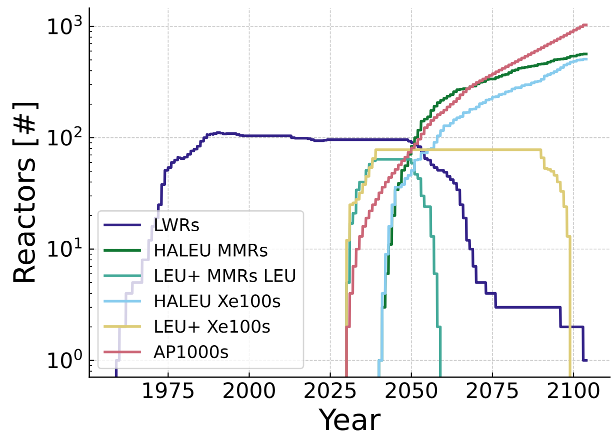


(b) Double.

Figure 3.4: Greedy multi-fuel reactor deployment.

A direct consequence of the greedy deployment scheme is that, in the doubling scenario, the AP1000 is deployed the most over time, whereas the no growth scenario shows the opposite. Another consequence of the deployment scheme is that the deployment rate for the single-fuel regime compared with the multi-fuel regime is identical, and future work could investigate further implications of transitioning from one fuel type to another regarding operation. Simply meeting energy demand is not how utilities make decisions and is not the intended use case of the broad generation of new nuclear reactors, so this is an upper-bounding case for the energy demand met by designs like the MMR or Xe-100.

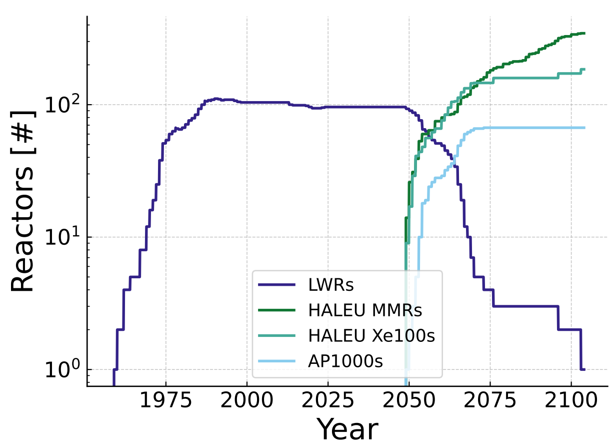


(a) No Growth.

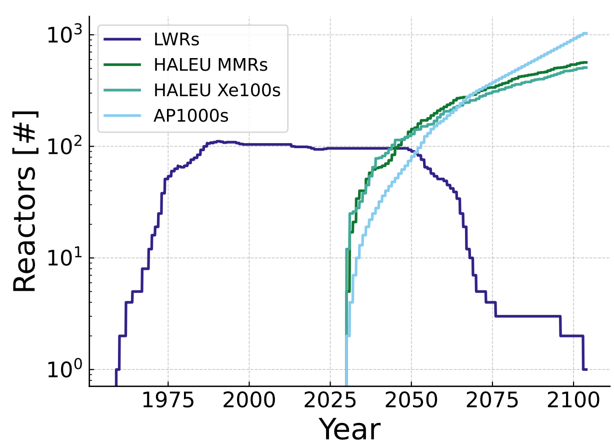


(b) Double.

Figure 3.5: Greedy single-fuel reactor deployment.

Table 3.6 shows how the average number of reactors by design is not influenced by the interstitial period included in this thesis. Compared to the no growth scenario, the double by 2050 scenario shows a significant increase in the average number of each design operating across the 2030-2104 timeline. Consequently, the average number of the AP1000s increases by 757% between the two growth scenarios, which is the largest increase of any design. The Xe-100 reactors show the second largest increase at 163%, followed by the MMR at 109%.

Table 3.6: Average greedy total operating reactors by design.

| Scenario | No Growth, Single | No Growth, Multiple | Double, Single | Double, Multiple |
|---|---|---|---|---|
| HALEU fueled MMRs | 131.613 | 131.613 | 274.493 | 257.427 |
| LEU+ fueled MMRs | – | – | – | 17.067 |
| HALEU fueled Xe-100s | 94.04 | 94.04 | 246.88 | 184.48 |
| LEU+ fueled Xe-100s | – | – | – | 62.4 |
| LEU fueled AP1000 | 38.667 | 38.667 | 331.387 | 331.387 |

### 3.3.2 SWU Results

In Figure 3.6, the yearly SWU demand periodically spikes as the demand for enrichment services grows to meet the fuel demand for the fleet. When reactors begin operation in the depicted no growth scenario around 2050, the SWU demand for the AP1000 peaks above the other two reactors, while the demand from Xe-100s exceeds the demand from MMRs. This trend is exacerbated in the double by 2050 scenarios shown in Figures 3.7b and 3.8b, where the SWU for AP1000 LEU fuel rises quickly and eventually exceeds the total SWU for the existing fleet.

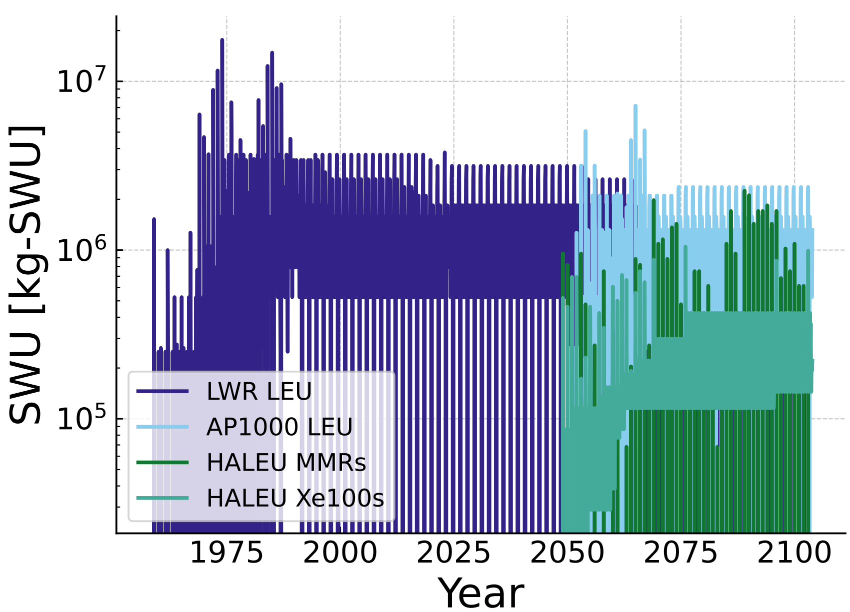


Figure 3.6: Greedy yearly SWU capacity multi-fuel, no growth scenario.

As the features of the yearly data are regular and dictated by the reactor's cycle, Figures 3.7 and 3.8 visualize the total cumulative SWU demand.

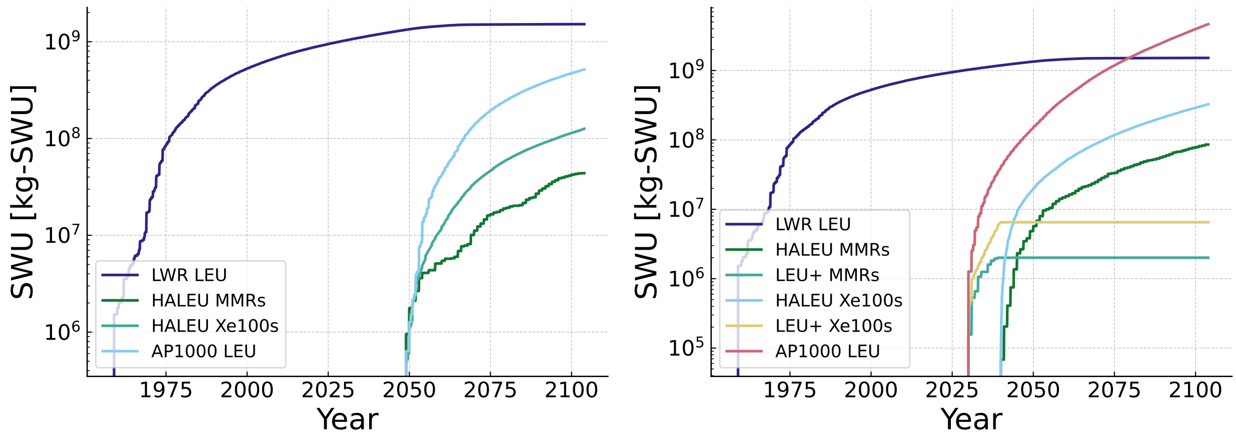


(a) No Growth.

(b) Double.

Figure 3.7: Greedy multi-fuel SWU.

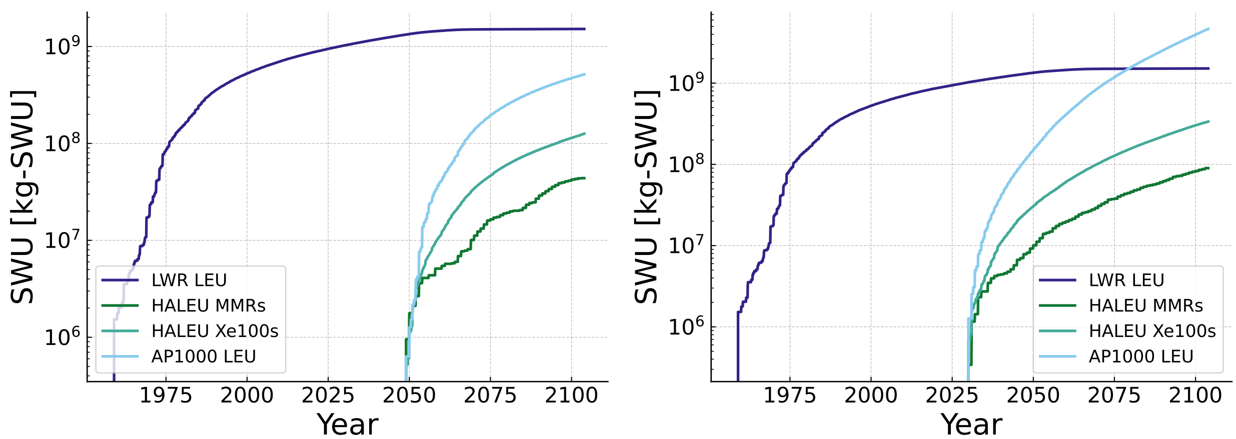


(a) No Growth.

(b) Double.

Figure 3.8: Greedy single-fuel SWU.

Table 3.7 shows how the SWU demand for the MMR and Xe-100 reactors are the same in the single and multi-fuel regimes for the no growth scenarios, consistent with the reactor deployment trends in Section 3.3.1. The SWU demand for the AP1000s increases by 800% from the no growth scenario to the double scenario, again consistent with the reactor deployment trends in the previous section. The SWU demand for Xe-100 HALEU increases by 167%, while the SWU demand for MMR HALEU increases by 105% from the no growth scenario to the double scenario.

Table 3.7: Average greedy yearly SWU by design in kSWU.

| Scenario | No Growth, Single | No Growth, Multiple | Double, Single | Double, Multiple |
|---|---|---|---|---|
| MMR HALEU | 48.699 | 48.699 | 99.974 | 95.127 |
| MMR LEU+ | – | – | – | 2.228 |
| Xe-100 HALEU | 139.926 | 139.926 | 374.323 | 362.312 |
| Xe-100 LEU+ | – | – | – | 7.227 |
| AP1000 LEU | 573.989 | 573.989 | 5167.815 | 5167.815 |

### 3.3.3 Fresh Fuel Results

Figures 3.9 and 3.10 show the fresh fuel demand for the reactors in the no growth and double by 2050 scenarios. The fresh fuel curves in each scenario follow the same pattern as the reactor deployment curves, as CYCLUS supplies fuel to each of the reactors as it is deployed.

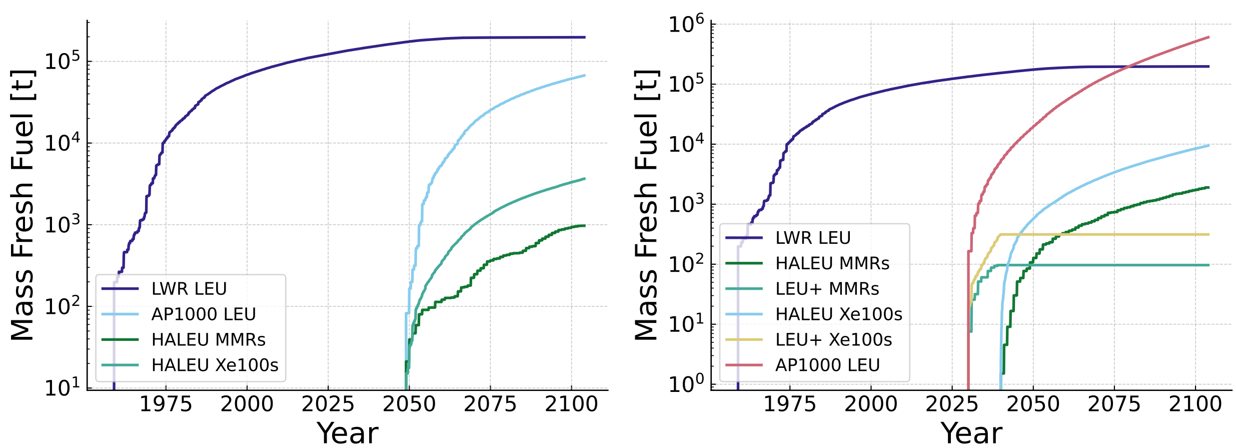


(a) No Growth.

(b) Double.

Figure 3.9: Greedy multi fresh fuel demanded.

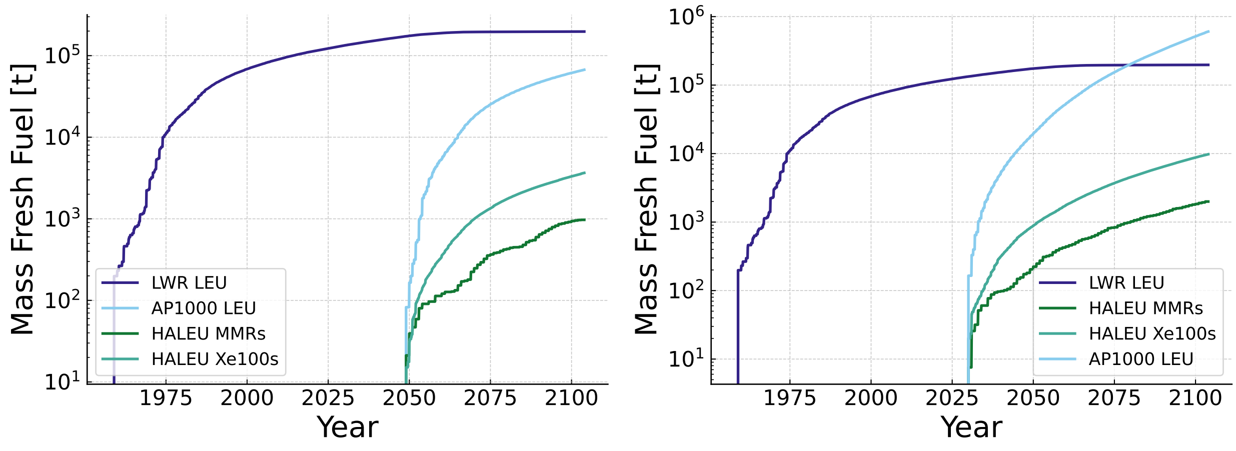


(a) No Growth.

(b) Double.

Figure 3.10: Greedy single fresh fuel demanded.

Table 3.8 quantifies the average yearly fresh fuel demand by design in the no growth and double by 2050 scenarios. The AP1000 LEU shows the largest increase in fresh fuel demand from the no growth scenario to the double scenario at 800%, followed by the Xe-100 HALEU at 159%. The MMR HALEU reactors show the smallest increase in fresh fuel demand at 105%.

Table 3.8: Average greedy yearly fresh fuel by design in tonnes.

| Scenario | No Growth, Single | No Growth, Multiple | Double, Single | Double, Multiple |
|---|---|---|---|---|
| MMR HALEU | 1.079 | 1.079 | 2.216 | 2.108 |
| MMR LEU+ | – | – | – | 0.107 |
| Xe-100 HALEU | 4.059 | 4.059 | 10.859 | 10.511 |
| Xe-100 LEU+ | – | – | – | 0.348 |
| AP1000 LEU | 74.636 | 74.636 | 671.976 | 671.976 |

### 3.3.4 Used Fuel Results

Figures 3.11 and 3.12 describe the used fuel demand for the reactors in the no growth and double by 2050 scenarios. The used fuel curves in each scenario lag the reactor deployment curves, as CYCLUS removes the used fuel after the appropriate number of cycles from each operating and eventually decommissioning reactor.

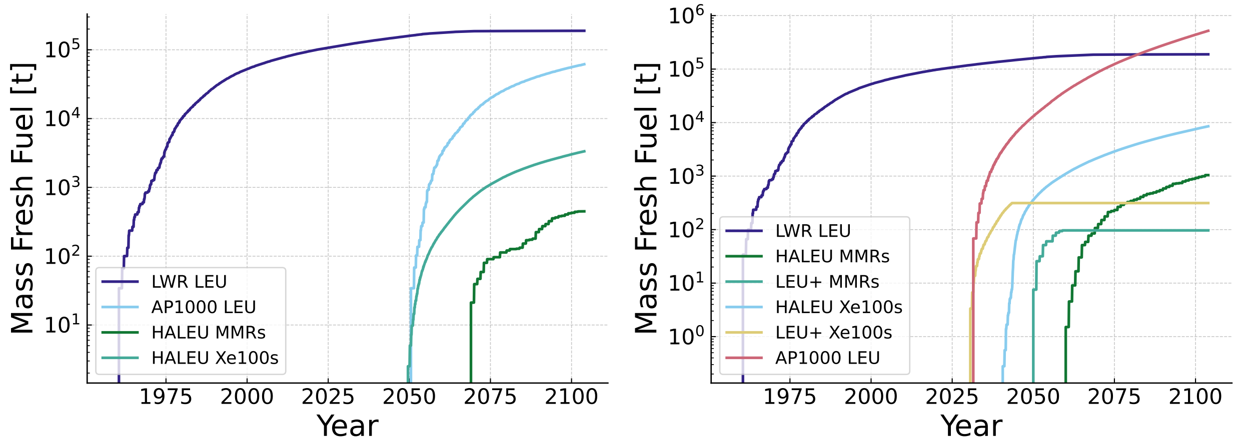


(a) No Growth.

(b) Double.

Figure 3.11: Greedy multi used fuel accumulation.

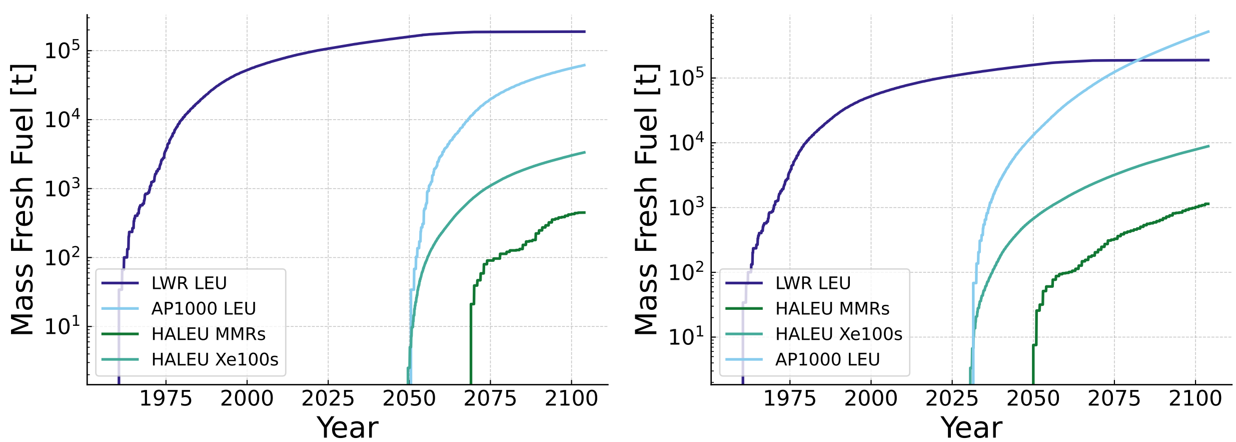


(a) No Growth.

(b) Double.

Figure 3.12: Greedy single used fuel accumulation.

Table 3.9 itemizes the average yearly used fuel by design in the no growth and double by 2050 scenarios. The AP1000 LEU shows the largest increase in used fuel demand from the no growth scenario to the double scenario at 743%, followed by the Xe-100 HALEU at 164%. The MMR HALEU reactors show the smallest increase in used fuel demand at 154%.

Table 3.9: Average greedy yearly used fuel by design in tonnes.

| Scenario | No Growth, Single | No Growth, Multiple | Double, Single | Double, Multiple |
|---|---|---|---|---|
| MMR HALEU | 0.499 | 0.499 | 1.267 | 1.160 |
| MMR LEU+ | – | – | – | 0.107 |
| Xe-100 HALEU | 3.714 | 3.715 | 9.826 | 9.477 |
| Xe-100 LEU+ | – | – | – | 0.348 |
| AP1000 LEU | 68.496 | 68.496 | 577.484 | 577.484 |

## 3.4 Random Deployment

Advanced reactor concepts, like the ones outlined in this thesis, are often designed for use cases ranging from industrial steam production to microgrid integration. Reactor deployment is a complex problem that requires a nuanced understanding of the energy market, regulatory environment, intended use of the technology, and the technical capabilities of the reactor.

This random deployment is a proxy for the complexity of the real-world problem; however, it does not include the nuance of how individual deployments meet an end user's needs, which will drive the strategic decisions that utilities and ratepayers behind the meter make in their reactor choices. The random deployment scheme has the potential to capture some of the complexities in overall market development, but the extent to which it captures these details is not explored in this thesis.

The random deployment scheme is implemented by randomly selecting reactors from the list of deployable reactors until the demand is covered. Figure 3.13 illustrates this scheme, which shows the single loop in the logic from the top down. There is an irreducible demand that cannot be met because the power capacity is assumed to be constant. At its best, the random deployment scheme will meet the demand but has the potential to fall short of the demand by one of the smallest capacity reactors. This thesis implements a rough random case that deploys until the randomly selected reactor exceeds the demand to reduce the computational cost. This rough approximation is coupled with the greedy deployment scheme in the initially random, greedy deployment scheme in Section 3.5.

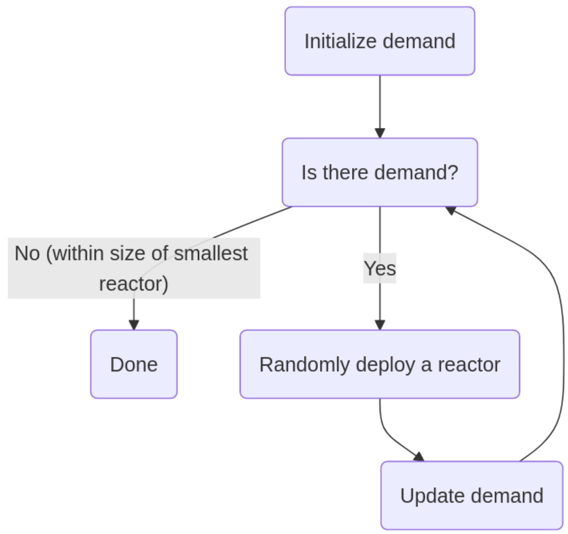


Figure 3.13: Random deployment diagram.

The seed, which was set to 20240527121205 for every run for this scheme, for the random number generator is set by the date and time of the simulation, which allows for the reproducibility of the results. This scheme is a proxy for aggregate decisions by actors and would fail to reliably capture individual actor decisions. This scheme is most useful for scenarios or timescales where there is a high degree of uncertainty in the deployment of reactors.

### 3.4.1 Number of Reactors

As discussed in Section 3.3.1, the difference between the no growth and double scenarios in Figures 3.14 and 3.15 is that the double scenario requires new reactors to be deployed immediately during the transition. A consequence of the random reactor deployment scheme is that the reactors in Figures 3.14a and 3.14b grows similarly over time as they are sampled for deployment. This scheme has the potential to stochastically capture the complexity of deploying reactors in the real world but likely represents an extreme where utilities are not narrowing in on a single reactor design to reduce deployment costs.

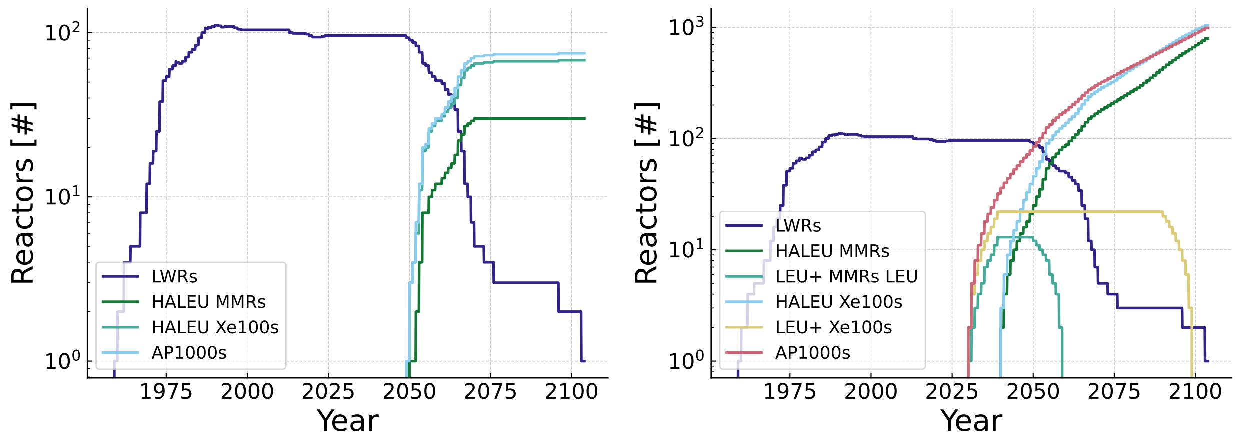


(a) No Growth.

(b) Double.

Figure 3.14: Multiple fuels random reactor deployment.

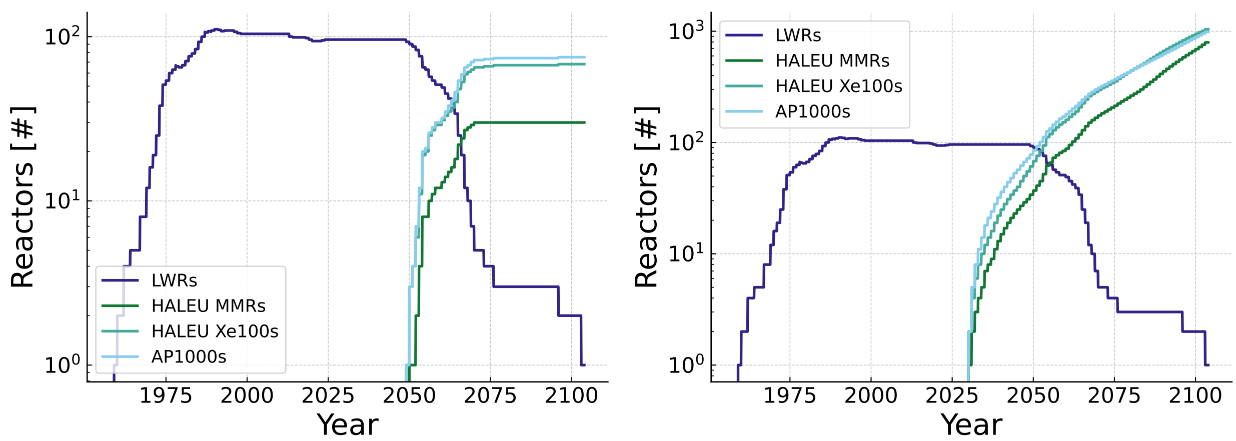


(a) No Growth.

(b) Double.

Figure 3.15: Single-fuel random reactor deployment.

Table 3.10 shows the average total number of reactors for the no growth and double scenarios in the single and multi-fuel regimes. There is a 740% increase in the AP1000s deployed from the no growth scenario to the double scenario. The Xe-100 reactors show a 249% increase, while the MMR reactors show a 62% increase in the reactors deployed from the no growth scenario to the double scenario in the single-fuel regime. Unlike the reactor deployment under the greedy scheme in Section 3.3.1 and the initially random then greedy scheme in Section 3.5.1, the random deployment scheme results for the single-fuel and multi-fuel regimes are not the same.

In the multi-fuel regime, the AP1000 reactors show a 660% increase in the reactors deployed from the no growth scenario to the double scenario. The Xe-100 reactors show a 746% increase, while the MMR reactors show an 1138%

increase in the reactors deployed from the no growth scenario to the double scenario.

Table 3.10: Average random total operating reactors by design.

| Scenario | No Growth, Single | No Growth, Multiple | Double, Single | Double, Multiple |
|---|---|---|---|---|
| HALEU fueled MMRs | 131.613 | 17.267 | 213.707 | 210.24 |
| LEU+ fueled MMRs | – | – | – | 3.467 |
| HALEU fueled Xe-100s | 94.04 | 38.813 | 328.173 | 310.573 |
| LEU+ fueled Xe-100s | – | – | – | 17.6 |
| LEU fueled AP1000s | 38.667 | 42.72 | 324.68 | 324.68 |

### 3.4.2 SWU Results

Figure 3.16 visualizes the yearly SWU demand periodically spike as reactors begin operation in the depicted no growth scenario around 2050. The SWU demand for the AP1000 LEU rises above the other two reactors where the demand from Xe-100s overlaps heavily with the demand from MMRs. This trend is exacerbated in the double by 2050 scenarios shown in Figures 3.7b and 3.8b, where the SWU for AP1000 LEU fuel rises quickly and eventually exceeds the total SWU for the existing fleet.

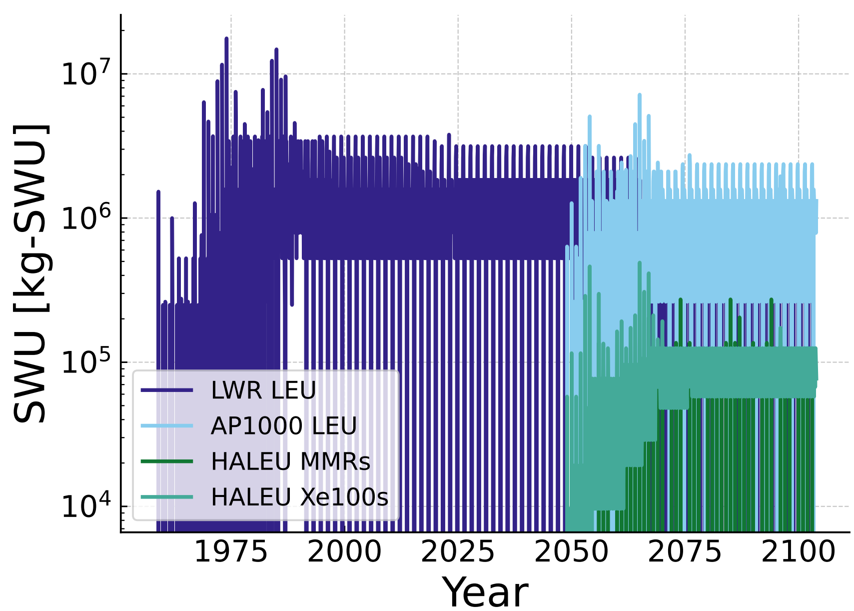


Figure 3.16: Random reactor yearly SWU capacity.

As the features of the yearly data are regular, dictated by the cycles of the reactors, and overlapping, Figures 3.17 and 3.18 visualize the total cumulative SWU demand in the.

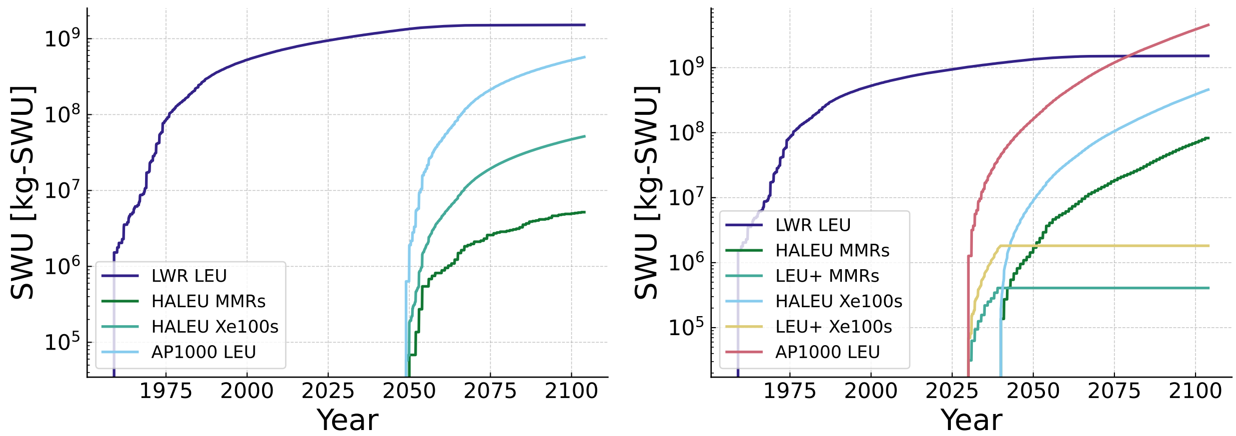


(a) No Growth.

(b) Double.

Figure 3.17: Random reactor multi-fuel SWU.

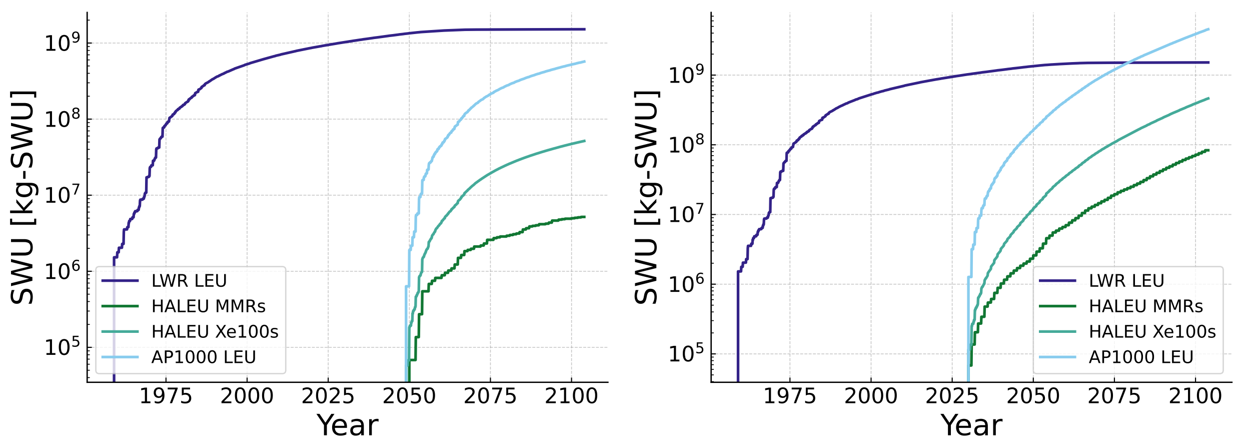


(a) No Growth.

(b) Double.

Figure 3.18: Random reactor single-fuel SWU.

Table 3.11 shows the average total yearly SWU capacity for the no growth and double scenarios in the single and multi-fuel regimes under the random deployment scheme. The Xe-100 reactors show a 796% increase in the average total yearly SWU capacity from the no growth scenario to the double scenario in the single-fuel regime. The MMR reactors show a 1511% increase in the average total yearly SWU capacity from the no growth scenario to the double scenario in the single-fuel regime. The AP1000 reactors show a 697% increase in the average total yearly SWU capacity from the no growth scenario to the double scenario in the single-fuel regime.

Table 3.11: Average random yearly SWU by design in tonnes of SWU.

| Scenario | No Growth, Single | No Growth, Multiple | Double, Single | Double, Multiple |
|---|---|---|---|---|
| MMR HALEU | 5.756 | 5.756 | 92.703 | 91.719 |
| MMR LEU+ | – | – | – | 0.453 |
| Xe-100 HALEU | 57.327 | 57.327 | 513.746 | 510.388 |
| Xe-100 LEU+ | – | – | – | 2.021 |
| AP1000 LEU | 634.554 | 634.554 | 5050.323 | 5050.323 |

### 3.4.3 Fresh Fuel Results

Figures 3.19 and 3.20 show the fresh fuel demand for the reactors in the no growth and double by 2050 scenarios. The fresh fuel curves in each scenario follow the same pattern as the reactor deployment curves from Figures 3.14 and 3.15, as CYCLUS supplies fuel to each of the reactors as they deploy.

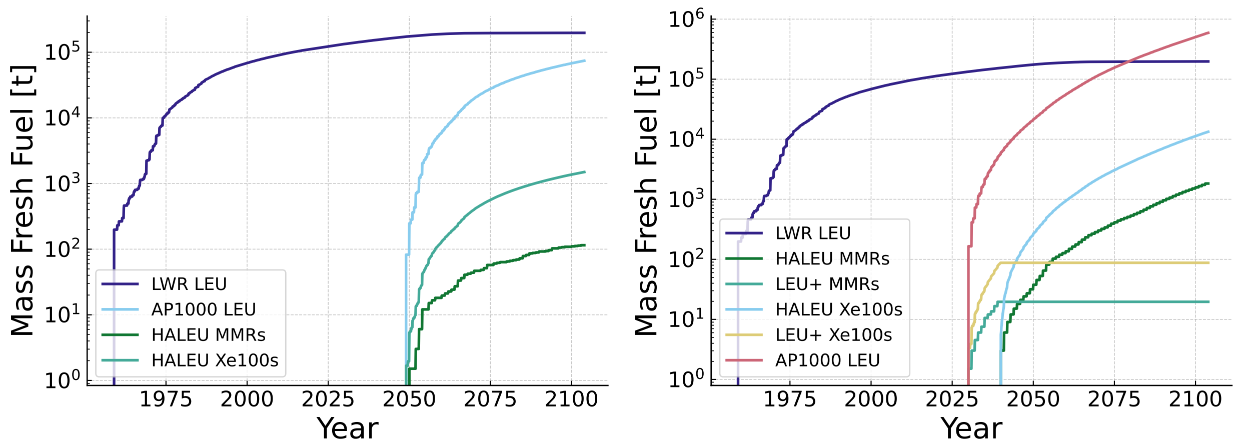


(a) No Growth.

(b) Double.

Figure 3.19: Random multi fresh fuel demanded.

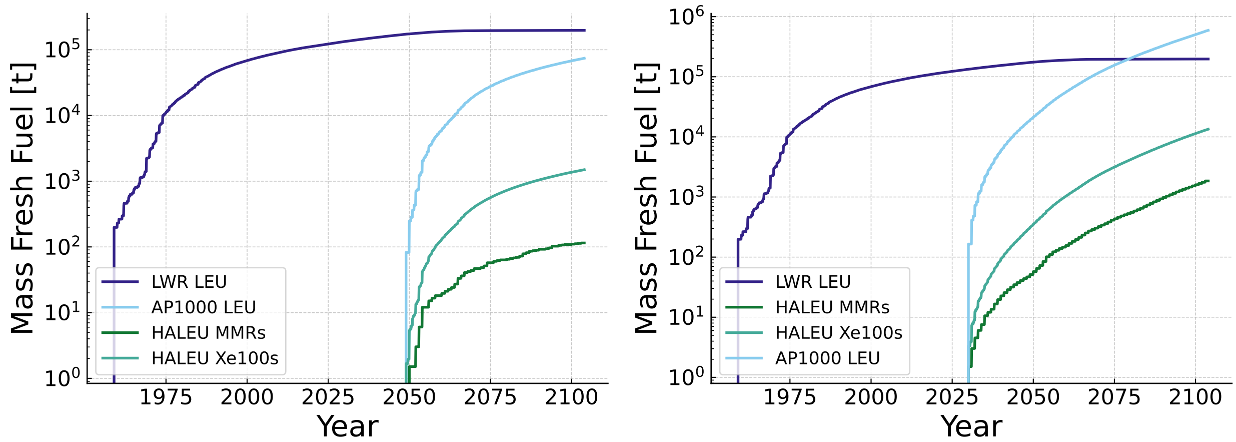


(a) No Growth.

(b) Double.

Figure 3.20: Random single fresh fuel demanded.

Table 3.12 shows the average total yearly fresh fuel for the no growth and double scenarios in the single and multi-fuel regimes under the random deployment scheme. The Xe-100 reactors show a 796% increase in the average total yearly fresh fuel from the no growth scenario to the double scenario in the single-fuel regime. The MMR reactors show a 1505% increase in the average total yearly fresh fuel from the no growth scenario to the double scenario in the single-fuel regime. The AP1000 reactors show a 696% increase in the average total yearly fresh fuel from the no growth scenario to the double scenario in the single-fuel regime.

Table 3.12: Average random yearly fresh fuel by design in tonnes.

| Scenario | No Growth, Single | No Growth, Multiple | Double, Single | Double, Multiple |
|---|---|---|---|---|
| MMR HALEU | 0.128 | 0.128 | 2.055 | 2.033 |
| MMR LEU+ | – | – | – | 0.107 |
| Xe-100 HALEU | 1.663 | 1.663 | 14.904 | 14.806 |
| Xe-100 LEU+ | – | – | – | 0.022 |
| AP1000 LEU | 82.512 | 82.512 | 656.698 | 656.698 |

### 3.4.4 Used Fuel Results

Figures 3.21 and 3.22 depict the used fuel accumulation for the reactors in the no growth and double by 2050 scenarios. The used fuel curves in each scenario follow the reactor deployment curves with a lag corresponding to the cycle length of the reactor from Figures 3.14 and 3.15, as CYCLUS removes fuel from each reactor.

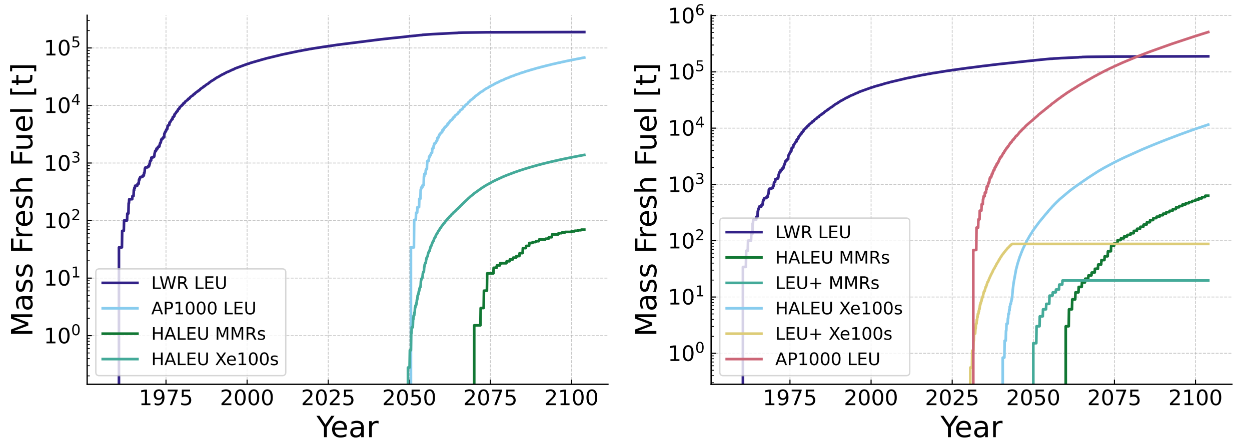


(a) No Growth.

(b) Double.

Figure 3.21: Random multi used fuel accumulation.

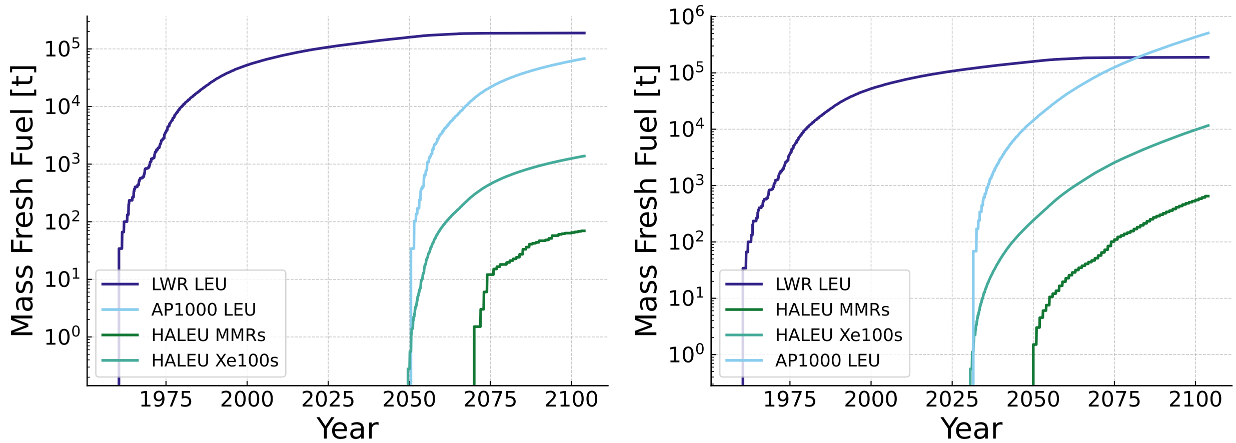


(a) No Growth.

(b) Double.

Figure 3.22: Random single used fuel accumulation.

Table 3.13 show the average total yearly used fuel for the no growth and double scenarios in the single and multi-fuel regimes under the random deployment scheme. The Xe-100 reactors show a 742% increase in the average total yearly used fuel from the no growth scenario to the double scenario in the single-fuel regime. The MMR reactors show a 838% increase in the average total yearly used fuel from the no growth scenario to the double scenario in the single-fuel regime. The AP1000 reactors show a 649% increase in the average total yearly used fuel from the no growth scenario to the double scenario in the single-fuel regime.

Table 3.13: Average random yearly used fuel by design in tonnes.

| Scenario | No Growth, Single | No Growth, Multiple | Double, Single | Double, Multiple |
|---|---|---|---|---|
| MMR HALEU | 0.077 | 0.077 | 0.722 | 0.700 |
| MMR LEU+ | – | – | – | 0.107 |
| Xe-100 HALEU | 1.536 | 1.536 | 12.930 | 12.833 |
| Xe-100 LEU+ | – | – | – | 0.022 |
| AP1000 LEU | 75.638 | 75.638 | 566.239 | 566.239 |

## 3.5 Initially Random, Greedy Deployment

Combining the random and greedy deployment schemes allows us to inject uncertainty as to which reactor will be deployed at any given time while ensuring that the demand is met efficiently. This scheme does not give us more insight than the random or greedy deployment; it merely allows us to leverage the strengths of both.

In this deployment scheme, we randomly deploy reactors until a reactor bigger than the remaining capacity is proposed for each year, then fill the remaining capacity with a greedy algorithm. We outline this scheme in Figure 3.23, which shows the two loops (first random, then greedy) in the logic from the top down.

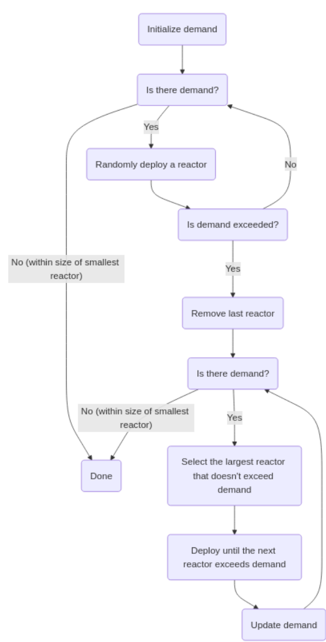


Figure 3.23: Initially random, greedy deployment diagram.

As highlighted in Section 3.4, we did not implement the initially random, greedy deployment scheme to capture additional realism in the deployment problem. This scheme combines random and greedy deployment schemes and inherits their realistic and unrealistic elements. The random deployment scheme captures some of the complexity of the deployment problem but does not guarantee the capture of the nuance of future user needs. The greedy deployment scheme captures the efficiency of the deployment problem but does not capture the complexity of the deployment problem. This scheme is a compromise between the two and does not capture the nuance of the deployment problem.

The seed, which was set to 20240527121205 for every run for this scheme, for the random number generator is set by the date and time of the simulation, which allows for the reproducibility of the results. The degree to which this scheme captures features of the random or greedy deployment schemes varies with the number of reactors deployed in the random phase. Instead of randomly deploying until the demand is met, this implementation randomly deploys until the selected reactor exceeds the demand. This means that when the reactors are different sizes, there is a chance that the random phase will deploy a reactor larger than the demand, and the greedy phase will make up more of the deployment.

### 3.5.1 Number of Reactors

As with the random deployment scheme, Figures 3.24 and 3.25 show that the share of reactors by design is much closer than the greedy deployment scheme. The reactors in the no growth scenarios (shown in Figures **??** and **??**) are deployed close to 2050, whereas the advanced reactors in the double scenarios (shown in Figures **??** and **??**) are deployed close to 2030.

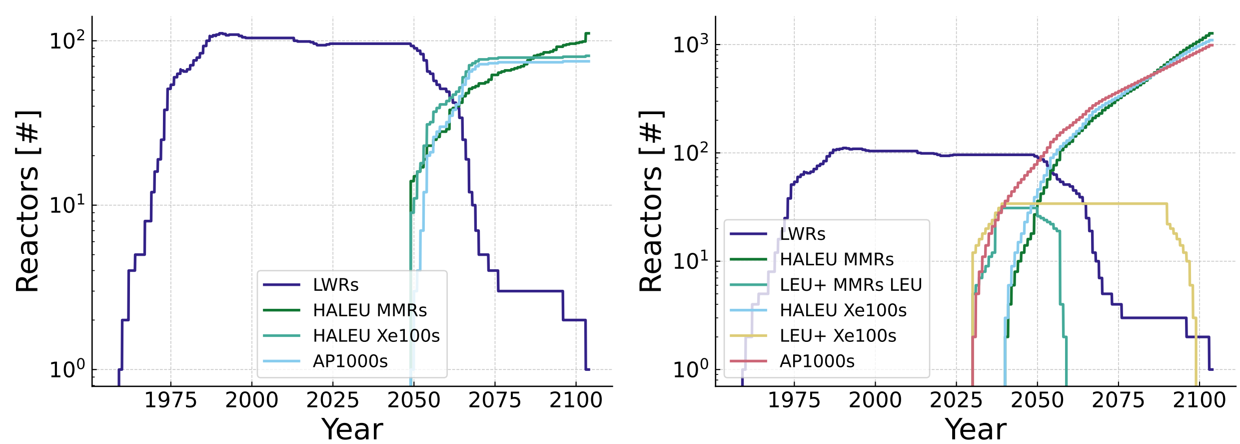


(a) No Growth.

(b) Double.

Figure 3.24: Multiple fuels initially random, then greedy reactor deployment.

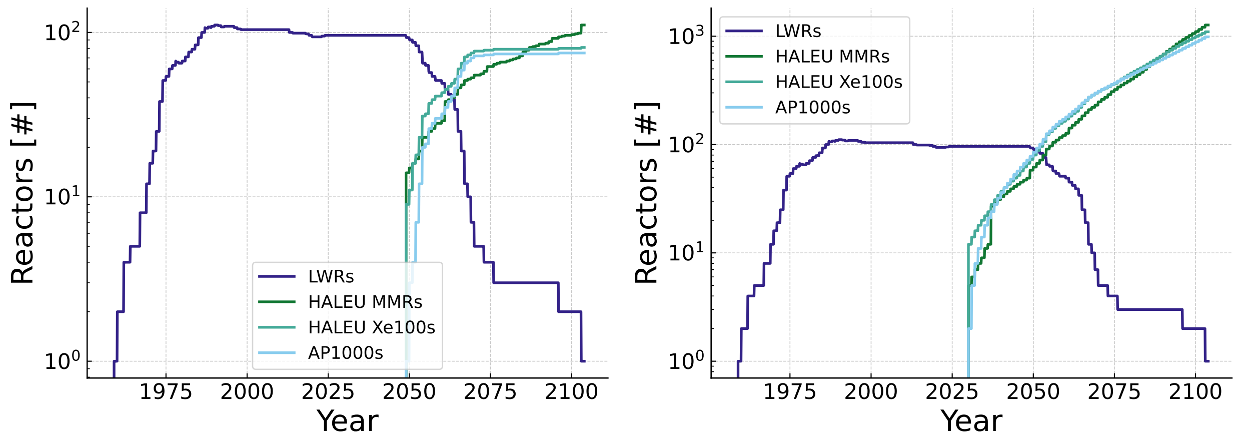


(a) No Growth.

(b) Double.

Figure 3.25: Single-fuel initially random, then greedy reactor deployment.

In Table 3.14, we show the average total operating reactors by design for the no growth and double growth scenarios for the multi and single-fuel regimes. The HALEU fueled MMR and Xe-100 deployment is unchanged in the single and multi-fuel regimes for the no growth scenarios. The number of AP1000 reactors increases 660% from the no growth to the double growth scenario in the multi-fuel regime. The number of HALEU fueled Xe-100 reactors increases 626%, while the number of HALEU fueled MMR reactors increases 649%.

Table 3.14: Average initially random, then greedy total operating reactors by design.

| Scenario | No Growth, Single | No Growth, Multiple | Double, Single | Double, Multiple |
|---|---|---|---|---|
| HALEU fueled MMRs | 44.547 | 44.547 | 333.613 | 325.347 |
| LEU+ fueled MMRs | – | – | – | 8.267 |
| HALEU fueled Xe-100s | 47.52 | 47.52 | 344.88 | 317.68 |
| LEU+ fueled Xe-100s | – | – | – | 27.2 |
| LEU fueled AP1000 | 42.72 | 42.72 | 324.68 | 324.68 |

### 3.5.2 SWU Results

In Figure 3.26, we show the yearly SWU demand periodically spike as reactors begin operation in the depicted no growth scenario around 2050. The SWU demand for the AP1000 LEU rises above the other two reactors while the demand from Xe-100s overlaps heavily with the demand from MMRs. This trend is exacerbated in the double by 2050 scenarios shown in Figures 3.27b and 3.28b where the SWU for AP1000 LEU fuel rises quickly and eventually exceeds the total SWU for the existing fleet.

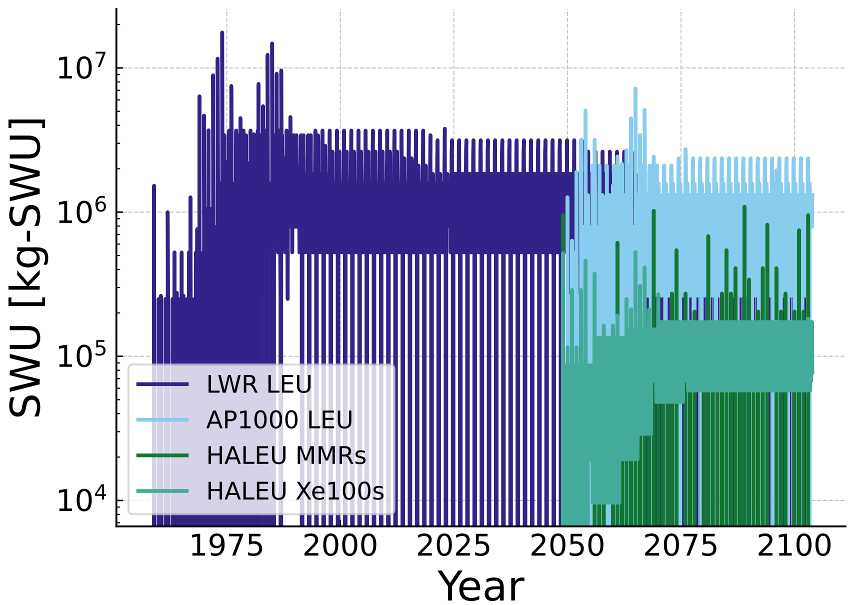


Figure 3.26: Initially random, then greedy yearly SWU capacity.

As the features of the yearly data are regular, dictated by the cycles of the reactors, and overlapping, we will visualize the total SWU demand in the cumulative plots in Figures 3.27 and 3.28.

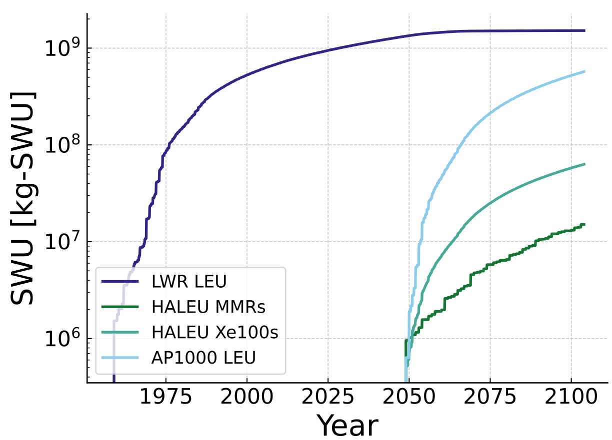


(a) No Growth.

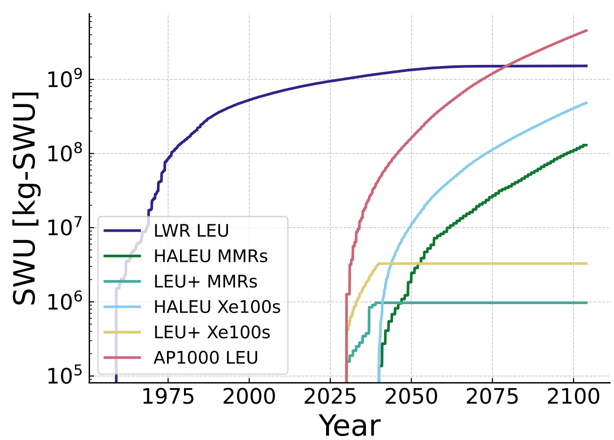


(b) Double.

Figure 3.27: Initially random, then greedy multi-fuel SWU.

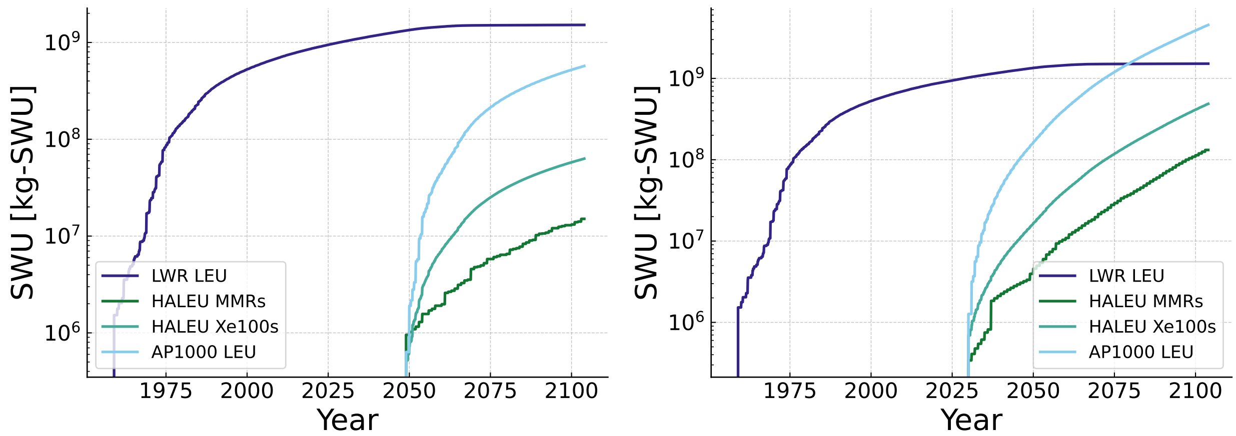


(a) No Growth.

(b) Double.

Figure 3.28: Initially random, then greedy single-fuel SWU.

In Table 3.15, we show the average yearly SWU for the no growth and double growth scenarios for the multi and single-fuel regimes. The SWU demand for the MMR and Xe-100 reactors is the same in the single and multi-fuel regimes for the no growth scenarios, which is consistent with the reactor deployment trends in the Section 3.5.1. Across scenarios, the demand for SWU for AP1000 LEU fuel increases 696% from the no growth to the double growth scenario in the single-fuel regime. The demand for SWU for HALEU fuel in the MMR and Xe-100 reactors increases 775% and 672% respectively from the no growth to the double growth scenario in the multi-fuel regime.

Table 3.15: Average initially random, then greedy yearly SWU by design in kSWU.

| Scenario | No Growth, Single | No Growth, Multiple | Double, Single | Double, Multiple |
|---|---|---|---|---|
| MMR HALEU | 16.738 | 16.738 | 146.477 | 144.129 |
| MMR LEU+ | – | – | – | 1.079 |
| Xe-100 HALEU | 70.066 | 70.066 | 540.613 | 534.559 |
| Xe-100 LEU+ | – | – | – | 3.624 |
| AP1000 LEU | 634.553 | 634.553 | 5050.323 | 5050.323 |

### 3.5.3 Fresh Fuel Results

In Figures 3.29 and 3.30, we show the fresh fuel demand for the reactors in the no growth and double by 2050 scenarios. The fresh fuel curves in each scenario follow the same pattern as the reactor deployment curves from Figures 3.24 and 3.25, as CYCLUS supplies fuel to each of the reactors as it they deploy.

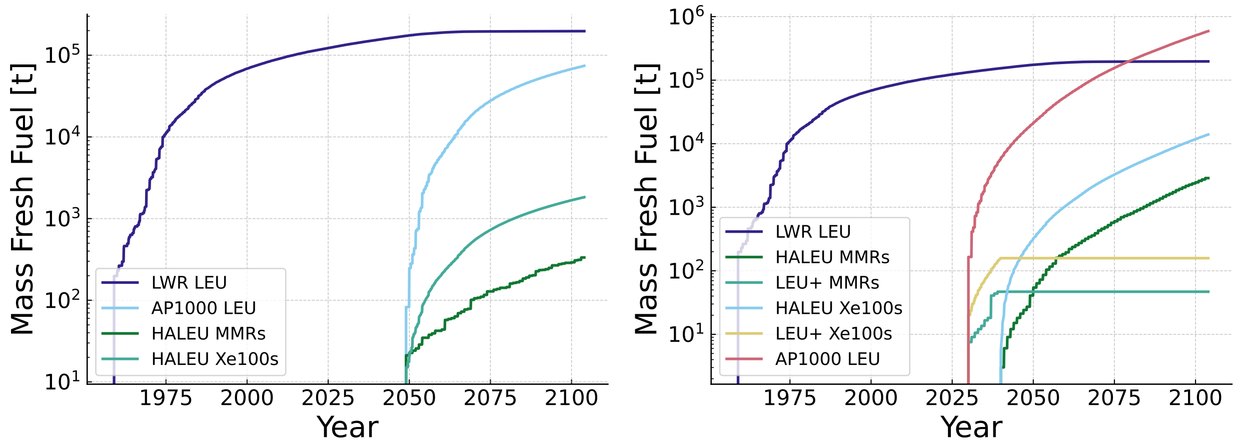


(a) No Growth.

(b) Double.

Figure 3.29: Initially random, then greedy multi fresh fuel demanded.

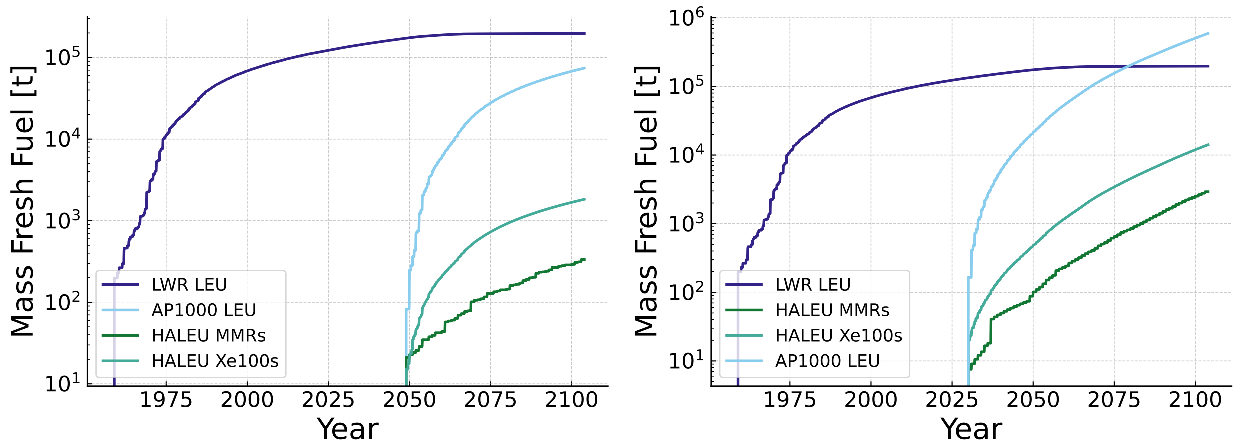


(a) No Growth.

(b) Double.

Figure 3.30: Initially random, then greedy single fresh fuel demanded.

In Table 3.16, we show the average yearly fresh fuel by design in tonnes for the no growth and double growth scenarios for the multi and single-fuel regimes. The fresh fuel demand for the reactors is the same in the single and multi-fuel regimes for the no growth scenarios, which is consistent with the reactor deployment trends in the Section 3.5.1. Across scenarios, the demand for fresh fuel for AP1000 LEU fuel increases 696% from the no growth to the double growth scenario in the single-fuel regime. The demand for fresh fuel for HALEU fuel in the MMR and Xe-100 reactors increases 775% and 671% respectively from the no growth to the double growth scenario in the multi-fuel regime.

Table 3.16: Average initially random, then greedy yearly fresh fuel by design in tonnes.

| Scenario | No Growth, Single | No Growth, Multiple | Double, Single | Double, Multiple |
|---|---|---|---|---|
| MMR HALEU | 0.371 | 0.371 | 3.247 | 3.194 |
| MMR LEU+ | – | – | – | 0.052 |
| Xe-100 HALEU | 2.033 | 2.033 | 15.683 | 15.507 |
| Xe-100 LEU+ | – | – | – | 0.176 |
| AP1000 LEU | 82.512 | 82.512 | 656.698 | 656.698 |

### 3.5.4 Used Fuel Results

In Figures 3.31 and 3.32, we depict the used fuel accumulation for the reactors in the no growth and double by 2050 scenarios. The used fuel curves in each scenario follow the reactor deployment curves with a lag corresponding to the cycle length of the reactor from Figures 3.24 and 3.25, as CYCLUS removes fuel from each reactor.

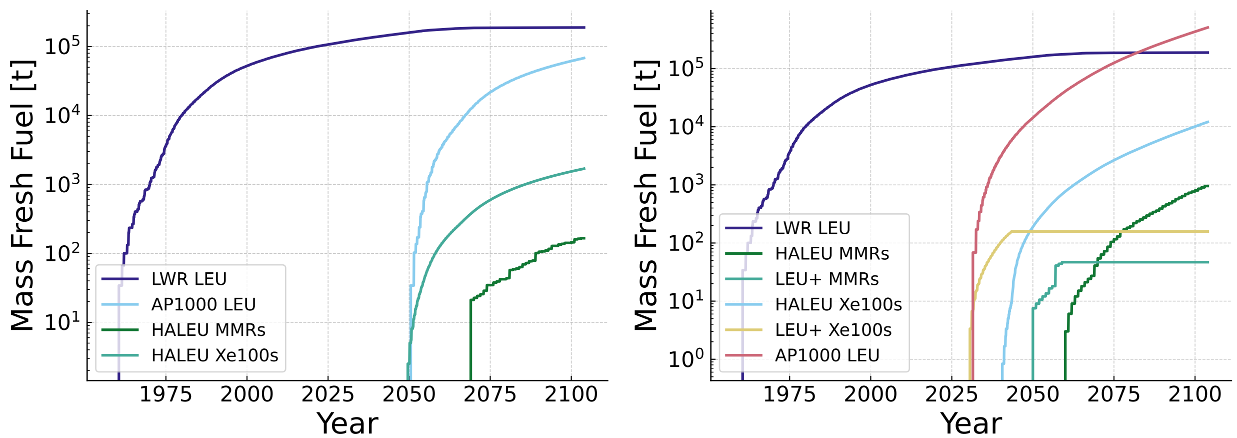


(a) No Growth.

(b) Double.

Figure 3.31: Initially random, then greedy multi used fuel accumulation.

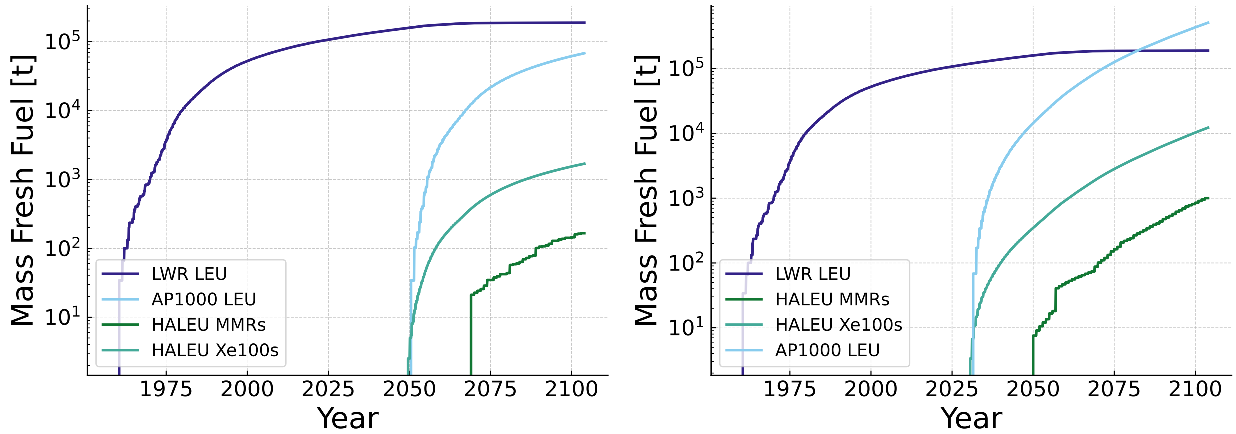


(a) No Growth.

(b) Double.

Figure 3.32: Initially random, then greedy single used fuel accumulation.

In Table 3.17, we show the average yearly used fuel by design in tonnes for the no growth and double growth scenarios for the multi and single-fuel regimes. The used fuel demand for the reactors is the same in the single and multi-fuel regimes for the no growth scenarios, which is consistent with the reactor deployment trends in the Section 3.5.1. Across scenarios, the demand for used fuel for AP1000 LEU fuel increases 649% from the no growth to the double growth scenario in the single-fuel regime. The demand for used fuel for HALEU fuel in the MMR and Xe-100 reactors increases 503% and 620% respectively from the no growth to the double growth scenario in the multi-fuel regime.

Table 3.17: Average initially random, then greedy yearly used fuel by design in tonnes.

| Scenario | No Growth, Single | No Growth, Multiple | Double, Single | Double, Multiple |
|---|---|---|---|---|
| MMR HALEU | 0.185 | 0.185 | 1.115 | 1.063 |
| MMR LEU+ | – | – | – | 0.052 |
| Xe-100 HALEU | 1.882 | 1.882 | 13.549 | 13.419 |
| Xe-100 LEU+ | – | – | – | 0.176 |
| AP1000 LEU | 75.638 | 75.638 | 566.239 | 566.239 |

# Chapter 4

# Reactor Power and Market Interactions

In this chapter, we will explore how altering the frequency with which the CYCAMORE reactor interacts with the Dynamic Resource Exchange (DRE) in CYCLUS impacts the computational efficiency of a simulation and how to make the power output from a reactor more realistic.

## 4.1 Archetypes and Time Management

Throughout the CYCLUS ecosystem, archetypes interact with the DRE and each other in a fixed, user-defined time step, forcing the entire simulation to operate on the smallest universal time step. For example, if a fabrication facility can produce material every 2 months but the enrichment facility can only provide material every 3 months, we would need to use a 1-month time step to capture both. When the time step is smaller than the minimum for a given facility, that facility still participates in the DRE with a zero bid. These zero bids, across hundreds of facilities, add complexity and inefficiencies to solving the transaction problem at each time step.

Examining the CYCLUS ecosystem, we identified an archetype called PatternSink wherein the user can alter the frequency at which the sink, often called the repository, can accept the material. We have created an example of this archetype with a simple A-B-C scenario, shown in Figure 4.1. In this scenario, material is received from a source (A) to a reactor (B) with a final (C) sink that can only accept material at a specific frequency.

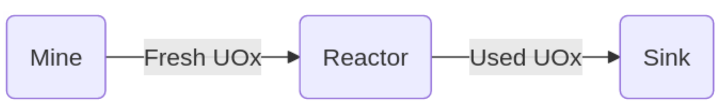


Figure 4.1: Simple A-B-C scenario.

If we track the material the sink receives, it becomes clear that this frequency alters how frequently the archetype updates its internal understanding of time. It appears in Figure 4.2 as though multiple groups of material are received in one time step despite this archetype not having an idea of individual shipments. This archetype accomplishes the artificial restriction on accepting material by simply not updating the time step that the archetype is at until the next universal time step is met. Regardless of function, this is the only example of the timekeeping flexibility we found in the ecosystem.

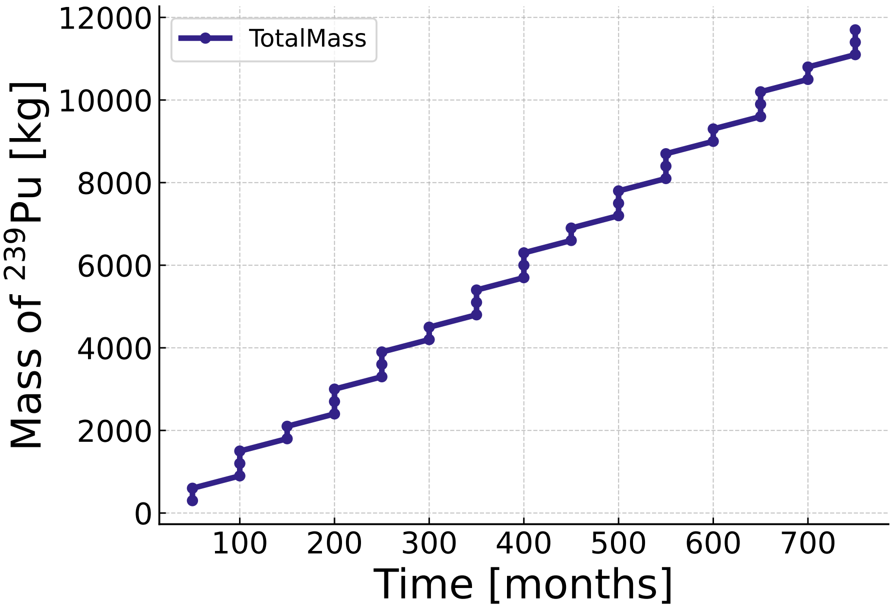


Figure 4.2: Acceptance of $^{239}$Pu into the sink with a frequency of 50 months.

While archetypes like PatternSink introduce new internal capabilities, they all inherit a set of base capabilities from the CYCLUS toolkit. The CYCLUS toolkit provides a modular and extensible framework for modeling nuclear fuel cycles (NFCs), allowing users to create custom archetypes that simulate various facilities and processes. These base capabilities standardize how archetypes create material buffers, interact with the DRE, and connect to the internal clock of the simulation, which are essential for coordinating the agents and commodities across their complex interactions within an NFC. In this work, we examine the fundamental toolkit capabilities of the CYCLUS ecosystem and identify time-intensive components of the current CYCAMORE Reactor. We also examine a modified reactor archetype we call the Trading On-Demand (TOD) reactor, that interacts with the DRE only when it is time to refuel.

The toolkit's modular architecture allows users to integrate new archetypes and models, promoting innovation and collaboration within the CYCLUS community. We will contribute a reactor archetype called Dynamic Power Reactor (DPR) to the ecosystem that can adjust the power of the reactor based on user inputs to better capture real fluctuations in reactor operation. Through this archetype, we will explore incorporating historical realism and allow for small timescale simulations to better capture the power output dynamics of the reactor fleet.

## 4.2 Trading On-Demand Reactor

We use Valgrind's [33] Callgrind [34] tool to profile a source-reactor-sink scenario and establish which parts of the CYCAMORE reactor code generate the most instructions. 52.27% of the 9,897,385,005 instructions come from the exchange manager in CYCLUS, and the reactor's tock (which appends each time step) is the source of 13.26% of the instructions. The reactor's tick (which pre-pends each time step) is the source of 4.66% of the instructions.

The basic structure of each time step is fundamental to aligning the material transactions and bids in the existing DRE, but we can find a way to reduce the computational cost of engaging with the tick and tock phases. This reduction comes from checking whether or not it is time to refuel before engaging with the calculations that take place when the reactor needs to refuel. This new archetype is called the TOD reactor, and when we performed the same analysis, tock was the source of 11.5% of the 9,519,845,814 instructions, while tick was the source of 2.77% of the instructions.

We ran ten duplicates of a simple source-reactor-sink scenario to further compare how the CYCAMORE and TOD reactors perform and collected statistics with the Linux tool Perf [29]. In these scenarios, CYCLUS deploys 1000 reactors over the first ten time steps, and the reactors operate for three time steps before refueling for two. This scenario demonstrates an intensive deployment to exacerbate the differences between the two reactor archetypes. The mean, maximum, minimum, and standard deviation of the time clock, number of instructions, and instructions per cycle are in Table 4.1.

Table 4.1: TOD reactor and CYCAMORE reactor profiles.

| Reactor | Metric | Mean | Max | Min | StDev |
|---|---|---|---|---|---|
| CYCAMORE Reactor | Time Clock [sec] | 3.286 | 3.333 | 3.242 | 0.026 |
| | Instructions | $1.209 \times 10^{10}$ | $1.211 \times 10^{10}$ | $1.207 \times 10^{10}$ | $1.328 \times 10^{7}$ |
| | Instructions per Cycle | 0.800 | 0.808 | 0.791 | 0.005 |
| TOD Reactor | Time Clock [sec] | 3.166 | 3.195 | 3.142 | 0.016 |
| | Instructions | $1.174 \times 10^{10}$ | $1.176 \times 10^{10}$ | $1.167 \times 10^{10}$ | $2.692 \times 10^{7}$ |
| | Instructions per Cycle | 0.807 | 0.811 | 0.801 | 0.003 |

The results in Table 4.1 indicate an average speedup of 1.038, going from the CYCAMORE reactor to the TOD reactor. As Figure 4.3 indicates, these time results are significant outside their combined standard deviations.

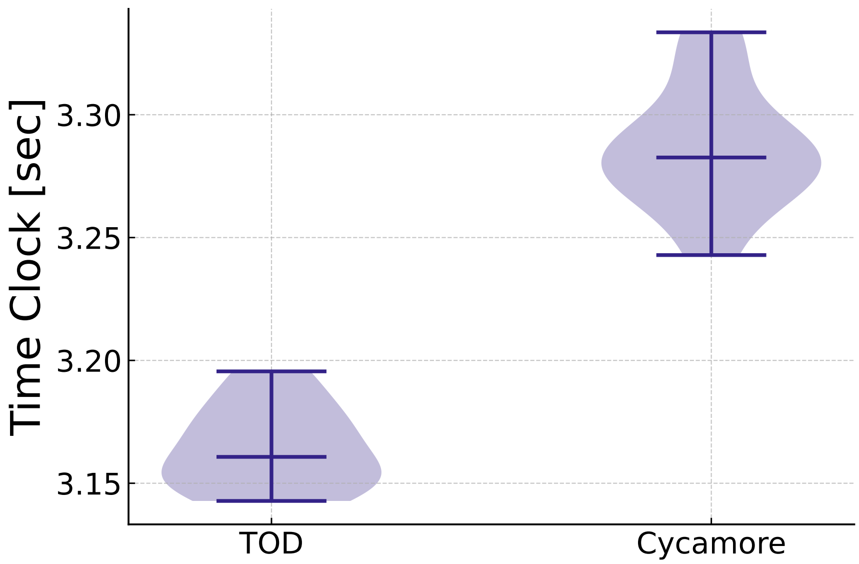


Figure 4.3: Time clock values for the TOD and CYCAMORE reactors.

The time clock values can vary by machine, architecture, and other demands during operation; however, the number of instructions issued using these archetypes, shown in Figure 4.4, is distinct between the TOD and CYCAMORE reactors and is specific to the code, not the machine. The distributions of instructions per cycle, presented alongside the instructions, overlap but indicate that the average TOD reactor simulation has a higher utilization than the CYCAMORE reactor.

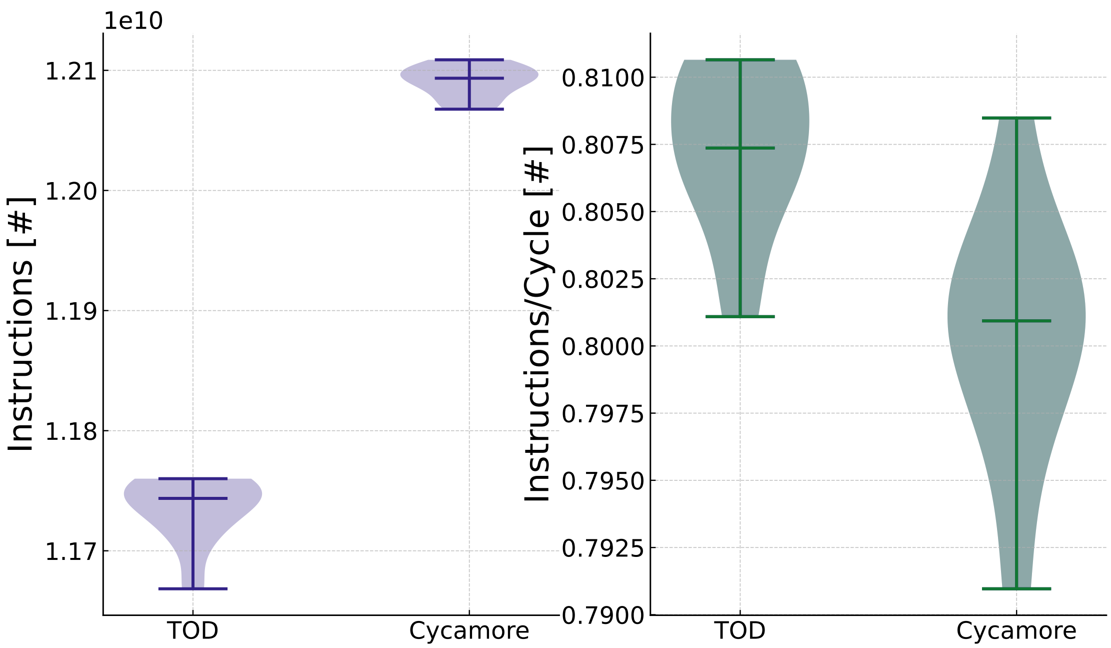


Figure 4.4: Number of instructions and instructions per cycle from the TOD and CYCAMORE reactors.

## 4.3 Dynamic Power Reactor

The U.S. Nuclear Regulatory Commission (NRC) publishes a daily Power Reactor Status report for each reactor under its jurisdiction [36]. These reports contain, amongst other things, the percentage of the total power capacity at which the operators say the reactor operated. In the case of a fuel cycle simulation containing a small number of reactors or a full-fleet simulation over a short time, the differences in the power predicted by the CYCAMORE reactor and reality can diverge.

In Figure 4.5, we examine the single reactor operating at the Clinton Clean Energy Center (Clinton), with a reference unit power capacity (i.e., net power) of 1062 MWe according to the International Atomic Energy Agency (IAEA) Power Reactor Information System (PRIS) database [25], and compare it to the results from the CYCAMORE reactor modeled over the same time frame. This figure excludes the startup of the CYCAMORE reactor, which we set several months before this window to ensure that it was operating on the same schedule as the data from the NRC suggest the reactor was operating from the start of 2021 through the end of 2024.

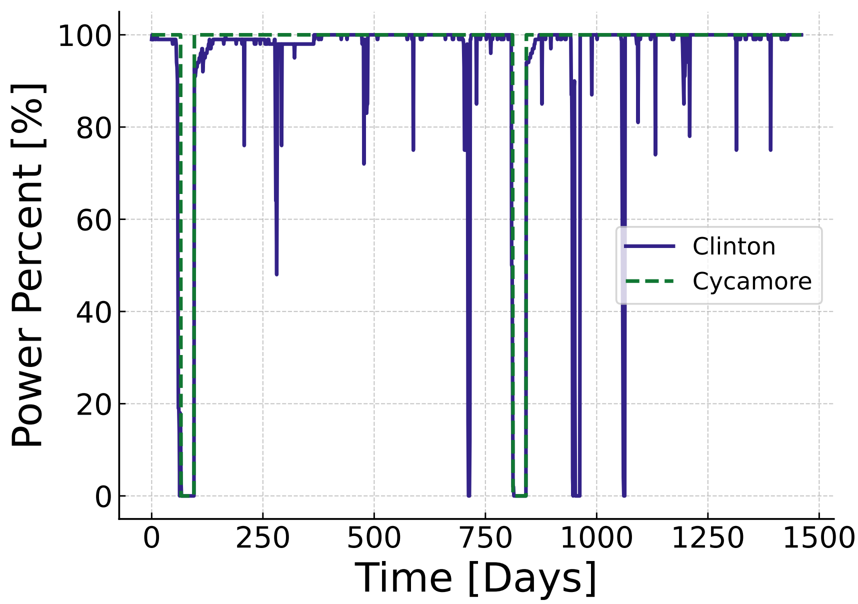


Figure 4.5: Clinton reactor daily power percent 2021-2024.

Performing a simple numerical integration, we find that the total energy capacity of both reactors differs by just under 51 GWe with a percent difference of 3.52%. This difference can be negated by comparing it to a base case, but for our small-scale model, users might be interested in incorporating realistic fluctuations in power and find that the two scenarios in Figure 4.5 were not equal on 908 days, or 62.2%, of the 1460-day simulation. For this work, we introduce the DPR to mirror this variability in power we see in Figure 4.5. DPR functions the same way as the CYCAMORE reactor, except the user can input the percentage of the total power capacity the reactor is outputting at any given time step.

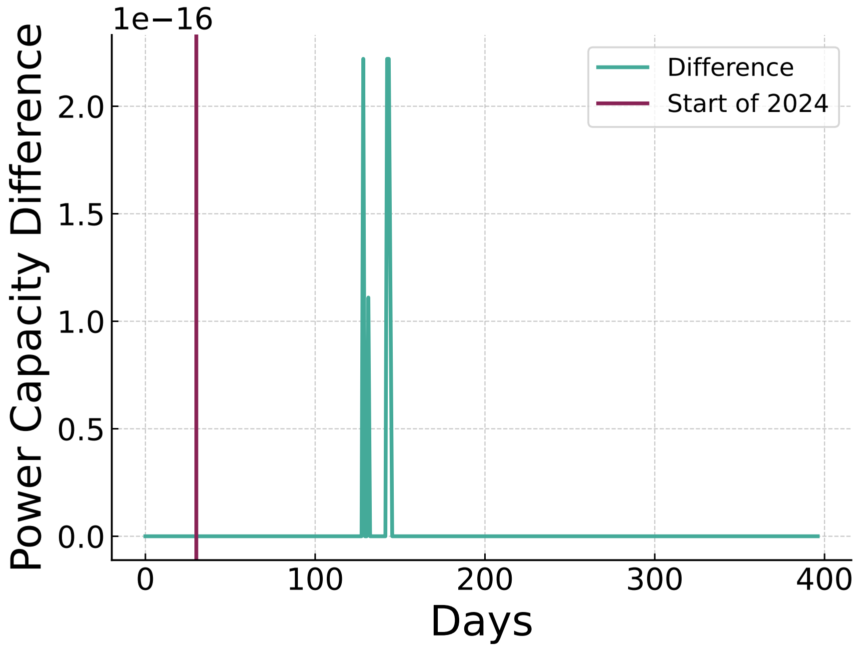


Figure 4.6: Difference in daily power capacity between DPR and Clinton.

If we narrow the scope of this study to 2024, Figure 4.6 shows how DPR replicates power capacity fluctuations with the difference between the reported values from the NRC [36] and the results from our CYCLUS simulation. The maximum difference between the two is $2.22 \times 10^{-16}$, which is explainable by floating point error in calculations as this value matches a double point machine epsilon value. Figure 4.7 compares DPR to the CYCAMORE reactor. As the reactors are assumed to start operations before 2024, we have added a buffer month in which the reactors fuel. With a vertical line, we indicate when 2024 begins to show the period over which we compare the results from CYCLUS.

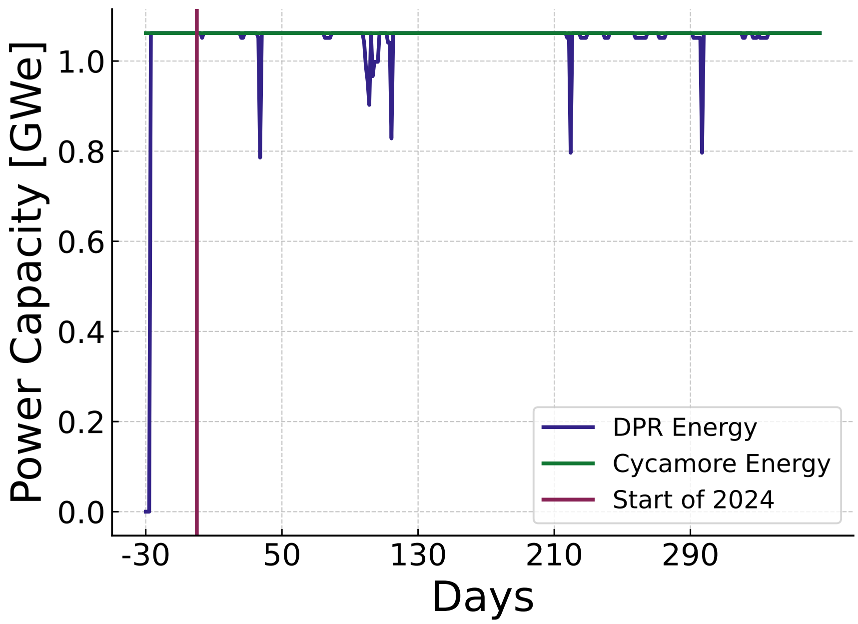


Figure 4.7: 2024 power capacity of the CYCAMORE reactor and DPR.

# Chapter 5

# Conclusions

## 5.1 Transition Scenarios Conclusions

In this work, we have characterized bounding scenarios of reactor deployment in the United States (U.S.) as we transition to a new fleet of nuclear reactors using an interstitial fuel cycle involving low-enriched uranium plus (LEU+) TRi-structural ISOtropic (TRISO) fuel. The results of this work show that the reactor deployment scheme has an understandable and identifiable impact on the separative work units (SWU) required to meet the energy demand.

In the transition scenarios of this work, we propose a series of fuel cycles that include and contextualize the deployment of new nuclear reactors in the U.S. using TRISO fuels at high-assay low-enriched uranium (HALEU) and LEU+ enrichment levels. These fuel cycles meet the energy demand growths predicted by the U.S. Energy Information Administration (EIA) and the U.S. Department of Energy (DOE). The increase in demand assumes that nuclear energy's generation share remains constant over time. When we say a 15% increase in demand, we mean a 15% increase in nuclear energy generation (as the EIA numbers [58] reflect the total energy demand, this conversion is only possible by assuming that the percentage share of nuclear capacity is the same). This assumption is not reflected in the demand scenarios from the DOE liftoff report [26], which are specific to nuclear deployment increases, and the number is agnostic to the total increase. The liftoff report scenarios are assumed to continue beyond the initial 2050 projection.

The Light Water Reactor (LWR) fleet deviates from reality as we assume they all have regular 18-month cycles with regular 1-month outages. Related to this consistent cycle length, we assume that the reactors have constant power outputs (when not in an outage) over their lifetime. Each LWR has an assembly size of 427.38589211618256 and a batch size of 80, further normalizing the fleet. After 2024, no new LWRs will be built other than the AP1000s deployed under the various schemes.

We assume that the supply chain is not a limiting factor in new reactors. This allows us to characterize the upper bound of what needs to be in place to achieve the projected deployment scenarios. Additionally, we treat the fabrication and enrichment of fuel as a black box, not factoring in variations in time, resources, or regulations associated with the fuels included.

We based the models used for the Micro Modular Reactor (MMR) and X-Energy Xe-100 (Xe-100) Serpent simulations on limited publicly available information and do not rely on confidential or proprietary data, another limitation is they assume that when the reactors accept LEU+ fuel and operate with the same power levels and burnup rates. As we have discussed, the intended use of many advanced reactors extends beyond simply meeting energy demand, so modeling them entirely in on-the-grid applications is not necessarily the only way they will deploy. These reactors could provide a range of services that can contribute to decarbonizing the economy.

The result of these assumptions is that we expect the changes in SWU to be the most significant metric to compare the scenarios. In Table 5.1, we show the average yearly percentage SWU increases from the no-growth scenario to the double scenario. We can see the impacts of the deployment scheme in these values, where the greedy scheme regularly prefers the highest capacity reactors, leading to the most significant increase in the SWU for AP1000 low-enriched uranium (LEU). The randomness in the other two schemes levels the reactor preferences and leads to more consistent increases across fuel types.

Table 5.1: Average yearly percentage SWU increases from the no-growth scenario to the double scenario.

| Scheme | MMR HALEU | Xe-100 HALEU | AP1000 LEU |
|---|---|---|---|
| Greedy Deployment | 105% | 167% | 800% |
| Random Deployment | 1511% | 796% | 697% |
| Initially Random Greedy | 775% | 672% | 696% |

### 5.1.1 Future Work

This work could be expanded in various ways to contextualize the deployment of advanced reactors in the U.S.. Outside of simply removing the assumptions outlined above, two immediate additions to this work would be to incorporate isotope calculations for used fuel to understand the accumulation of isotopes of interest. This would allow for a more detailed understanding of the waste stream and the potential for recycling. The second addition would be to compare the no growth and double nuclear scenarios to the triple nuclear scenario from the DOE liftoff report [26]. These two additions were not included in this work due to computational limitations and the sheer size of the data needed.

The next steps in expanding this work would be to translate the base metrics presented here (SWU, mass, energy, and deployment) into costs for fuel and energy. The mass of used fuel would be a good starting point for repository space considerations and transportation costs. This work could leverage CYCLUS's ability to track latitude and longitude to understand the transportation time between facilities.

As we highlighted in our discussion of LEU+, the categories of enrichment facilities are critical components in the cost and logistics of a fuel cycle. SWU is a good starting point for understanding the relative effort required to deploy the reactors, but the cost of that effort is a critical component of the deployment for making policy recommendations. Combining SWU and masses of fuel, we can start to understand how international cooperation with nations that have existing enrichment facilities could help the U.S. meet its energy goals.

## 5.2 Reactor Power and Market Interaction Conclusions

As we identified in Section 4.2, the CYCAMORE reactor enters the tick and tock phases of each time step whether or not it is time to refuel. We performed the same analysis on the Trading On-Demand (TOD) reactor and uncovered that both the tick and tock phases were the source of less instructions than the CYCAMORE reactor. Overall, our analysis shows that the TOD reactor archetype represents an alteration in the logic of the widely used CYCAMORE reactor that increases the utilization, decreases the number of instructions, and maintains consistent performance with the CYCAMORE reactor.

With the 2024 test case examining the power output of the Clinton Clean Energy Center (Clinton), we identified in Section 4.3 that the CYCAMORE reactor's constant power capacity results in a 3.52% difference between the cumulative power capacity of Clinton and the CYCAMORE reactor modeling Clinton. By introducing the Dynamic Power Reactor (DPR), we are able to replicate historic and realistic power outputs from a reactor with the only differences between DPR and Clinton arising from floating point error below the machine epsilon.

### 5.2.1 Future Work

In the future, the TOD effort can be expanded to find other ways to reduce the number of instructions germane to the simulation; our profiling revealed that the exchange method for the Dynamic Resource Exchange (DRE) was routinely a larger source of instructions than the tick and tock methods. Outside of the reactor, incorporating checks in other fuel cycle facilities would be the next step to allowing users to develop complex purchasing agreements restricted by external factors other than material availability.

The DPR is currently a stand-alone implementation of historical variation, and future work could contribute a method to generate realistic predictions of power capacity over time for the LWR fleet. There is also a need to apply this method to creating bounding cases for the advanced reactor fleet that we propose in Section 2.5, although each reactor model will exhibit different behavior that would require additional work to characterize. With this feature, the number of reactors deployed to meet demand can mirror the anticipated planning utilities will engage with. Outside of power capacity variation, the current scheme approximates the output and usage of fuel as constant over time, and implementing a similar variability in the masses and burnups of fuel, as we discuss in Section 2.6.1, would strengthen the conclusions of future CYCLUS simulations.

# References

[1] Amanda M. Bachmann, O. Y. and Munk, M. (2024). An open-source coupling for depletion during fuel cycle modeling. *Nuclear Science and Engineering*, 0(0):1–14.

[2] Bachmann (2023a). MMR-like Serpent Model.

[3] Bachmann, A. M. (2023b). *Investigation of the impacts of deploying reactors fueled by high-assay low enriched uranium.* Thesis, University of Illinois at Urbana-Champaign.

[4] Bachmann, A. M., Fairhurst-Agosta, R., Richter, Z., Ryan, N., and Munk, M. (2021). Enrichment dynamics for advanced reactor HALEU support. *EPJ Nuclear Sciences & Technologies*, 7:22.

[5] Bae, J. W., Rykhlevskii, A., Chee, G., and Huff, K. D. (2020). Deep learning approach to nuclear fuel transmutation in a fuel cycle simulator. *Annals of Nuclear Energy*, 139.

[6] Carlsen, R. W., Gidden, M., Huff, K., Opotowsky, A. C., Rakhimov, O., Scopatz, A. M., and Wilson, P. (2014). Cycamore v1.0.0. *Figshare*.

[7] Costa Peluzo, B. M. T. and Kraka, E. (2022). Uranium: The Nuclear Fuel Cycle and Beyond. *International Journal of Molecular Sciences*, 23(9):4655. Number: 9 Publisher: Multidisciplinary Digital Publishing Institute.

[8] Demkowicz, P. A., Liu, B., and Hunn, J. D. (2019). Coated particle fuel: Historical perspectives and current progress. *Journal of Nuclear Materials*, 515:434–450.

[9] Dotson, S. G. and Munk, M. (2024). Osier: A python package for multi-objective energy system optimization. *Journal of Open Source Software*, 9(104):6919.

[10] EIA Electricity Supply & Uranium Statistics & Product Innovation Team (2024). 2023 Domestic Uranium Production Report. Technical report, US Energy Information Administration.

[11] Eisenhower, P. D. D. (1953). Atoms for Peace Speech. Publisher: IAEA.

[12] European Commission. Joint Research Centre. (2021). *GHG emissions of all world: 2021 report.* Publications Office, LU.

[13] F. B. Daniels (1944). Suggestions for a High-Temperature Pebble Pile. Technical report, The University of Chicago Metallurgical Laboratory, Chicago, IL.

[14] Farokhi Soofi, A., D. Manshadi, S., and Saucedo, A. (2022). Farm electrification: A road-map to decarbonize the agriculture sector. *The Electricity Journal*, 35(2):107076.

[15] Feng, B., Dixon, B., Sunny, E., Cuadra, A., Jacobson, J., Brown, N. R., Powers, J., Worrall, A., Passerini, S., and Gregg, R. (2016). Standardized verification of fuel cycle modeling. *Annals of Nuclear Energy*, 94:300–312.

[16] Framatome (2024). Press Release: Framatome's enhanced accident tolerant fuel assemblies first to complete lifecycle operations in U.S.

[17] GFP Limited (2019). Project Description for the Micro Modular Reactor™ Project at Chalk River. Technical Report CRP-LIC-01-001, Global First Power, Chalk River.

[18] Gurban, I. and Laaksoharju, M. (2001). Hydrochemical stability of groundwaters surrounding a spent nuclear fuel repository in a 100,000 year perspective. Technical Report 951-652-107-X, POSIVA OY, Finland. POSIVA–01-06 INIS Reference Number: 33020732.

[19] Helm, D. (2002). Energy policy: security of supply, sustainability and competition. *Energy Policy*, 30(3):173–184.

[20] Hiraishi, T., Nyenzi, B., Gillet, M., Meijer, J., Pullus, T., Simmons, T., Tichy, M., Adi, A. C., Chandra, M., Emmanuel, S., Fontelle, J.-P., Fott, P., Lamotta, S., Lieberman, E., Mareckova, K., Amous, S., Olsson, A., Hossain, I., Gomez, D., Miroslav, M., Oi, M., Rajarathnam, U., Tuhkanen, S., Zhang, J., Walsh, M., Mowafy, S., and Eggleston, S. (2000). Good Practice Guidance and Uncertainty Management in National Greenhouse Gas Inventories. Technical report, Task Force on National Greenhouse Gas Inventorie, Intergovernmental Panel on Climate Change.

[21] Honnold, P., Crabtree, L., Higgins, M., Williams, A., Finch, R., Cipiti, B., Ammerman, D., Farnum, C., Kalinina, E., Ruehl, M., and Hawthorne, K. (2022). PRO-X Fuel Cycle Transportation and Crosscutting Progress Report. Technical Report SAND2022-13387R, 1890069, 710373, Sandia National Laboratories.

[22] Huff, K. D., Gidden, M. J., Carlsen, R. W., Flanagan, R. R., McGarry, M. B., Opotowsky, A. C., Schneider, E. A., Scopatz, A. M., and Wilson, P. P. H. (2016). Fundamental concepts in the Cyclus nuclear fuel cycle simulation framework. *Advances in Engineering Software*, 94:46–59.

[23] Hyland, B., Edwards, G., Kitson, C., and Chshyolkova, T. (2013). Post-closure performance assessment of a deep geological repository for advanced heavy water reactor fuels. Technical report, Canadian Nuclear Laboratories, Canada. AECL-CW–10192-CONF-001 INIS Reference Number: 49101296.

[24] IAEA (2016). List of Member States. Publisher: IAEA.

[25] International Atomic Energy Agency, I. (2024). Power reactor information system (pris) database. Accessed: 2024-09-30.

[26] Julie Kozeracki, Chris Vlahoplus, Ken Erwin, Alan Propp, Sonali Razdan, Rasheed Auguste, Tim Stuhldreher, Christina Walrond, Melissa Bates, Erica Bickford, Andrew Foss, Derek Gaston, Cheryl Herman, Rory Stanley, Billy Valderrama, Katheryn Scott, Tomotaroh Granzier-Nakajima, Paul Donohoo-Vallett, Tom Fanning, Brent Dixon, Abdalla Abou Jaoude, and Chris Lohse (2024). Pathways to Commercial Liftoff: Advanced Nuclear. *DOE Liftoff Report*.

[27] Laha, P. and Chakraborty, B. (2017). Energy model – A tool for preventing energy dysfunction. *Renewable and Sustainable Energy Reviews*, 73:95–114.

[28] Li, G. and Yao, J. (2024). A Review of In Situ Leaching (ISL) for Uranium Mining. *Mining*, 4(1):120–148. Number: 1 Publisher: Multidisciplinary Digital Publishing Institute.

[29] Linux Foundation (2025). perf. `https://perf.wiki.kernel.org/`. Version 6.8.12.

[30] López-Luna, J., Francois, J.-L., Castillo, A., and Ortiz-Servin, J. J. (2025). Design of a 24-month equilibrium cycle of a bwr with extended low enrichment fuel using metaheuristic optimization techniques. *Annals of Nuclear Energy*, 213:111129.

[31] Mallapragada, D. S., Dvorkin, Y., Modestino, M. A., Esposito, D. V., Smith, W. A., Hodge, B.-M., Harold, M. P., Donnelly, V. M., Nuz, A., Bloomquist, C., Baker, K., Grabow, L. C., Yan, Y., Rajput, N. N., Hartman, R. L., Biddinger, E. J., Aydil, E. S., and Taylor, A. D. (2023). Decarbonization of the chemical industry through electrification: Barriers and opportunities. *Joule*, 7(1):23–41.

[32] NEA (2023) (2023). Uranium 2022: Resources, Production and Demand. Biannual 29, OECD Publishing, Paris.

[33] Nethercote, N. and Seward, J. (2007). Valgrind: a framework for heavyweight dynamic binary instrumentation. In *Proceedings of the 28th ACM SIGPLAN Conference on Programming Language Design and Implementation*, PLDI '07, pages 89–100, New York, NY, USA. Association for Computing Machinery.

[34] Nethercote, N., Walsh, R., and Fitzhardinge, J. (2006). Building workload characterization tools with valgrind. In *Proceedings of the 2006 IEEE International Symposium on Workload Characterization, IISWC 2006, October 25-27, 2006, San Jose, California, USA*, page 2. IEEE Computer Society.

[35] Nuclear Regulatory Commission (2017). 10 CFR § 70.4 Definitions.

[36] Nuclear Regulatory Commission (2025). Power Reactor Status Reports.

[37] NuScale (2018). Chapter One Introduction and General Description of the Plant.

[38] Papadis, E. and Tsatsaronis, G. (2020). Challenges in the decarbonization of the energy sector. *Energy*, 205:118025.

[39] Pfenninger, S., Hawkes, A., and Keirstead, J. (2014). Energy systems modeling for twenty-first century energy challenges. *Renewable and Sustainable Energy Reviews*, 33:74–86.

[40] Plazas-Niño, F. A., Ortiz-Pimiento, N. R., and Montes-Páez, E. G. (2022). National energy system optimization modelling for decarbonization pathways analysis: A systematic literature review. *Renewable and Sustainable Energy Reviews*, 162:112406.

[41] Posner, M. V. (1973). Fuel policy. A study in applied economics. *ETDEWEB World Energy Base*.

[42] Price, M. S. T. (2012). The Dragon Project origins, achievements and legacies. *Nuclear Engineering and Design*, 251:60–68.

[43] Regalbuto, M. C. (2020). High-Assay Low Enriched Uranium Demand and Deployment Options 2020 HALEU Workshop Report. Technical Report INL/EXT-21-61768, Idaho National Laboratory, Idaho National Laboratory.

[44] Richards, S. and Feng, B. (2021). Application of sensitivity analysis in DYMOND/Dakota to fuel cycle transition scenarios. *EPJ Nuclear Sciences & Technologies*, 7:26. Published: = https://www.epj-n.org/articles/epjn/abs/2021/01/epjn210022/epjn210022.html.

[45] Richter, Z. (2022a). ISOTOPIC AND REACTOR PHYSICS CHARACTERIZATION OF A GAS-COOLED, PEBBLE-BED MICROREACTOR. *UIUC Ideals*.

[46] Richter, Z. (2022b). Isotopic fuel compositions in the sangamon200 model.

[47] Romano, P. K., Horelik, N. E., Herman, B. R., Nelson, A. G., Forget, B., and Smith, K. (2015). OpenMC: A state-of-the-art Monte Carlo code for research and development. *Annals of Nuclear Energy*, 82:90–97.

[48] Schneider, E. and Scopatz, A. (2016). An Integrated Fuel Depletion Calculator for Fuel Cycle Options Analysis. Technical Report 12-4065, 1258475, battelle Energy Alliance, LLC.

[49] Schneider, E. A., Bathke, C. G., and James, M. R. (2005). NFCSim: A Dynamic Fuel Burnup and Fuel Cycle Simulation Tool. *Nuclear Technology*, 151(1):35–50.

[50] Shaw, A. M. and Clarity, J. B. (2022). Impacts of leu+ and atf on fresh fuel storage criticality safety. Technical report, Oak Ridge National Laboratory (ORNL), Oak Ridge, TN (United States).

[51] Skutnik, S. E., Sly, N. C., and Littell, J. L. (2016). CyBORG: An ORIGEN-Based Reactor Analysis Capability for Cyclus. In *Transactions of the American Nuclear Society*, volume 115 of *Fuel Cycle and Waste Management: General—II*, pages 299–301, Las Vegas, Nevada, United States. American Nuclear Society.

[52] Texas Comptroller of Public Accounts, T. (2023). ERCOT: Texas Energy Tour of Economy.

[53] Treasury, G. B. (1967). *Nationalised Industries: A Review of Economic and Financial Objectives*. C (Series) (Great Britain. Parliament). H.M. Stationery Office.

[54] Ultra Safe Nuclear Corporation (2021). USNC Micro Modular Reactor (MMR™ Block 1) Technical Information. *USNC*, page 36.

[55] Ultra Safe Nuclear Corporation (2024). USNC: Press & News, Media Kit.

[56] U.S. Department of Energy (2024). Biden-Harris Administration Invests $1.5 Billion to Bolster the Nation's Electricity Grid and Deliver Affordable Electricity to Meet New Demands.

[57] U.S. Department of Energy, Grid Deployment Office (2024). National Transmission Planning Study. Technical report, U.S. Department of Energy, Washington D.C. United States.

[58] U.S. Energy Information Administration (2023a). Annual Energy Outlook 2023. Government, U.S. Energy Information Administration.

[59] U.S. Energy Information Administration (2023b). Statement on the Annual Energy Outlook and EIA plan to enhance long-term modeling capabilities.

[60] U.S. Energy Information Administration (2024). Monthly Energy Review September 2024. Technical Report DOE/EIA-0035(2024/9), U.S.Energy Information Administration.

[61] US Energy Information Administration (2024). U.S. EIA What is U.S. electricity generation by energy source?

[62] X-Energy (2024). X-Energy Media Kit (Triso-X).

[63] X-energy (2024). X-Energy Media Kit (Xe-100).

[64] Yacout, A., Jacobson, J., Matthern, G., Piet, S., Shropshire, D., and Laws, C. (2006). VISION–Verifiable Fuel Cycle Simulation of Nuclear Fuel Cycle Dynamics. *Waste Management*.

[65] York, R. (2012). Do alternative energy sources displace fossil fuels? *Nature Climate Change*, 2(6):441–443. Number: 6 Publisher: Nature Publishing Group.

[66] York, R. and Bell, S. E. (2019). Energy transitions or additions?: Why a transition from fossil fuels requires more than the growth of renewable energy. *Energy Research & Social Science*, 51:40–43.

# Appendix A

# LWRs Simulated

In this work we pull publicly available information from the Power Reactor Information System (PRIS) database to simulate the Light Water Reactor (LWR) fleet in the United States (U.S.). The PRIS database is a collection of information on nuclear power plants around the world, and is maintained by the International Atomic Energy Agency (IAEA). For the sake of completeness and replication of this work in Tables A.1, A.2, and A.3; we have also included the LWR fleet that we have simulated in this work and a notebook is available on GitHub (((((((((((cite))))))))))) to pull the same information we used.

Table A.1: LWR fleet simulated, A-K.

| Name | State | Type | Vendor | Core size | Startup date | License | Shut Down | Power cap |
|---|---|---|---|---|---|---|---|---|
| ANO 1 | AR | PWR | B&W | 177 | 1974 | 2034 | | 836.0 |
| ANO 2 | AR | PWR | CE | 177 | 1978 | 2038 | | 988.0 |
| Beaver Valley 1 | PA | PWR | WE | 157 | 1976 | 2036 | | 908.0 |
| Beaver Valley 2 | PA | PWR | WE | 157 | 1987 | 2047 | | 905.0 |
| Big Rock Point | MI | BWR | GE | 84 | 1964 | | 1997 | 67.0 |
| Braidwood 1 | IL | PWR | WE | 193 | 1987 | 2046 | | 1194.0 |
| Braidwood 2 | IL | PWR | WE | 193 | 1988 | 2047 | | 1160.0 |
| Browns Ferry 1 | AL | BWR | GE | 764 | 1973 | 2033 | | 1200.0 |
| Browns Ferry 2 | AL | BWR | GE | 764 | 1974 | 2034 | | 1200.0 |
| Browns Ferry 3 | AL | BWR | GE | 764 | 1976 | 2036 | | 1210.0 |
| Brunswick 1 | NC | BWR | GE | 560 | 1976 | 2036 | | 938.0 |
| Brunswick 2 | NC | BWR | GE | 560 | 1974 | 2034 | | 932.0 |
| Byron 1 | IL | PWR | WE | 193 | 1985 | 2044 | | 1164.0 |
| Byron 2 | IL | PWR | WE | 193 | 1987 | 2046 | | 1136.0 |
| Callaway | MO | PWR | WE | 193 | 1984 | 2044 | | 1215.0 |
| Calvert Cliffs 1 | MD | PWR | CE | 217 | 1974 | 2034 | | 877.0 |
| Calvert Cliffs 2 | MD | PWR | CE | 217 | 1976 | 2036 | | 855.0 |
| Catawba 1 | SC | PWR | WE | 193 | 1985 | 2043 | | 1160.0 |
| Catawba 2 | SC | PWR | WE | 193 | 1986 | 2043 | | 1150.0 |
| Clinton 1 | IL | BWR | GE | 624 | 1987 | 2026 | | 1062.0 |
| Columbia | WA | BWR | GE | 764 | 1984 | 2043 | | 1131.0 |
| Comanche Peak 1 | TX | PWR | WE | 193 | 1990 | 2030 | | 1205.0 |
| Comanche Peak 2 | TX | PWR | WE | 193 | 1993 | 2033 | | 1195.0 |
| Cook 1 | MI | PWR | WE | 193 | 1974 | 2034 | | 1030.0 |
| Cook 2 | MI | PWR | WE | 193 | 1977 | 2037 | | 1168.0 |
| Cooper Station | NE | BWR | GE | 548 | 1974 | 2034 | | 769.0 |
| Crystal River 3 | FL | PWR | B&W | 177 | 1976 | | 2013 | 860.0 |
| Davis-Besse | OH | PWR | B&W | 177 | 1977 | 2037 | | 894.0 |
| Diablo Canyon 1 | CA | PWR | WE | 193 | 1984 | 2024 | | 1138.0 |
| Diablo Canyon 2 | CA | PWR | WE | 193 | 1985 | 2025 | | 1118.0 |
| Dresden 1 | IL | BWR | GE | 464 | 1959 | 2029 | 1978 | 197.0 |
| Dresden 2 | IL | BWR | GE | 724 | 1969 | 2029 | | 894.0 |
| Dresden 3 | IL | BWR | GE | 724 | 1971 | 2031 | | 879.0 |
| Duane Arnold | IA | BWR | GE | 368 | 1974 | 2034 | 2020 | 601.0 |

Table A.2: LWR fleet simulated, L-St.

| Name | State | Type | Vendor | Core size | Startup date | License | Shut Down | Power cap |
|---|---|---|---|---|---|---|---|---|
| La Crosse | WI | BWR | AC | 72 | 1967 | | 1987 | 48.0 |
| LaSalle County 1 | IL | BWR | GE | 764 | 1982 | 2042 | | 1137.0 |
| LaSalle County 2 | IL | BWR | GE | 764 | 1983 | 2043 | | 1140.0 |
| Limerick 1 | PA | BWR | GE | 764 | 1985 | 2044 | | 1134.0 |
| Limerick 2 | PA | BWR | GE | 764 | 1989 | 2049 | | 1134.0 |
| Maine Yankee | ME | PWR | CE | 217 | 1973 | | 1996 | 860.0 |
| McGuire 1 | NC | PWR | WE | 193 | 1981 | 2041 | | 1158.0 |
| McGuire 2 | NC | PWR | WE | 193 | 1983 | 2043 | | 1158.0 |
| Millstone 1 | CT | BWR | GE | 580 | 1970 | | 1998 | 641.0 |
| Millstone 2 | CT | PWR | CE | 217 | 1975 | 2035 | | 869.0 |
| Millstone 3 | CT | PWR | WE | 193 | 1986 | 2045 | | 1210.0 |
| Monticello | MN | BWR | GE | 484 | 1970 | 2030 | | 628.0 |
| Nine Mile Point 1 | NY | BWR | GE | 532 | 1969 | 2029 | | 613.0 |
| Nine Mile Point 2 | NY | BWR | GE | 764 | 1987 | 2046 | | 1277.0 |
| North Anna 1 | VA | PWR | WE | 157 | 1978 | 2038 | | 948.0 |
| North Anna 2 | VA | PWR | WE | 157 | 1980 | 2040 | | 944.0 |
| Oconee 1 | SC | PWR | B&W | 177 | 1973 | 2033 | | 847.0 |
| Oconee 2 | SC | PWR | B&W | 177 | 1973 | 2033 | | 848.0 |
| Oconee 3 | SC | PWR | B&W | 177 | 1974 | 2034 | | 859.0 |
| Oyster Creek | NJ | BWR | GE | 560 | 1969 | 2029 | 2018 | 619.0 |
| Palisades | MI | PWR | CE | 204 | 1971 | 2031 | | 805.0 |
| Palo Verde 1 | AZ | PWR | CE | 241 | 1985 | 2045 | | 1311.0 |
| Palo Verde 2 | AZ | PWR | CE | 241 | 1986 | 2046 | | 1314.0 |
| Palo Verde 3 | AZ | PWR | CE | 241 | 1987 | 2047 | | 1312.0 |
| Peach Bottom 2 | PA | BWR | GE | 764 | 1973 | 2053* | | 1300.0 |
| Peach Bottom 3 | PA | BWR | GE | 764 | 1974 | 2054* | | 1331.0 |
| Perry 1 | OH | BWR | GE | 748 | 1986 | 2026 | | 1240.0 |
| Pilgrim 1 | MA | BWR | GE | 580 | 1972 | 2032 | 2019 | 677.0 |
| Point Beach 1 | WI | PWR | WE | 121 | 1970 | 2030 | | 591.0 |
| Point Beach 2 | WI | PWR | WE | 121 | 1971 | 2033 | | 591.0 |
| Prairie Island 1 | MN | PWR | WE | 121 | 1973 | 2033 | | 522.0 |
| Prairie Island 2 | MN | PWR | WE | 121 | 1974 | 2034 | | 519.0 |
| Quad Cities 1 | IL | BWR | GE | 724 | 1972 | 2032 | | 908.0 |
| Quad Cities 2 | IL | BWR | GE | 724 | 1972 | 2032 | | 911.0 |

Table A.3: LWR fleet simulated, Su-Z.

| Name | State | Type | Vendor | Core size | Startup date | License | Shut Down | Power cap |
|---|---|---|---|---|---|---|---|---|
| Summer 1 | SC | PWR | WE | 157 | 1982 | 2042 | | 973.0 |
| Surry 1 | VA | PWR | WE | 157 | 1972 | 2032 | | 838.0 |
| Surry 2 | VA | PWR | WE | 157 | 1973 | 2033 | | 838.0 |
| Susquehanna 1 | PA | BWR | GE | 764 | 1982 | 2042 | | 1257.0 |
| Susquehanna 2 | PA | BWR | GE | 764 | 1984 | 2044 | | 1257.0 |
| TMI 1 | PA | PWR | B&W | 177 | 1974 | 2034 | 2019 | 819.0 |
| TMI 2 | PA | PWR | B&W | 177 | 1978 | 2038 | 1979 | 880.0 |
| Trojan | OR | PWR | WE | 193 | 1975 | | 1992 | 1095.0 |
| Turkey Point 3 | FL | PWR | WE | 157 | 1972 | 2052* | | 837.0 |
| Turkey Point 4 | FL | PWR | WE | 157 | 1973 | 2053* | | 821.0 |
| Vermont Yankee | VT | BWR | GE | 368 | 1972 | 2032 | 2014 | 605.0 |
| Vogtle 1 | GA | PWR | WE | 193 | 1987 | 2047 | | 1150.0 |
| Vogtle 2 | GA | PWR | WE | 193 | 1989 | 2049 | | 1117.0 |
| Vogtle 3 | GA | PWR | WE | 193 | 2023 | 2062 | | 1117.0 |
| Vogtle 4 | GA | PWR | WE | 193 | 2024 | 2063 | | 1117.0 |
| Waterford 3 | LA | PWR | CE | 217 | 1985 | 2044* | | 1168.0 |
| Watts Bar 1 | TN | PWR | WE | 193 | 1996 | 2035 | | 1157.0 |
| Watts Bar 2 | TN | PWR | WE | 193 | 2016 | 2055 | | 1164.0 |
| Wolf Creek 1 | KS | PWR | WE | 193 | 1985 | 2045 | | 1200.0 |
| Yankee Rowe | MA | PWR | WE | 76 | 1960 | | 1991 | 167.0 |
| Zion 1 | IL | PWR | WE | 193 | 1973 | | 1997 | 1040.0 |
| Zion 2 | IL | PWR | WE | 193 | 1973 | | 1996 | 1040.0 |

# Appendix B

# Considered Deployment Schemes

In addition to the deployment schemes outlined in 3.3, 3.4, and 3.5, we also considered a few others that we did not include in the final analysis. We examined these schemes for their potential to capture the complexity of the deployment problem but were ultimately not included due to the egregious nature of approximation required to implement or the lack of a clear benefit over the other schemes for the questions explored in this work.

## B.1 Capped Deployment

This scheme places a constant limit on the number of specific reactors deployed at any given time step. This is a simple way to model aggregate supply chain constraints that could limit vendors from deploying reactors freely. With the right constraints, this scheme would better succeed at roughly incorporating the limits of a workforce over a short to medium time scale. As workforce constraints are outside the scope of this work, we implement this scheme but do not incorporate it into this work.

To use this deployment scheme, a user needs to understand the supply chain constraints that will limit the deployment of the reactors they are deploying. We illustrate the defining steps of the capped deployment scheme in Figure B.1. The main loop in the logic is consistent with the greedy deployment scheme but adds a check to see if the current deployment exceeds the limit on that reactor. If it does, the reactor is removed from the list of reactors to be deployed in that time step.

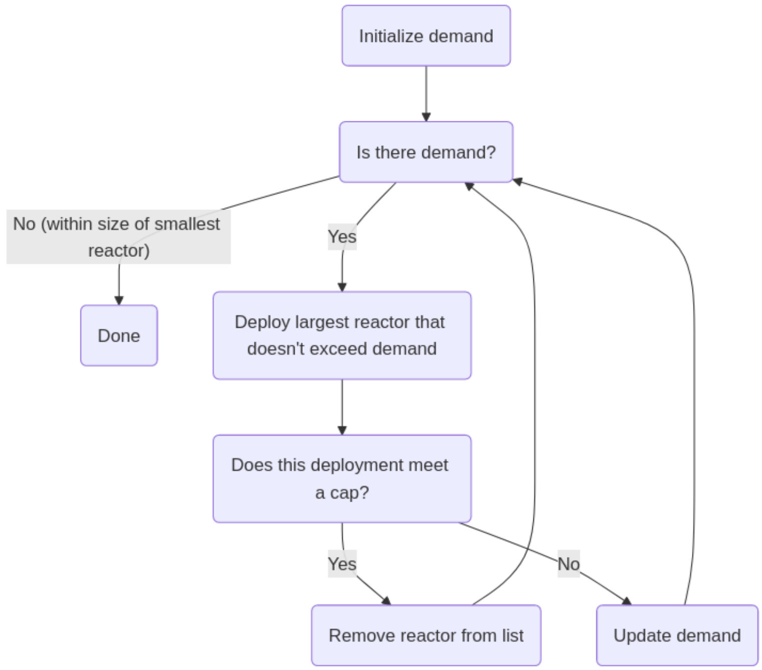


Figure B.1: Capped deployment diagram.

The realism of this deployment scheme mirrors some elements of the pre-determined distribution (this is a flat distribution after all), but the cap is a less granular way to account for supply chain constraints. This scheme is most useful for scenarios or timescales where there is a known limit on the workforce. The unrealistic element of this deployment scheme comes from two places: 1) the current implementation requires one reactor to be unrestrained (preferably the smallest reactor from the deployment standpoint); 2) the cap is a flat distribution, which is not a realistic representation of the supply chain constraints for most technologies.

When the unconstrained reactor is not the smallest power reactor, this scheme will fall below demand moreso than when the unconstrained reactor is the smallest in power. This scheme has the potential to overperform by one reactor in the case where the unconstrained reactor is the smallest in power as it can over-deploy by one reactor's capacity in that case.

## B.2 Pre-Determined Distribution Deployment

This deployment scheme allows users to incorporate the projections and commitments of ratepayers and utilities by setting a distribution over the simulation time. In this scheme, the distribution serves as a cap to the number of reactors deployed in a time step, and we preferentially deploy reactors first to meet those caps. After completion, we deploy the remaining reactors without caps to meet the demand. In this way, we incorporate knowledge of supply chain constraints for specific technologies without having to model the supply chain in detail.

To use this deployment scheme, a user needs some idea of the distribution of reactors deployed over the simulation time. We illustrate the defining steps of the pre-determined distribution deployment scheme in Figure B.2. The main loop in the logic is consistent with the greedy deployment scheme but adds a check to see if the current deployment exceeds the limit on that reactor. If it does, the scheme removes the reactor from the list of deployable reactors in that time step. This scheme varies from the capped deployment scheme in that the distribution is not flat, but a more granular distribution that varies by year.

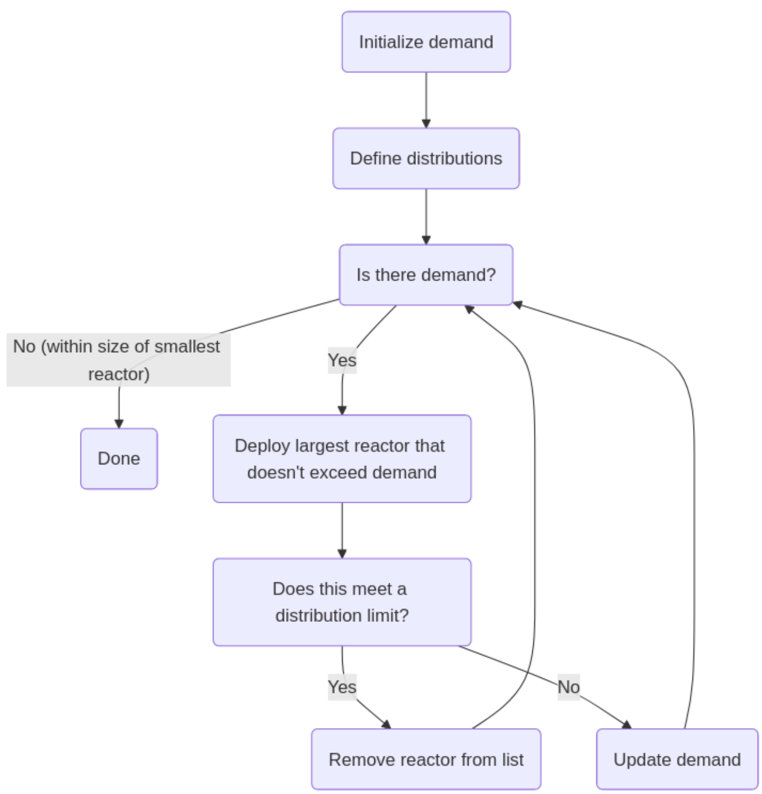


Figure B.2: Pre-determined distribution deployment diagram.

The realism of this deployment scheme mirrors some elements of the capped deployment, but the distribution is a more granular way to account for supply chain constraints. This scheme is most useful when there are known commitments to specific technologies. It allows the user to indirectly incorporate the evolution of supply chains or workforce constraints over time, and to explicitly incorporate decisions from individual actors. If a user established the nuances of the supply chain constraints in other work, it could be incorporated through this scheme. Under and over-performance of this scheme is difficult to predict, as it depends on the distribution of reactors over time.

# Appendix C

# Availability of Work

The Dynamic Power Reactor (DPR) and Trading On-Demand (TOD) reactor archetypes are available on GitHub at `https://github.com/arfc/NEAR`.

While the low-enriched uranium plus (LEU+) versions of the advanced reactor models are available on Zenodo